ECREEE
Towards Sustainable Energy

PÖYRY

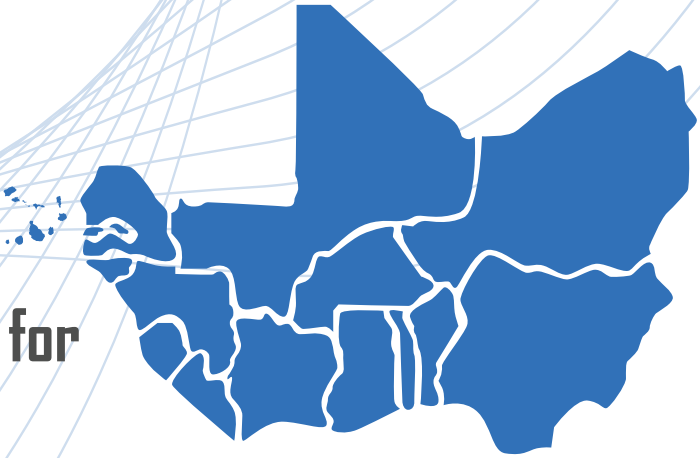

# Technical Report on Methodology and Lessons Learnt for

# ECOWAS COUNTRIES

## GIS Hydropower Resource Mapping and Climate Change Scenarios for the ECOWAS Region

ECOWAS Centre for Renewable Energy and Energy Efficiency
www.ecreee.org

AUSTRIAN DEVELOPMENT COOPERATION

Spanish Cooperation

**Imprint**

**Title:** GIS Hydropower Resource Mapping and Climate Change Scenarios for the ECOWAS Region - Technical Report on Methodology and Lessons Learnt for ECOWAS Countries

**Publisher:** ECOWAS Centre for Renewable Energy and Energy Efficiency (ECREEE), Praia, Cabo Verde. *All results and maps are published on the ECOWAS Observatory for Renewable Energy and Energy Efficiency - www.ecowrex.org/smallhydro*
**Contact:** info@ecreee.org

March 2017

**Program Responsibility:**

The ECOWAS Small-Scale Hydropower Program was approved by ECOWAS Energy Ministers in 2012. In the frame of this program ECREEE assigned Poyry Energy GmbH in 2015 for implementation of a GIS Hydro Resource Mapping and Climate Change Scenarios in ECOWAS countries with Hydropower potentials. Find the 14 country reports summarizing the GIS Hydro Resource mapping and climate change scenarios at **www.ecowrex.org/smallhydro**

**Project Team:**

**Pöyry Energy GmbH, Vienna, Austria**
Mr. Harald Kling (project management, team leader hydrology)
Mr. Martin Fuchs (team leader hydropower)
Mr. Philipp Stanzel (team leader climate change)
Ms. Maria Paulin
Mr. Bernhard Wipplinger
Mr. Stefan Wimmer
Ms. Elisabeth Freiberger
Mr. Christoph Libisch
Mr. Raimund Mollner
Mr. Rudolf Faber
Mr. Herbert Weilguni

**ECOWAS Centre for Renewable Energy and Energy Efficiency, Praia, Cabo Verde**
Mr. Mahama Kappiah, Executive Director
Mr. Hannes Bauer, Project Management, Lead hydropower Program
Mr. Daniel Paco, GIS Expert

**The ECOWAS Small-Scale Hydropower Program is managed by:**
ECOWAS Centre for Renewable Energy and Energy Efficiency (ECREEE)
Mr. Hannes Bauer, ECREEE
Contact: info@ecreee.org

**Project Funding**

Austrian Development Cooperation – ADC
Spanish Ministry of External Affairs and Cooperation - AECID

## TABLE OF CONTENTS

# 1 ABBREVIATIONS AND DEFINITIONS

**Abbreviations:**

ADA: Austrian Development Agency

AECID: Spanish Development Agency

ASTER: Advanced Spaceborne Thermal Emission and Reflection Radiometer (DEM)

CDO: Climate Data Operators

Climwat: CLIMWAT is a climatic database to be used in combination with the computer program CROPWAT

CORDEX: Co-ordinated Regional Downscaling Experiment

CROPWAT: CROPWAT is a decision support tool developed by the Land and Water Development Division of FAO

CRU: Climatic Research Unit

DEM: Digital Elevation Model

DWD: Deutscher Wetterdienst (German meteorological service)

ECOWAS: Economic Community of West African States

ECOWREX: ECOWAS Observatory for Renewable Energy

ECREEE: ECOWAS Centre for Renewable Energy & Energy Efficiency

FAO: Food and Agricultural Organization

FEWS: Famine Early Warning System

GCM: Global Climate Model (a.k.a. General Circulation Model)

GDP: Gross Domestic Product

GIS: Geographical Information System

GPCC: Global Precipitation Climatology Centre

GRDC: Global Runoff Data Centre

H2O: EartH2Observe “Global Earth Observation for Integrated Water Resource Assessment”

HPP: hydropower plant

Hydrosheds: HYDROological data and maps based on SHuttle Elevation Derivatives at multiple Scales

JICA: Japanese International Cooperation Agency

LHS: Liberian Hydrological Service

MAP: Mean Annual Precipitation

MoEP: Ministry of Energy and Power (Sierra Leone)

MW: Megawatt

NBA: Niger Basin Authority

OMVS: Senegal Basin Authority

Qobs: Observed discharge

Qsim: Simulated discharge

RCP: Representative Concentration Pathway

RFE: Rainfall Estimator (satellite rainfall data product)

RCM: Regional Climate Model

SE4ALL: Sustainable Energy For All (program)

SIEREM: Système d'Informations Environnementales sur les Ressources en Eau et leur Modélisation

SRTM: Shuttle Radar Topography Mission (DEM)

TRMM: Tropical Rainfall Measurement Mission (satellite rainfall data product)

USGS: United States Geological Survey

VBA: Volta Basin Authority

**Definitions:**

Pico/micro/mini HPP: Installed capacity < 1 MW

Small HPP: Installed capacity 1-30 MW

Medium/large HPP: Installed capacity > 30 MW

# 2 INTRODUCTION

The 15 countries of the Economic Community of West African States (ECOWAS) face a constant shortage of energy supply, which has negative impacts on social and economic development, including also strongly the quality of life of the population. In mid 2016 the region has about 50 operational hydropower plants and about 40 sites are under construction or refurbishment. The potential for hydropower development – especially for small-scale plants – is assumed to be large, but exact data were missing in the past.

The ECOWAS Centre for Renewable Energy and Energy Efficiency (ECREEE), founded in 2010 by ECOWAS, ADA, AECID and UNIDO, responded to these challenges and developed the ECOWAS Small-Scale Hydropower Program, which was approved by ECOWAS Energy Ministers in 2012. In the frame of this program ECREEE assigned Pöyry Energy GmbH in 2015 for implementation of a hydropower resource mapping by use of Geographic Information Systems (GIS) for 14 ECOWAS member countries (excluding Cabo Verde). The main deliverable of the project is a complete and comprehensive assessment of the hydro resources and computation of hydropower potentials as well as possible climate change impacts for West Africa. Main deliverables of the GIS mapping include:

- River network layer: GIS line layer showing the river network for about 500,000 river reaches with attributes including river name (if available), theoretical hydropower potential, elevation at start and end of reach, mean annual discharge, mean monthly discharge, etc.

- Sub-catchment layer: GIS polygon layer showing about 1000 sub-catchments with a size of roughly 3000 km² each. This layer summarizes the data of all river reaches located within the sub-catchment.

Hydropower plants are investments with a lifetime of several decades. Therefore, possible impacts of climate change on future discharge were incorporated into the river network and sub-catchment GIS layers.

The GIS layers are available in the ECREEE Observatory for Renewable Energy and Energy Efficiency (www.ecowrex.org).

For each of the 14 countries separate reports were prepared that summarize the results of the GIS layers, including:

- Climate

- Hydrology

- Hydropower potential

- Climate change

In addition to these 14 country reports, where the focus was on summarizing the results, the present report focusses on technical aspects, including:

- Data sources

- Methodology
- Results overview (meta-data)
- Evaluation of accuracy of results
- Recommendations and conclusions

Several different data layers were produced in this project. Accordingly, this report includes separate sections for description of:

- Layer showing existing hydropower plants
- Layer D1 Climatic zones
- Hydropower resource mapping:
  - Layer D2 River network
  - Layer D3 Sub-areas
- Layer D4 Country reports
- Climate change scenarios: Results incorporated into layers D1-D4

Note that apart from the existing hydropower plants layer, all of the data published in the GIS layers is based on modelling results. The objective of the data layers is to provide a regional overview and to enable identification of sub-catchments and rivers with attractive theoretical hydropower potential. This provides the basis for follow-up studies and to start targeted discharge measurement campaigns.

Throughout this report the following definitions are used for hydropower plants (HPPs) of different plant size:

- Pico/micro/mini HPP: Installed capacity < 1 MW
- Small HPP: Installed capacity 1-30 MW
- Medium/large HPP: Installed capacity > 30 MW

# 3 EXISTING HYDROPOWER PLANTS

## 3.1 Objective

The objective is to prepare an up-to-date GIS layer that shows the location and meta-data of all existing hydropower plants in West Africa. This information is required to identify those river reaches where the hydropower potential is already utilized. A first screening of data availability showed that a homogeneous data set with correct geo-referencing was not available in the past.

As information about small and especially pico/micro/mini hydropower plants is usually hard to obtain the focus was on identifying all existing hydropower plants with installed capacity above 30 MW. However, during preparation of the GIS layer also smaller hydropower plants were included if information was available.

## 3.2 Data sources

Various different data sources were used for creating the existing hydropower plants layer, including data from:

- ECOWREX (ECREEE)
- Global Reservoir and Dam (GranD) data base
- Aquastat
- International Journal on Hydropower & Dams: Water Storage and Hydropower Development for Africa (2015)
- JICA (Japan) data for Nigeria Master Plan
- Small Hydropower (SHP) News
- World Small HPP Development Report 2013
- Water Power & Dam Construction Yearbook 2012
- Various sources provided by ECREEE
- Internet research
- Maps
- Satellite images

## 3.3 Methodology

The following methodology was used for creating the existing hydropower plants layer:

- Create list of existing hydropower plants

- Start with list of 30 existing hydropower plants in ECOWREX (ECREEE)
- Include data from GranD
- Include data from International Journal on Hydropower & Dams (2015)
- Include data from Aquastat
- Include data from JICA for Nigeria HPPs
- Include data from various other sources (see chapter 3.2)

· Validate/update geo-referencing of each hydropower plant

- Use satellite image to verify or update correct geo-referencing.
- In case of missing coordinates first a literature review was required to determine the approximate location (near town X, at river Y), before manually determining the coordinates with satellite images.

· Update list/geo-referencing with data from various sources

The most time-consuming task was the correct geo-referencing of the hydropower plants, as in many cases the reported coordinates were either inaccurate or missing at all. Geo-referencing was done manually by use of satellite images (see example in Figure 1). This required manual screening of satellite images along the river where the hydropower plant was expected to be located. For smaller hydropower plants the identification of the correct river in the satellite image to start the search was the most difficult part.

In several cases there were conflicting data from different sources for the same hydropower plant (for example different values for installed capacity). Here, expert judgement, combined with additional literature research was used to decide which source to trust more. It was also found that the data sources included duplicates of the same hydropower plant, but with different names. The duplicates were removed and data merged.

The list also includes proposed or identified hydropower plants where the data were obtained from ECREEE and SE4ALL. Here, Pöyry did not check or update the data (because it was outside the scope of this study). As a consequence, it is likely that for many of these sites the data are not accurate, especially the geo-referencing.

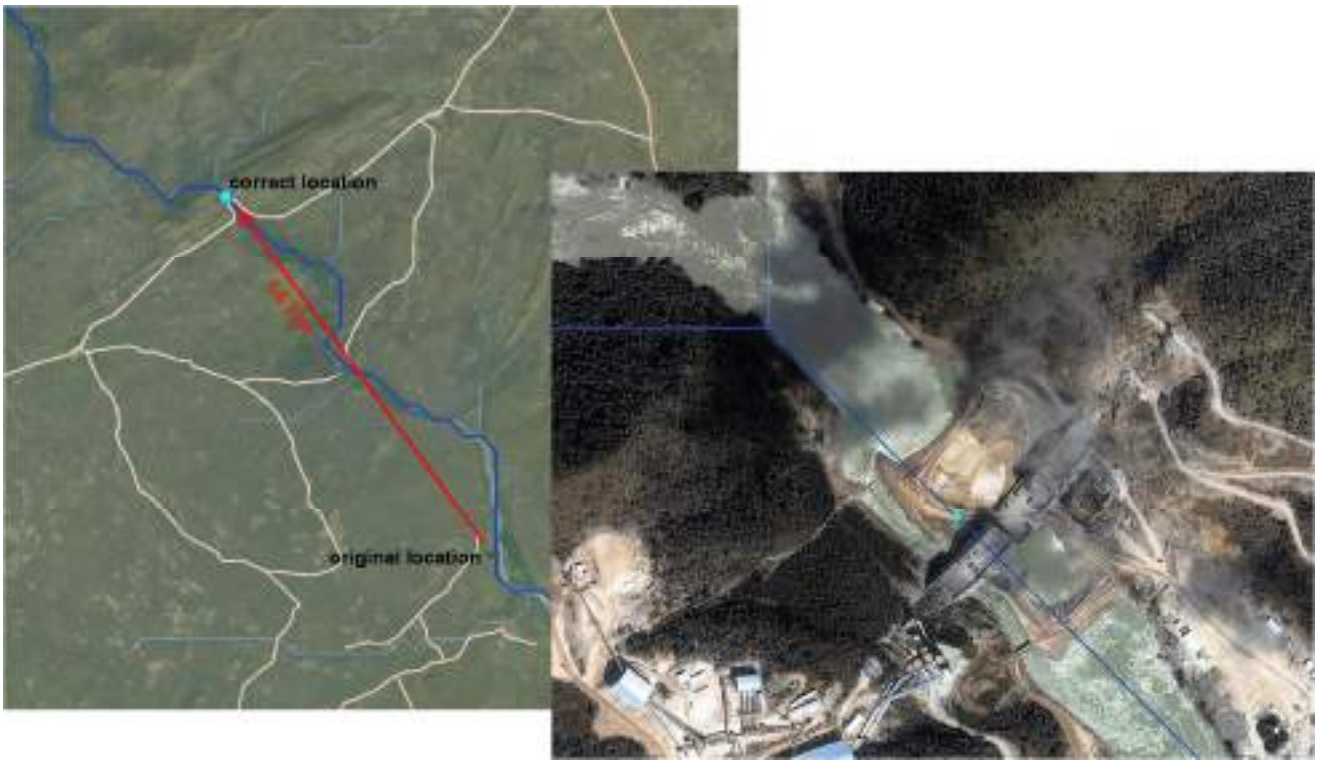


**Figure 1: Manual geo-referencing of existing hydropower plants by use of satellite images. Example for the recently constructed Bui HPP in Ghana. Here, the HPP was misplaced by 14 km with the originally reported coordinates.**

## 3.4 Results: Layer showing existing hydropower plants

The results are published as a GIS point shape file named “Layer Existing HPPs”. Figure 2 displays a map showing the location of the existing hydropower plants. Overall there are 91 existing hydropower plants, 24 large HPPs (installed capacity > 100 MW), 17 medium HPPs (installed capacity 30-100 MW) and 50 small HPPs (installed capacity < 30 MW). Of the overall 91 hydropower plants 56 are operational and 35 are under construction or refurbishment.

For each of the 91 existing hydropower plants 22 attributes are provided in the shape file (see Table 1). In addition to the 91 existing hydropower plants the layer also includes 115 proposed or identified hydropower plants, where the data were not checked or updated by Pöyry.


**Figure 2: Map showing existing hydropower plants.**

**Table 1: Attributes of the GIS shape file "Layer Existing HPPs".**

| Attribute | Units | Description |
|---|---|---|
| Comment | text | Any comment possible. |
| Name | text | Name of HPP. |
| Name_alt | text | Alternative name of HPP, if known. |
| Country | text | Country of location of the HPP. |
| ISO | text | Three letter country name acronym. |
| Existing | text | Main status division (yes/no), further divided in the status attribute (see status attribute). |
| Hpp_class | text | Capacity class according to the ECOWAS classification (small < 30MW, medium 30-100 MW, large > 100 MW). |
| Status | text | Describes the status of the HPP in six categories: operational, under refurbishment, under construction (these three have the value Yes in the Existing attribute); identified, planned, proposed (these three have the value No in the Existing attribute). |
| Lat | deg | Latitude of the location, snapped to the river network. |
| Lon | deg | Longitude of the location, snapped to the river network. |
| River | text | Name of the river where the HPP is located. Value n/a if not known. |
| River_alt | text | Alternative river name, if applicable. |
| Year | none | Year of start of operation for existing HPPs. Estimated for HPPs under construction and under refurbishment. Value n/a if not known. Not used for HPP with status not existing. |
| Dam_height | m | Height (m) of the main dam for existing HPPs. Estimated for HPPs under construction and under refurbishment. Value n/a if not known. Not used for HPP with status not existing. |
| Cap_Instal | MW | Installed capacity (MW) for operational HPPs and HPPs under refurbishment. Value n/a if not known and for HPPs under construction. Not used for HPP with status not existing. |
| Cap_Availa | MW | Currently available capacity (MW) for operational HPPs. Value n/a if not differing from installed capacity or if not known, and for HPPs under refurbishment and under construction. Not used for HPP with status not existing. |
| Cap_Planned | MW | Planned capacity (MW) for HPPs under construction, under refurbishment and all types of HPPs with status not existing. Value n/a if not known. For operational HPPs, a value is given if a planned extension is known, otherwise n/a. |
| Volume | $hm^3$ | Reservoir volume ($hm^3$) for existing HPPs. Value n/a if not known. Not used for HPP with status not existing. |
| Lake_area | $km^2$ | Reservoir area ($km^2$) for existing HPPs. Value n/a if not known. Not used for HPP with status not existing. |
| Data_Provider | text | Source of information, with values ECREEE (data from the ECOWREX database before Dec 2015), SE4ALL (data from the database of Pascal Habay of "Programme d'Assistante Technique pour l'Afrique Occidentale et Centrale" under the Sustainable Energy for All Programme, SE4ALL) and Poyry (data collected in the GIS hydropower resource mapping project from various sources). |
| Data_Source | text | More specific information on the original source of data, if known (information from the ECOWREX database before Dec 2015). |
| Owner | text | Owner of the HPP (information from the ECOWREX database before Dec 2015). |

## 3.5 Lessons learned

Different sources (reports, data bases) often gave conflicting information about existing hydropower plants in West Africa. It is difficult to decide which source to trust more. Ideally, field visits would be required to each existing hydropower plant to confirm the data. However, this would require a significant amount of time and budget.

Another problem is that it cannot be ruled out that for some hydropower plants inaccurate data are copied from one report to the next report. In such a case different

sources appear to confirm the accuracy of the data, but in reality the data are not accurate.

Basic information about hydropower plants, such as installed capacity or dam height, was easier to obtain than to determine the exact location. Here, often only vague information is available in reports (e.g. upstream of city X on river Y). Therefore, satellite images were used to manually geo-reference the location of the hydropower plants. However, for smaller hydropower plants this was a tedious and very time-consuming task.

## 3.6 Conclusions and recommendations

The results of the mapping of existing hydropower plants allow the following conclusions:

- A considerable number of small, medium and large hydropower plants already exist in West Africa. About half of the existing plants are operational and the other half are under construction or refurbishment.
- There are hardly any pico/micro/mini hydropower plants existing in West Africa. Or at least, in the available data bases there is no information available about pico/micro/mini hydropower plants.
- Some of the existing small hydropower plants have installed capacities that differ from a conventional hydropower design for the river of a given size:
    - Some hydropower plants are located at large rivers, but using only a small share of total river discharge. Examples are Yele HPP at the Teye River in Sierra Leone or Sotuba HPP at the Niger River near Bamako in Mali.
    - Some hydropower plants are part of multi-purpose schemes, combining irrigation (main use) and hydropower (secondary use). For many of these locations a single-purpose hydropower plant would probably not be viable due to too high investment costs. One example is Bakolori scheme at the Sokoto River in Nigeria, where at the reservoir for the large-scale irrigation scheme also includes a hydropower plant (which currently is not operational).

The published GIS shape file “Layer Existing HPPs” represents the current status of knowledge about existing hydropower plants, as of the year 2016. We recommend to continuously update the layer as new information about new or existing hydropower plants becomes available. The updating should be done at least once a year, but ideally continuously directly when new information becomes available. However, as there are often conflicting pieces of information the data sources should be thoroughly and critically checked, to avoid updates with inaccurate data.

# 4 CLIMATIC ZONES

## 4.1 Objective

The objective is to create a GIS layer that shows the regional distribution of the diverse climatic conditions in West Africa. This dataset is not intended for local studies but only for regional comparison.

## 4.2 Data sources

Various different data sources were used for the climatic zones layer (see Table 2). This includes rainfall data, air temperature data, and potential evapotranspiration data. For climate model data see chapter 6.

**Table 2: Data sources used for the climatic zones.**

| Variable | Product | Spatial resolution | Temporal resolution | Period | Description |
|---|---|---|---|---|---|
| Precipitation | TRMM 3B42 V7 | 0.25 deg raster | daily | 1998-2014 | Tropical Rainfall Measurement Mission (TRMM) of NASA (USA) and JAXA (Japan), satellite based measurements merged with ground based rain gauges |
| Air temperature | CRU TS3.22 | 0.5 deg raster | monthly | 1901-2013 | Climatic Research Unit, University of East Anglia (UK), interpolated station measurements |
| Potential evapo-transpiration | CRU TS3.22 | 0.5 deg raster | monthly | 1901-2013 | Climatic Research Unit, University of East Anglia (UK), computed with Penman-Monteith method using interpolated station data (air temperature, relative humidity, etc.) |

## 4.3 Methodology

The dataset was created using the following methodology:

1. A climatic zones classification was determined based on an existing classification by L'Hôte et al. (1996) that has been developed with a special focus on West Africa and applicability for hydrological purposes, summarizing and consolidating many previous attempts of classifying West African climate. The classification is widely used in regional studies, as e.g. in the Andersen et al. (2005) study on the Niger River Basin, from which the English denominations of the originally French climatic zone names were derived. Climatic zone limits are based on mean annual and seasonal precipitation:

    a. Desert: Mean Annual Precipitation (MAP) < 100 mm

    b. Semiarid desert: MAP < 400 mm

    c. Semiarid tropical: MAP < 700 mm

d. Pure tropical: MAP < 1000 mm

e. Transitional tropical: MAP > 1000 mm, one wet season

f. Transitional equatorial: MAP > 1000 mm, two wet seasons

2. The geographical location of the climatic zone boundaries was derived from the long-term annual mean of daily precipitation data for 1998-2014 of the Tropical Rainfall Measuring Mission (TRMM, a joint U.S.-Japan satellite mission to monitor tropical and subtropical precipitation). Limits between zone (e), transitional tropical climate, and zone (f), transitional equatorial climate, were adopted from the map of L`Hôte et al. 1996. Their limits are based on seasonal precipitation and on previous climate zone classification limits.

3. The resulting polygons were generalized (smoothing of polygon boundaries, removal of islands).

For each climatic zone several attributes were computed by spatial averaging of the data listed in chapter 4.2.

- Mean annual rainfall for the period 1998-2014.
- Mean monthly rainfall for the period 1998-2014.
- Mean annual air temperature for the period 1998-2013.
- Mean monthly air temperature for the period 1998-2013.
- Mean annual potential evapotranspiration for the period 1998-2013.
- Mean monthly potential evapotranspiration for the period 1998-2013.
- Mean monthly climatic water balance computed as difference between rainfall and potential evapotranspiration.

In addition, also climate change projections were summarized for each climatic zone (see chapter 6).

The following tools were used for creating this dataset:

- ArcGIS 10.0: Conversion of raster data sets to polygons, smoothing and generalization of polygons
- ArcGIS 9.2: Definition of interpolation points
- ArcView 3.1: Data import of large raster data sets
- Fortran: Calculation of mean annual and mean monthly values of climatic variables for West Africa
- MS Excel: Data pre-processing and visualization

- Libre Office: Manipulation of dbf data tables
- CDO: Climate Data Operators for processing of CORDEX-Africa climate model data
- Shell scripts: For automatic file processing of climate model data
- Batch scripts: For automatic calls to Fortran programs

## 4.4 Results: Layer D1 Climatic Zones

The results are published as a GIS polygon shape file named "Layer D1 Climatic Zones". The shape file shows the spatial distribution of climatic zones in West Africa. Two figures are attached to each climatic zone showing seasonality in rainfall, air temperature, potential evapotranspiration and climatic water balance.

Figure 3 displays a map showing Layer D1. Figure 4 to Figure 9 display the figures attached to the climatic zones.

Table 3 lists the attributes of Layer D1. Overall there are 24 attributes for the six climatic zones.

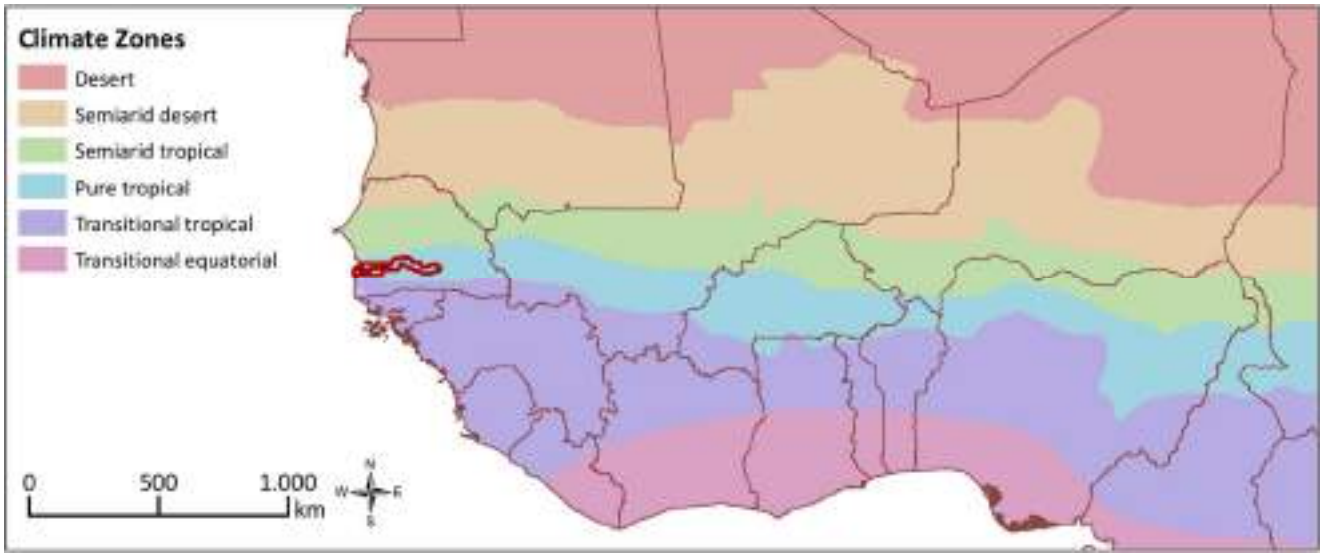


**Figure 3: Map showing Layer D1 Climatic Zones.**

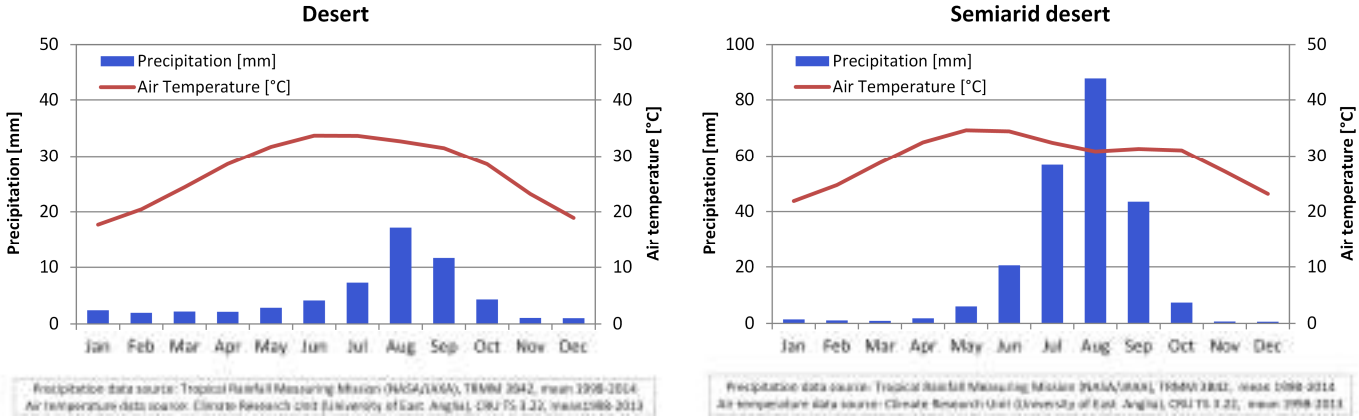


**Figure 4: Seasonality in rainfall and air temperature in climatic zones "Desert" (left) and "Semiarid desert" (right).**

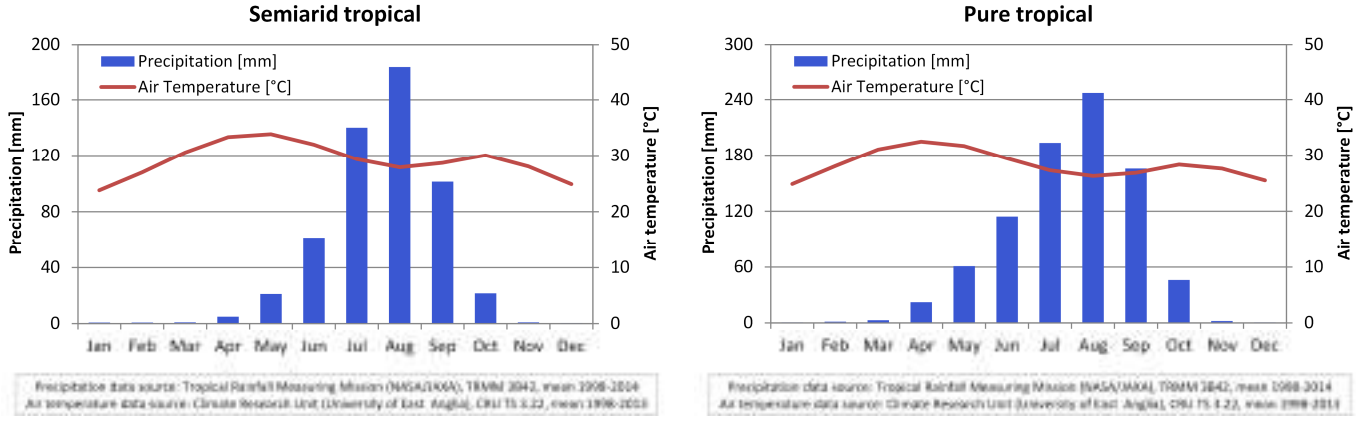


**Figure 5: Seasonality in rainfall and air temperature in climatic zones "Semiarid tropical" (left) and "Pure tropical" (right).**

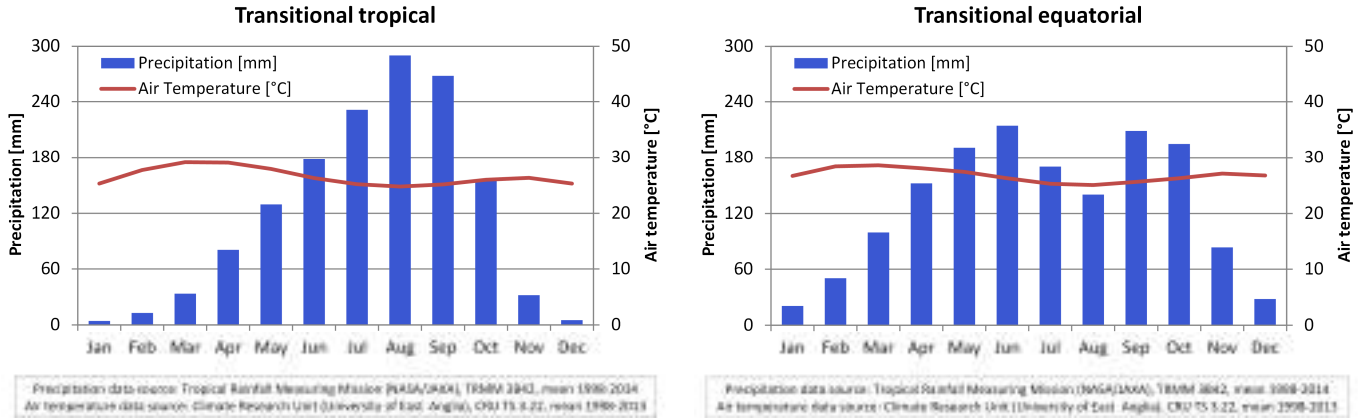


**Figure 6: Seasonality in rainfall and air temperature in climatic zones "Transitional tropical" (left) and "Transitional equatorial" (right).**

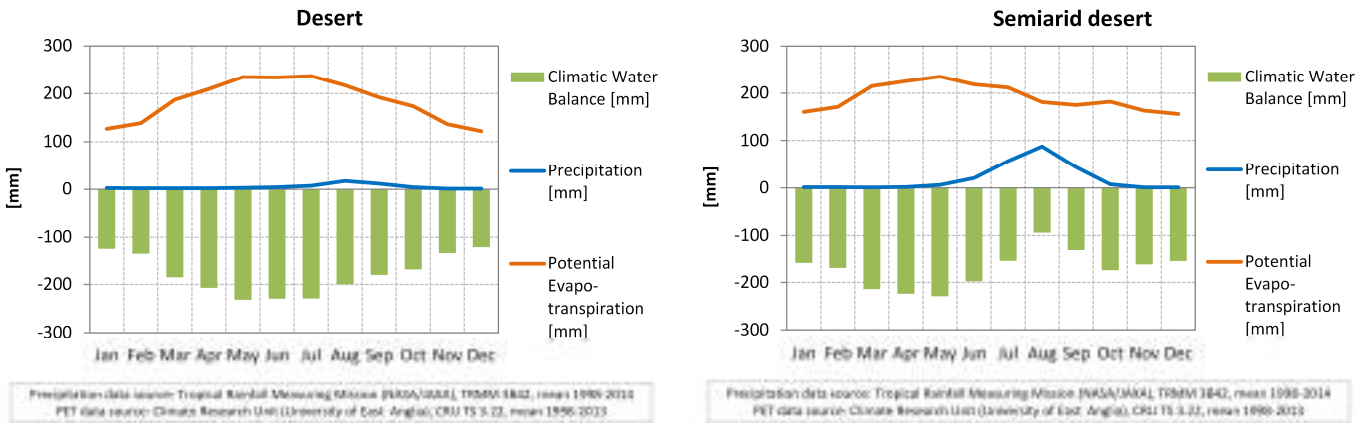


**Figure 7: Climatic water balance (rainfall minus potential evapotranspiration) in climatic zones "Desert" (left) and "Semiarid desert" (right).**

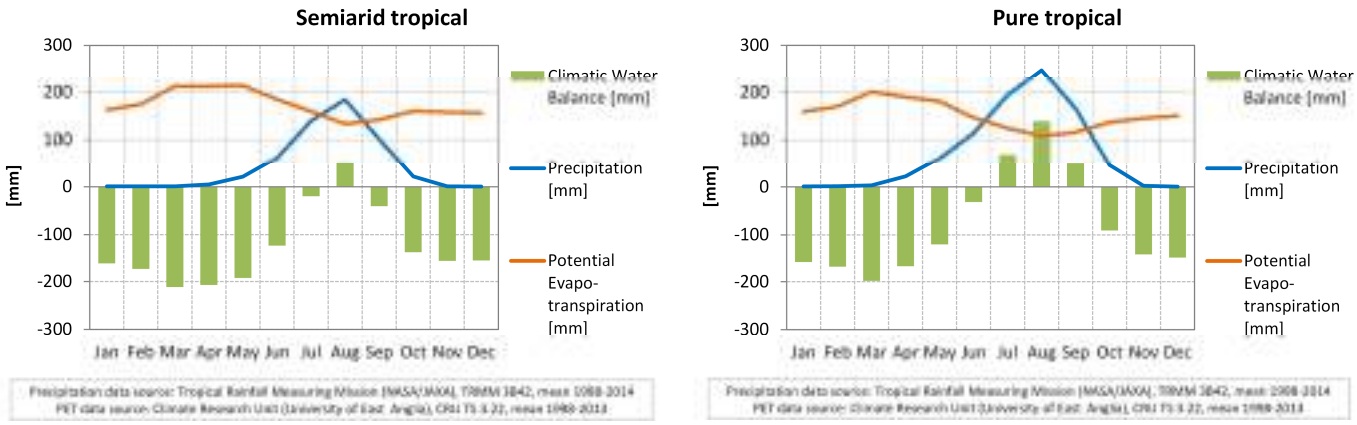


**Figure 8: Climatic water balance (rainfall minus potential evapotranspiration) in climatic zones "Semiarid tropical" (left) and "Pure tropical" (right).**

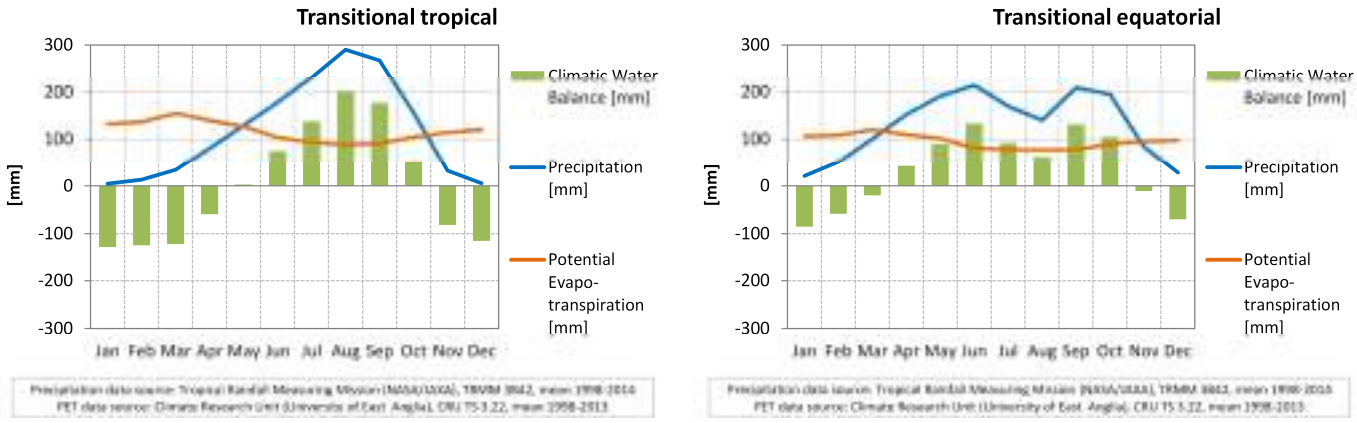


**Figure 9: Climatic water balance (rainfall minus potential evapotranspiration) in climatic zones "Transitional tropical" (left) and "Transitional equatorial" (right).**

**Table 3: Attributes of the GIS shape file "Layer D1 Climatic Zones".**

| Attribute | Units | Description |
|---|---|---|
| CLZ_ID | / | ID number of climate zone |
| NAME_FR | text | Climatic zone denomination in French |
| NAME_ENG | text | Climatic zone denomination in English |
| PRECIP_Y | mm | Mean annual precipitation (mm) in the period 1998-2014 |
| TEMP_Y | °C | Mean annual air temperature (°C) in the period 1998-2014 |
| ETP_Y | mm | Mean annual potential evapotranspiration (mm) in the period 1998-2014 |
| P_2035_P25 | % | Change in future mean annual precipitation in % (2026-2045 vs. 1998-2014) for the lower quartile projection of 30 climate model runs in the CORDEX-Africa ensemble (RCP4.5 and RCP8.5) |
| P_2035_P50 | % | Change in future mean annual precipitation in % (2026-2045 vs. 1998-2014) for the median projection of 30 climate model runs in the CORDEX-Africa ensemble (RCP4.5 and RCP8.5) |
| P_2035_P75 | % | Change in future mean annual precipitation in % (2026-2045 vs. 1998-2014) for the upper quartile projection of 30 climate model runs in the CORDEX-Africa ensemble (RCP4.5 and RCP8.5) |
| P_2055_P25 | % | Change in future mean annual precipitation in % (2046-2065 vs. 1998-2014) for the lower quartile projection of 30 climate model runs in the CORDEX-Africa ensemble (RCP4.5 and RCP8.5) |
| P_2055_P50 | % | Change in future mean annual precipitation in % (2046-2065 vs. 1998-2014) for the median projection of 30 climate model runs in the CORDEX-Africa ensemble (RCP4.5 and RCP8.5) |
| P_2055_P75 | % | Change in future mean annual precipitation in % (2046-2065 vs. 1998-2014) for the upper quartile projection of 30 climate model runs in the CORDEX-Africa ensemble (RCP4.5 and RCP8.5) |
| T_2035_P25 | °C | Change in future mean annual air temperature in °C (2026-2045 vs. 1998-2014) for the lower quartile projection of 30 climate model runs in the CORDEX-Africa ensemble (RCP4.5 and RCP8.5) |
| T_2035_P50 | °C | Change in future mean annual air temperature in °C (2026-2045 vs. 1998-2014) for the median projection of 30 climate model runs in the CORDEX-Africa ensemble (RCP4.5 and RCP8.5) |
| T_2035_P75 | °C | Change in future mean annual air temperature in °C (2026-2045 vs. 1998-2014) for the upper quartile projection of 30 climate model runs in the CORDEX-Africa ensemble (RCP4.5 and RCP8.5) |
| T_2055_P25 | °C | Change in future mean annual air temperature in °C (2046-2065 vs. 1998-2014) for the lower quartile projection of 30 climate model runs in the CORDEX-Africa ensemble (RCP4.5 and RCP8.5) |
| T_2055_P50 | °C | Change in future mean annual air temperature in °C (2046-2065 vs. 1998-2014) for the median projection of 30 climate model runs in the CORDEX-Africa ensemble (RCP4.5 and RCP8.5) |
| T_2055_P75 | °C | Change in future mean annual air temperature in °C (2046-2065 vs. 1998-2014) for the upper quartile projection of 30 climate model runs in the CORDEX-Africa ensemble (RCP4.5 and RCP8.5) |
| E_2035_P25 | % | Change in future mean annual potential evapotranspiration in % (2026-2045 vs. 1998-2014) for the lower quartile simulation using 30 climate model runs of the CORDEX-Africa ensemble (RCP4.5 and RCP8.5) |
| E_2035_P50 | % | Change in future mean annual potential evapotranspiration in % (2026-2045 vs. 1998-2014) for the median simulation using 30 climate model runs of the CORDEX-Africa ensemble (RCP4.5 and RCP8.5) |
| E_2035_P75 | % | Change in future mean annual potential evapotranspiration in % (2026-2045 vs. 1998-2014) for the upper quartile simulation using 30 climate model runs of the CORDEX-Africa ensemble (RCP4.5 and RCP8.5) |
| E_2055_P25 | % | Change in future mean annual potential evapotranspiration in % (2046-2065 vs. 1998-2014) for the lower quartile simulation using 30 climate model runs of the CORDEX-Africa ensemble (RCP4.5 and RCP8.5) |
| E_2055_P50 | % | Change in future mean annual potential evapotranspiration in % (2046-2065 vs. 1998-2014) for the median simulation using 30 climate model runs of the CORDEX-Africa ensemble (RCP4.5 and RCP8.5) |
| E_2055_P75 | % | Change in future mean annual potential evapotranspiration in % (2046-2065 vs. 1998-2014) for the upper quartile simulation using 30 climate model runs of the CORDEX-Africa ensemble (RCP4.5 and RCP8.5) |

## 4.5 Conclusions

The new climatic zones layer gives a good regional overview about the diverse climatic conditions in West Africa. Obviously there are many different climatic classification systems readily available. The classification system adopted here is based on the objective of being useful for hydrological assessments, such as hydropower resource mapping.

The attributes and figures provided for each climatic zone give a first overview about the hydro-climatological characteristics and climate change projections. More detailed information is available for sub-areas and river reaches (see chapter 5).

# 5 HYDROPOWER RESOURCE MAPPING

## 5.1 Objective

The main purpose of this study is to provide a complete and comprehensive assessment of the hydro resources and computation of hydropower potentials in West Africa. To this end river network and sub-catchment GIS layers shall be created with relevant attributes showing the hydropower potential.

The objective of the GIS data layers is to provide a regional overview and to enable identification of sub-catchments and rivers with attractive theoretical hydropower potential. This provides the basis for follow-up studies and to start targeted discharge measurement campaigns.

## 5.2 Data sources

The following tables list the data sources used in this study, including:

- Digital elevation models and derived products (Table 4).
- Hydro-meteorological data sources (Table 5)
- Observed discharge data (Table 6)

An important dataset for river network creation was the Hydrosheds data set (Lehner et al., 2008).

Figure 10 shows the temporal availability of precipitation data. GPCC covers the longest period from 1901 to 2010, whereas satellite-based precipitation data sets start in 1998 (TRMM). A comparison of long-term mean annual precipitation maps shows that GPCC and TRMM data correspond rather well, whereas RFE appears to be biased in some regions (Figure 11).

Figure 12 to Figure 16 show the temporal availability of discharge observation at gauges provided from different sources. The highest number of gauges is available between 1960 and 1990.

Additional data sources used in this study include:

- SIEREM: Coarse GIS river network layer, which was used as additional source for river names.
- Various maps (hard-copy and online) used as additional source for river names.
- Soil Atlas of Africa: Regional overview about soil types, water holding capacity of soils, etc., which was considered in the manual calibration of regional parameter values of the water balance model.
- Land-use maps from different sources: General information, which was considered in the manual calibration of regional parameter values of the water balance model.

- Satellite images (Google Earth): To visually identify the location of diversions for large-scale irrigation schemes.

**Table 4: Digital elevation models (DEM) and derived products data sources.**

| Product | Source | Spatial resolution | Tiles (individual GIS data sets) | Description | Comment |
|---|---|---|---|---|---|
| DEM unconditioned | Hydrosheds | 3s (~90m) | 41 | Unconditioned elevation of Hydrosheds | Used as input for further processing of longitudinal river profiles |
| DEM conditioned | Hydrosheds | 3s (~90m) | 41 | Hydrologically conditioned (stream burning) elevation of Hydrosheds | Only used for comparison, not used for final product |
| DEM | ASTER | 1s (~30m) | 840 | Elevation of ASTER with a fine spatial resolution | Only used for comparison, not used for final product |
| Flow direction | Hydrosheds | 15s (~450m) | 1 | Flow direction grid of Hydrosheds | Used for delineating new river-network |
| River-network | Hydrosheds | 15s (~450m) | 1 data-set, about 100,000 river reaches in West Africa | River-network vector GIS layer of Hydrosheds | Used for early processing, later replaced by own (more detailed) river network |

**Table 5: Hydro-meteorological data sources**

| Variable | Source | Spatial resolution | Temporal resolution | Period | Description | Comment |
|---|---|---|---|---|---|---|
| Precipitation | TRMM 3B42 V7 | 0.25 deg raster | daily | 1998-2014 | Tropical Rainfall Measurement Mission (TRMM) of NASA (USA) and JAXA (Japan), satellite based measurements merged with ground based rain gauges | Used as input for the water balance model in the reference period 1998-2014 |
| Precipitation | GPCC | 0.5 deg raster | monthly | 1901-2010 | Global Precipitation Climatology Centre (GPCC) of DWD (Germany), interpolated station data | Used for model calibration before 1998 |
| Precipitation | RFE V2 | 0.1 deg raster | daily | 2001-2014 | Rainfall Estimate (RFE) developed for Africa by FEWS-NET (USGS, USA), satellite based measurements merged with ground based rain gauges | Only used for comparison, not used for final product |
| Air temperature | CRU TS3.22 | 0.5 deg raster | monthly | 1901-2013 | Climatic Research Unit, University of East Anglia (UK), interpolated station measurements | Used as a baseline for air temperature in the reference period |
| Potential evapo-transpiration | CRU TS3.22 | 0.5 deg raster | monthly | 1901-2013 | Climatic Research Unit, University of East Anglia (UK), computed with Penman-Monteith method using interpolated station data (air temperature, relative humidity, etc.) | Used as input for water balance model |
| Potential evapo-transpiration | Climwat 2.0 | station data | long-term monthly means | ~1971-2000 | Dataset provided by FAO for CROPWAT model, which uses Penman-Monteith method | Used for comparison and correction of CRU data in some regions |
| Potential evapo-transpiration | H2O | 0.5 deg raster | daily | 1979-2012 | EartH2Observe (H2O) “Global Earth Observation for Integrated Water Resource Assessment” funded by EU, Penman-Monteith method | Only used for comparison, not used for final product |

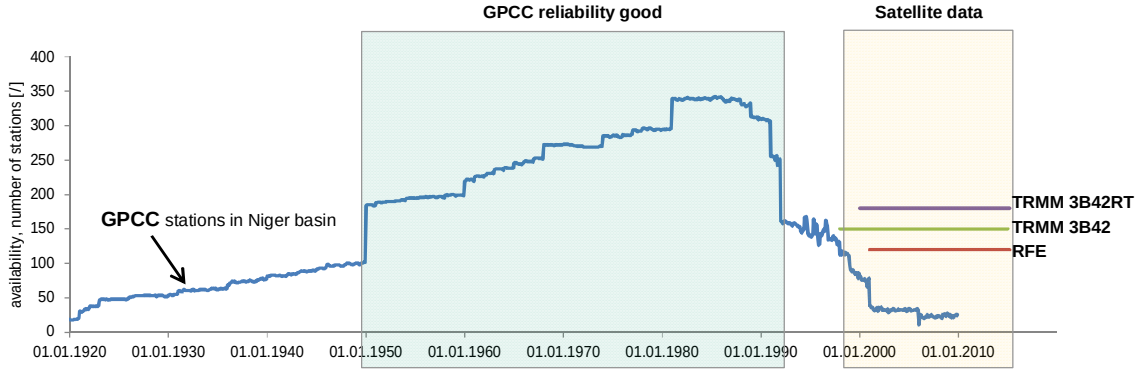


**Figure 10: Temporal availability of precipitation data sets for West Africa. The GPCC data cover the period 1901 to 2010, but with varying underlying station data (the blue line shows the number of stations available for GPCC in the Niger basin). Satellite-based precipitation data started with TRMM in the year 1998.**

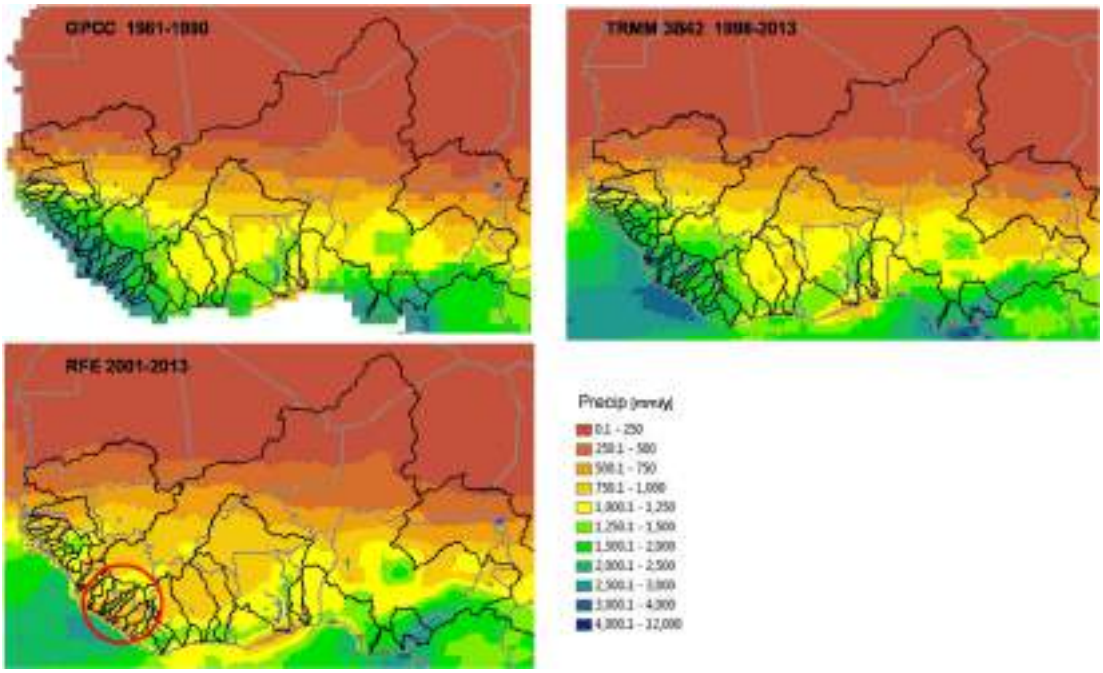


**Figure 11: Comparison of long-term mean annual precipitation maps derived from GPCC, TRMM and RFE. The GPCC and TRMM maps correspond well, whereas the RFE map shows quite low (biased) annual precipitation in the south-western part of West Africa (red circle).**

**Table 6: Observed discharge data sources. The different data sources include many duplicate gauges (with sometimes conflicting data). Period gives year of first and last record of all gauges (with many data gaps).**

| Source | Gauges | Temporal resolution | Period | Description |
|---|---|---|---|---|
| GRDC | 254 | daily | 1903-2012 | Global Runoff Data Centre (GRDC), Koblenz, Germany, daily discharge data for West Africa |
| GRDC | 361 | monthly | 1907-2007 | Global Runoff Data Centre (GRDC), Koblenz, Germany, monthly discharge data for West Africa |
| JICA | 101 | monthly | 1960-2011 | Japanese International Cooperation Agency (JICA), pre-processed monthly discharge data for Nigeria |
| VBA | 6 | irregular, 1 minute to daily | 1952-2012 | Volta Basin Authority, instantaneous discharge values (irregular time-steps) for selected key gauges in Burkina Faso and Ghana |
| NBA | 25 | monthly | 1955-2014 | Niger Basin Authority, monthly discharge data for selected key gauges in the Niger basin |
| OMVS | 8 | daily | 1950-2014 | Senegal Basin Authority (OMVS), daily discharge data for selected key gauges in the Senegal basin |
| LHS | 2 | daily | 2012-2015 | Liberian Hydrological Service, daily discharge data for two key gauges at the Lofa and St. Paul rivers |
| MoEP | 7 | daily | 1970-1976 | Daily discharge data of available gauges in Sierra Leone, provided by Ministry of Energy and Power – Water Supply Division |

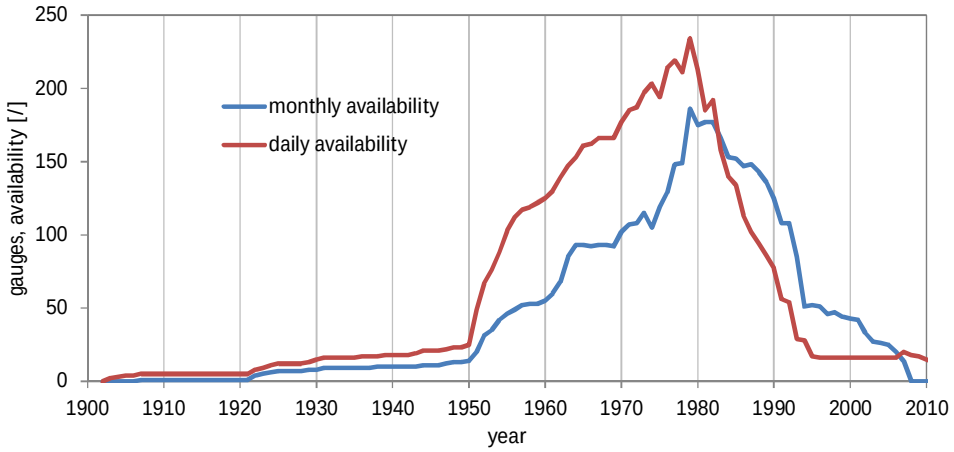


**Figure 12: Annual availability of observed discharge data at gauges provided by GRDC.**

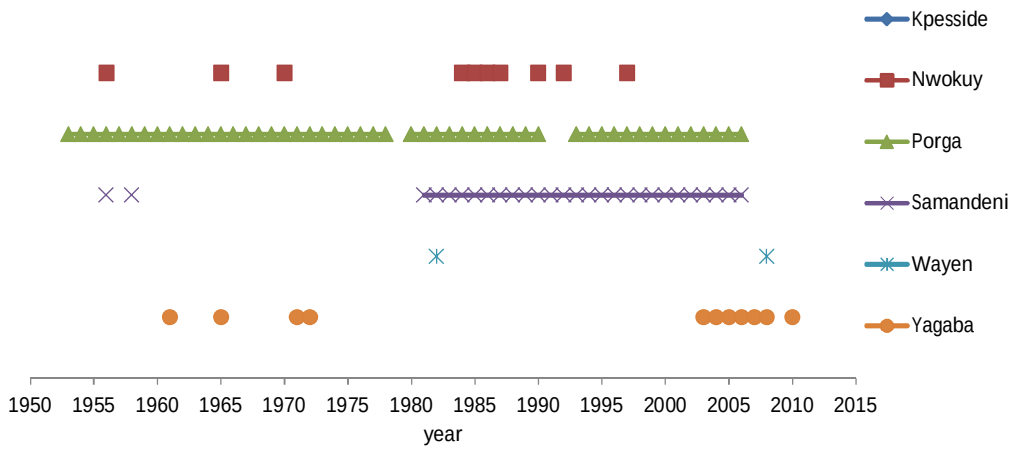


**Figure 13: Annual availability of observed discharge data at gauges provided by the Volta Basin Authority.**

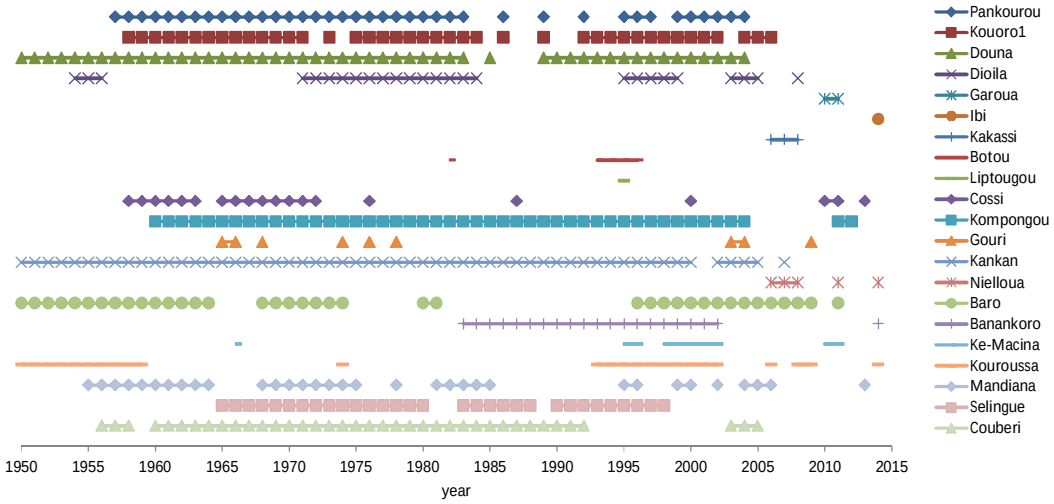


**Figure 14: Annual availability of observed discharge data at gauges provided by the Niger Basin Authority.**

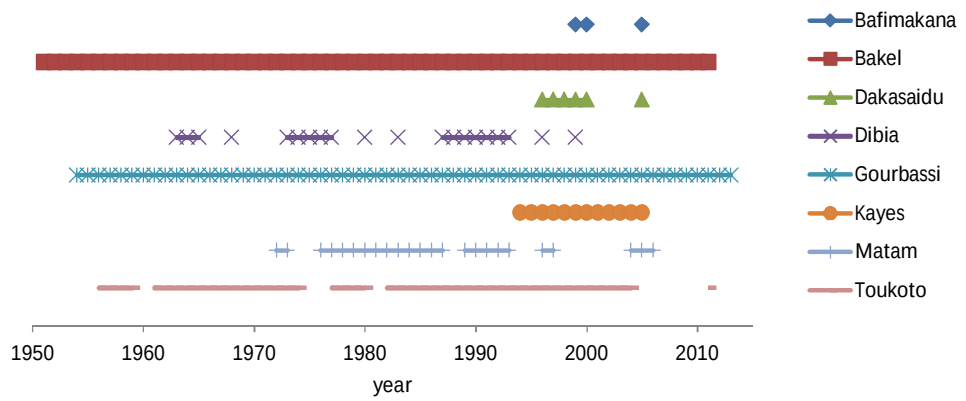


**Figure 15: Annual availability of observed discharge data at gauges provided by the Senegal Basin Authority.**

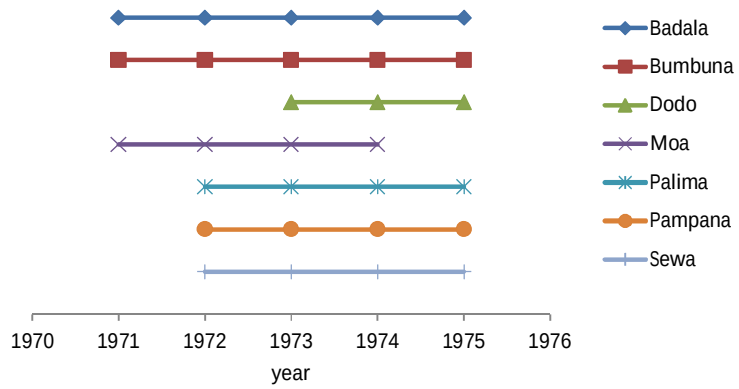


**Figure 16: Annual availability of observed discharge data at gauges provided by Sierra Leone Ministry of Energy and Power – Water Supply Division.**

## 5.3 Methodology

### 5.3.1 Pre-processing of observed discharge data

Pre-processing of observed discharge data included the following steps:

- Step 1: Merging of different data sources
- Step 2: Geo-referencing of gauges
- Step 3: Gap-filling and computation of annual values

In step 1 the 764 data-sets obtained from the eight different sources listed in Table 6 had to be merged into one consistent data-set. Duplicate gauges had to be removed – or if

the data from different sources covered different periods the two time-series had to be merged. Overall, data for 410 gauges were used in this study (Figure 17).

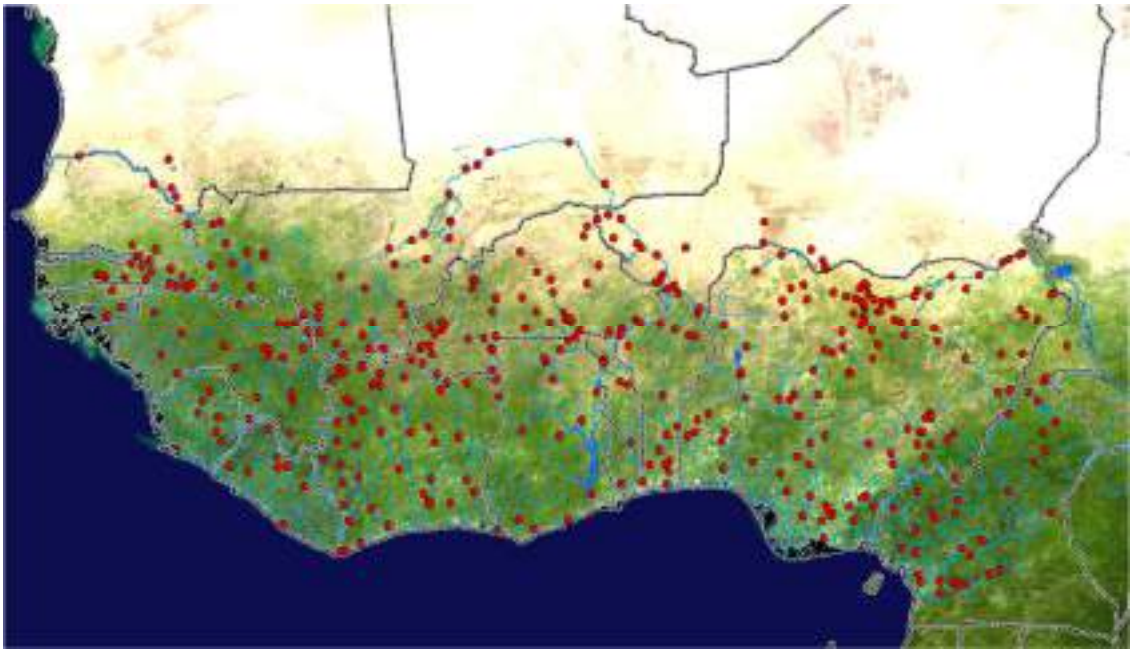

**Figure 17: Location of 410 gauges (red circles) used in this study.**

In step 2 the location coordinates of the 410 gauges were checked and updated. A requirement for the further GIS study was that the gauges are located at the river network. However, automatic GIS snapping was not feasible because of misplaced coordinates of many gauges. Therefore, a manual geo-referencing of all gauges was done based on the following information:

- River name
- Gauge name (Where is this village?)
- Satellite image (Where is nearest bridge or river access?)
- Catchment area reported vs. area computed
- Country (some gauges were even misplaced in the wrong country)
- SIEREM data base (however, also SIEREM proved to be quite inaccurate)
- Reports (internet search)

With the information above, all 410 gauges were manually snapped to the Hydrosheds river network. An example for manual geo-referencing in southern Mali is shown in Figure 18. Some gauges had to be moved by more than 100 km. The histogram in Figure 19 shows that for about half the gauges the distance between original and corrected location is less than 1 km (i.e. the original location is confirmed). However,

for a considerable number of gauges the distance is quite large, e.g. for 14 gauges it is between 20-50 km, and for 10 gauges it is even larger than 100 km. Typical errors in gauge coordinates included:

- Insufficient decimal places for latitude and longitude (e.g. lat = 7.5°)
- Inaccurate coordinates
- Apparent typing errors (e.g. lat = 7.531 reported, whereas correct location is at lat = 8.531)

Overall, the manual geo-referencing was an extremely time-consuming task. Therefore, the updated coordinates were provided to GRDC as a feedback, such that this information is available for future hydrological studies in West Africa.

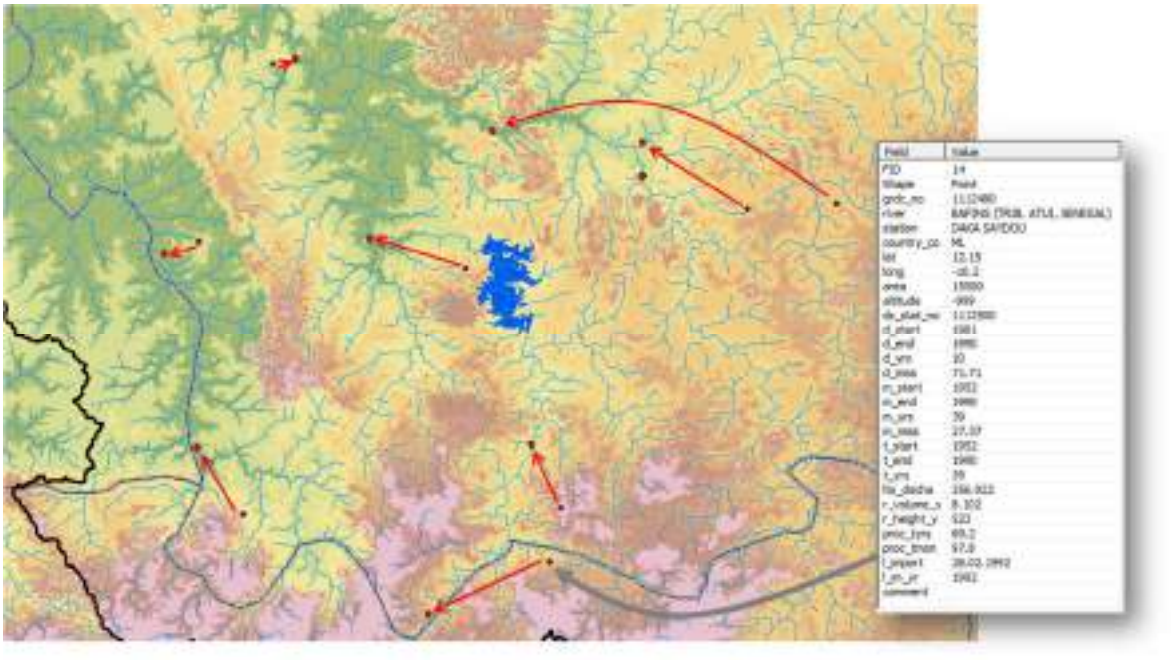

**Figure 18: Example for manual geo-referencing of gauges in southern Mali. The arrows show the correction of the original coordinates supplied with the gauge data and the updated (correct) location. The example shows the attribute table of a gauge that was misplaced into Guinea, but the correct (updated) location is in Mali.**

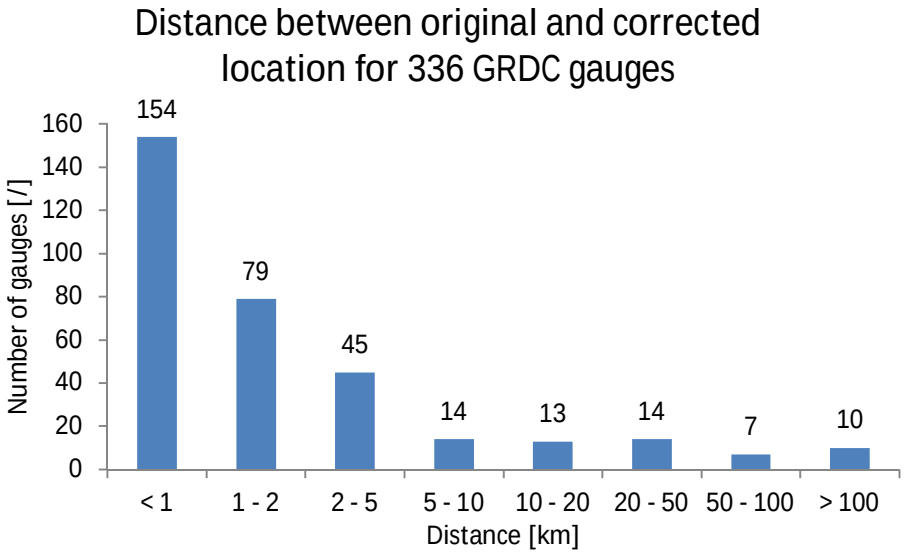


**Figure 19: Histogram showing for 336 GRDC gauges the distance between the original and the corrected location.**

The purpose of step 3 was to generate observed time-series of annual discharge. The following method was used:

- Instantaneous discharge data (in irregular minute intervals) of the Volta Basin Authority were converted to daily time-series.

- Daily data were aggregated to monthly time-steps. A threshold of a minimum 20 daily observations was used to compute monthly values. If observation days were fewer than 20 days then the month was flagged as “missing data”.

- Monthly time-series of each gauge was manually inspected to detect apparent errors (see examples in Figure 20 to Figure 22). Suspicious data were removed.

- In years where only a few months of observations were missing the data gaps were manually filled (see illustrative example in Figure 23). At many gauges of seasonal rivers this required to insert zero values during the dry season (no measurement campaign during the dry season). Missing values during the flood season were inserted by comparison with nearby other gauges. This procedure was required as otherwise many gauges would be removed from the analysis because of not a single year with complete data (12 monthly values, see example for Magou River at Tiele in Figure 23).

- Annual time-series values were computed from monthly time-series only in those years where all 12 monthly observations were available (after gap filling described in previous step). The strong seasonality in discharge requires that annual means are only computed from a complete set of 12 monthly values, otherwise biased annual values would be computed.

The procedure described above resulted in observed discharge data availability shown in Figure 24.

**Metchum @ GOURI** **1051704503**

**Débit journalier 1051704505-1 (m3/s)**

Latitude 6.2833

Longitude 10.0333

Aire du bassin versant 2116 km²

| Année | Valeurs moyennes mensuelles (m3/s) | | | | | | | | | | | | |
|---|---|---|---|---|---|---|---|---|---|---|---|---|---|
| | Jan | Fev | Mar | Avr | Mai | Jun | Jul | Aou | Sep | Oct | Nov | Dec | Annuel |
| 1964 | | (10.84) | 18.75 | 62.34 | (86.06) | (96.5) | 195.09 | 223.61 | (271.37) | (291.51) | (114.48) | 52.99 | (149.52) |
| 1965 | 28.18 | 69.95 | 28.03 | 47.91 | 60.07 | 137.24 | 259.92 | 255.9 | 290.8 | 212.9 | 85.62 | 31.09 | 126.02 |
| 1966 | 19.35 | 19.53 | 19.71 | 19.9 | 20.09 | 20.28 | 20.48 | 20.89 | 20.84 | 21.93 | 21.22 | 21.41 | 20.36 |
| 1967 | 21.62 | 13.55 | 13.24 | 48.57 | 102.94 | 100.66 | 255.55 | 273.39 | | (342.73) | 255.73 | 42.23 | (135.16) |
| 1968 | 23.14 | 23.9 | 24.66 | 25.43 | 26.2 | 26.98 | 27.75 | 28.53 | 29.3 | 30.08 | 30.85 | 31.62 | 27.36 |
| 1969 | (18.8) | 12.55 | | | (97.53) | 100.79 | 258.83 | 269.55 | 279.88 | 238.5 | 92.78 | (47.58) | (152.6) |
| 1970 | (23.98) | (16.93) | (21.01) | (26.82) | 66.38 | 98.77 | 149.11 | 197.4 | 281.88 | 180.44 | 191.42 | 36.37 | (103.02) |
| 1971 | (21.54) | (26.22) | 30.06 | 40.47 | 43 | 79.94 | 207.37 | 186.36 | | (100.97) | 68.79 | 33.21 | (93.66) |
| 1972 | (22.12) | | (17.91) | 27.99 | 66.71 | 112.89 | 161.69 | 200.67 | 212.1 | 166.04 | 74.97 | 30.46 | (109.24) |
| 1973 | (27.07) | (13.2) | 15.67 | 25.7 | 48.66 | 82.77 | 98.47 | 142.35 | 189.42 | 135.04 | 75.52 | | (84.19) |
| 1974 | 18.01 | 11.82 | 12.56 | 42.74 | 42.72 | 102.94 | 180.27 | 190.16 | 233.18 | 214.07 | 123.35 | 45.13 | 102.54 |
| 1975 | 23.88 | (21.39) | (29.73) | 45.45 | 51.01 | 83.42 | 142.59 | 156.53 | 233.41 | 239.34 | 85.34 | 47.58 | (104.4) |
| 1976 | 24.32 | 24.75 | 35.05 | 52.69 | 58.47 | 81.39 | 187.89 | 227.34 | 238.23 | 221.12 | 129.88 | 48.97 | 110.48 |
| 1977 | 27.05 | (16.53) | (9.28) | 16.43 | 41.25 | 99.82 | 208.15 | 188.11 | 251.38 | 197.36 | 89 | 31.82 | (107.24) |
| 1978 | 18.48 | 12.37 | 20.1 | 47 | 44.08 | 123.15 | 177.52 | 207.9 | 237.87 | 206.31 | 94.06 | 38.4 | 102.69 |
| 1979 | 28.58 | 15.86 | 18.9 | 20.49 | 67.17 | 115.4 | 182.45 | 263.06 | 184.78 | 172.8 | (147.18) | | (120.47) |
| 1980 | | | | | | | | | | | | | |
| 1981 | 30.67 | 30.78 | 30.7 | 30.62 | 30.54 | 30.45 | 30.37 | 30.28 | 30.2 | 30.12 | 30.03 | 29.95 | 30.41 |
| 1982 | 29.07 | 29.78 | 29.7 | 29.62 | 29.54 | 29.45 | 29.37 | 29.28 | 29.2 | 29.12 | 29.03 | 28.95 | 29.41 |
| 1983 | 28.87 | 28.78 | 28.7 | 28.62 | 28.54 | 28.45 | 28.37 | 28.28 | 28.2 | 28.12 | 28.03 | 27.95 | 28.41 |
| 1984 | 27.87 | 27.78 | 27.7 | 27.62 | 27.53 | 27.45 | 27.37 | 27.28 | 27.2 | 27.12 | 27.03 | 26.95 | 27.41 |
| 1985 | 26.88 | 26.78 | 26.7 | 26.62 | 26.53 | 26.45 | 26.37 | 26.28 | 26.2 | 26.12 | 26.03 | 25.95 | 26.41 |
| 1986 | 25.88 | 25.78 | 25.7 | 25.62 | 25.53 | 25.45 | 25.37 | 25.28 | 25.2 | 25.12 | 25.03 | 24.95 | 25.41 |
| 1987 | 24.88 | 24.78 | 24.7 | 24.62 | 24.53 | 24.45 | 24.37 | 24.28 | 24.2 | 24.12 | 24.03 | 23.95 | 24.41 |
| 1988 | 23.88 | 23.78 | 23.7 | 23.62 | 23.53 | 23.45 | 23.37 | 23.28 | 23.2 | 23.11 | 23.03 | 22.95 | 23.41 |

**Figure 20: Example for original data provided for the Metchum River at Gouri. The data highlighted in the red box obviously is erroneous. Such data had to be removed in the data pre-processing.**

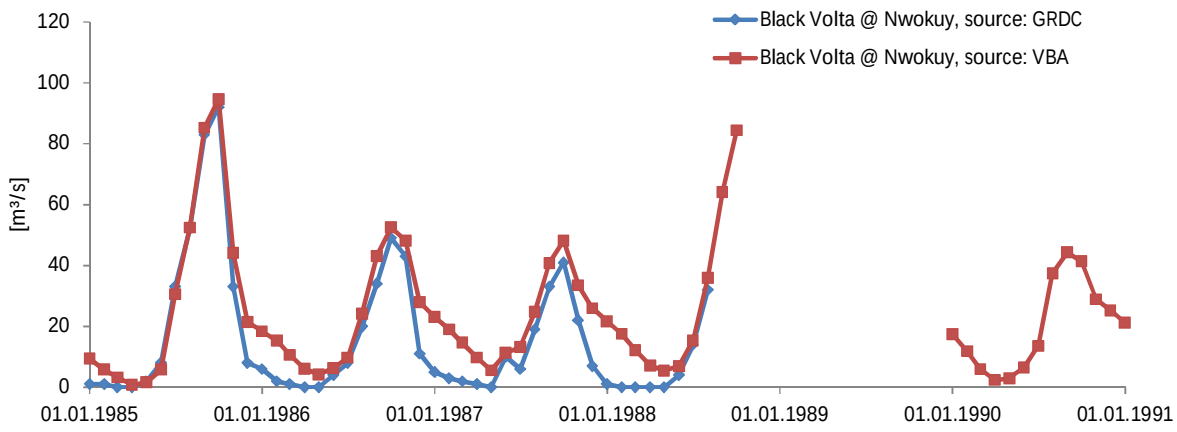


**Figure 21: Example for "observed" discharge data of the Black Volta River obtained from two different sources for the same gauge. Data of VBA during dry season are most likely biased (too high).**

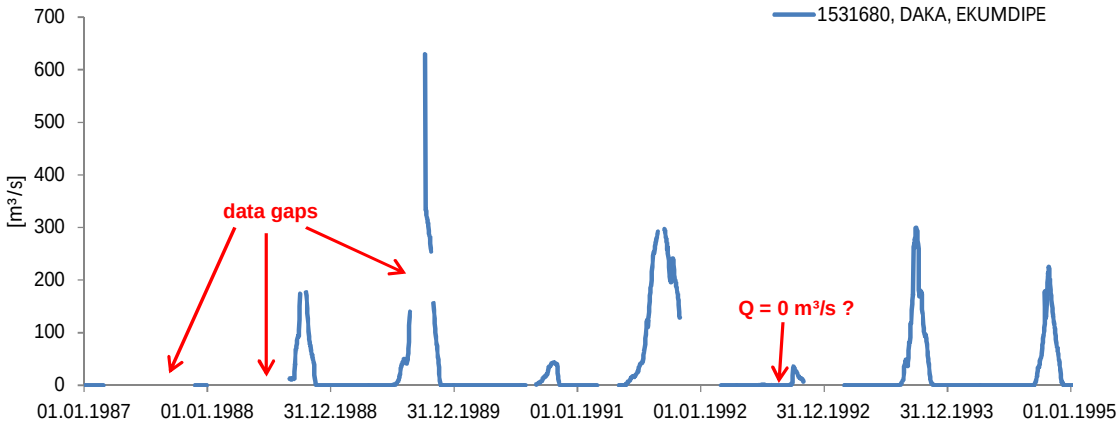


**Figure 22: Example for "observed" daily hydrograph of Daka River at Ekumdipe. Zero flow during rainy season 1992 is most likely erroneous. Therefore, such data were removed during data pre-processing.**

| RIVER | MAGOU | MONO | OUEME | ZOU | OUEME | OKPARA | ZOU | OUEME | OUEME | SO | MEKROU | ALIBORI | MEKROU |
|---|---|---|---|---|---|---|---|---|---|---|---|---|---|
| STATION | TIELE | ATHIEME | PONT DE I | ATCHERIG | PONT DE I | KABOUA | DOME | SAGON | BONOU | SO-AWA | KOMPONI | ROUTE KA | BAROU |
| COUNTRY | BJ | BJ | BJ | BJ | BJ | BJ | BJ | BJ | BJ | BJ | BJ | BJ | BJ |
| SOURCE | GRDC | GRDC | GRDC | GRDC | GRDC | GRDC | GRDC | GRDC | GRDC | GRDC | GRDC | GRDC | GRDC |
| 01.09.1966 | 15 | 587 | 139 | 43 | 363 | 90 | 48 | 477 | 582 | 97 | 61 | 164 | 105 |
| 01.10.1966 | 26 | 580 | 178 | 20 | 325 | 106 | 19 | 439 | 512 | 94 | 87 | 77 | 103 |
| 01.11.1966 | 1 | 350 | 23 | 5 | 64 | 30 | 9 | 161 | 153 | 55 | 20 | 5 | 30 |
| 01.12.1966 | 0 | 7 | 1 | 0 | 4 | 2 | 1 | 25 | 27 | 34 | 4 | 0 | 2 |
| 01.01.1967 | 0 | 2 | 0 | 0 | 0 | 0 | 0 | 4 | 5 | 29 | 0 | 0 | 0 |
| 01.02.1967 | 0 | 1 | 0 | 0 | 0 | 0 | 0 | 2 | 3 | 32 | 0 | 0 | 0 |
| 01.03.1967 | 0 | 2 | 0 | 0 | 0 | 0 | 4 | 1 | 4 | 35 | 0 | 0 | 0 |
| 01.04.1967 | 0 | 4 | 0 | 4 | 1 | 0 | 6 | 5 | 9 | 38 | 0 | 0 | 0 |
| 01.05.1967 | 0 | 7 | 0 | 2 | 0 | 0 | 3 | 5 | 7 | 37 | 0 | 2 | 0 |
| 01.06.1967 | 0 | 20 | 1 | 17 | 2 | 0 | 21 | 20 | 29 | 35 | 0 | 5 | 0 |
| 01.07.1967 | 0 | 100 | 44 | 13 | 72 | 0 | 21 | 85 | 80 | 30 | 1 | 19 | 5 |
| 01.08.1967 | 10 | 487 | 249 | 79 | 516 | 28 | 76 | 459 | 483 | 48 | 79 | 106 | 64 |
| 01.09.1967 | 30 | 659 | 348 | 67 | 767 | 123 | 68 | 796 | 846 | 128 | 162.07 | 302 | 219 |
| 01.10.1967 | 12 | 396 | 216 | 22 | 421 | 140 | 26 | 628 | 750 | 175 | 87 | 185 | 168 |
| 01.11.1967 | 0 | 300 | 21 | 2 | 46 | 24 | 3 | 124 | 142 | 61 | 20 | 3 | 24 |
| 01.12.1967 | 0 | 20 | 3 | 0 | 8 | 2 | 0 | 15 | 20 | 33 | 6 | 1 | 6 |
| 01.01.1968 | 0 | 10 | 1 | 0 | 1 | 0 | 0 | 5 | 6 | 33 | 1 | 0 | 1 |
| 01.02.1968 | 0 | 5 | 0 | 0 | 0 | 0 | 0 | 1 | 2 | 34 | 0 | 0 | 0 |
| 01.03.1968 | 0 | 1 | 0 | 0 | 0 | 0 | 0 | 1 | 2 | 39 | 0 | 0 | 0 |
| 01.04.1968 | 0 | 1 | 1 | 0 | 1 | 0 | 1 | 1 | 2 | 34 | 0 | 0 | 0 |
| 01.05.1968 | 0 | 4 | 3 | 3 | 5 | 0 | 4 | 10 | 13 | 39 | 0 | 3 | 1 |
| 01.06.1968 | 0 | 50 | 35 | 26 | 62 | 3 | 24 | 50 | 69 | 45 | 3 | 9 | 14 |
| 01.07.1968 | 8 | 601 | 198 | 252 | 303 | 30 | 122 | 355 | 540 | 55 | 54 | 89 | 27 |
| 01.08.1968 | 24 | 800 | 264 | 343 | 550 | 143 | 129 | 763 | 982 | 197 | 123 | 140 | 110 |
| 01.09.1968 | 25 | 756 | 384 | 345 | 907 | 359 | 120 | 928 | 1076 | 248 | 160.57 | 133 | 186 |
| 01.10.1966 | 19 | 500 | 180 | 150 | 429 | 187 | 114 | 800 | 948 | 216 | 91 | 64 | 113 |
| 01.11.1968 | 0 | 60 | 14 | 9 | 63 | 30 | 29 | 250 | 292 | 100 | 18 | 8 | 24 |
| 01.12.1968 | 0 | 10 | 3 | 0 | 6 | 3 | 3 | 30 | 40 | 42 | 2 | 1 | 7 |
| 01.01.1969 | 0 | 1 | 0 | 0 | 0 | 0 | 2 | 10 | 12 | 37 | 0 | 0 | 2 |
| 01.02.1969 | 0 | 1 | 0 | 0 | 0 | 0 | 1 | 4 | 6 | 38 | 0 | 0 | 0 |
| 01.03.1969 | 0 | 1 | 0 | 0 | 0 | 0 | 1 | 3 | 5 | 46 | 0 | 0 | 0 |
| 01.04.1969 | 0 | 7 | 0 | 2 | 0 | 0 | 2 | 5 | 7 | 41 | 0.01 | 0 | 0 |

**Figure 23: Example for gap-filling (yellow shaded cells) of monthly discharge data.**

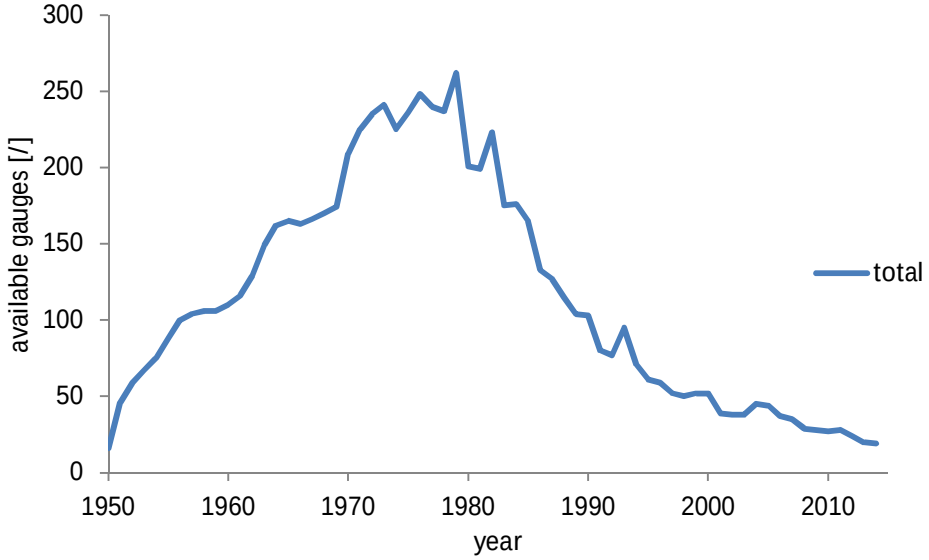


**Figure 24: Annual availability of observed discharge data after pre-processing.**

### 5.3.2 Definition of reference period

A definition of a reference period is required for the computation of the hydropower potential. The data availability described in the chapters 5.2 and 5.3.1 is summarized in Figure 25. To define a reference period the following considerations were made:

- General considerations:
  - Historically there have been considerable variations in annual flow between individual years and decades.
  - The reference period should be long enough to smooth out variability of individual years.
  - The reference period should be well accepted by stakeholders.
  - There should be good data availability in the reference period.
- Period 1961-1990:
  - Good availability of observed discharge data.
  - High number of stations available for GPCC precipitation data.
  - Includes prolonged drought of the 1980s.
  - 1990 was more than 25 years ago. Acceptance by stakeholders?
- Period 1998-2014:
  - Poor data availability for observed discharge data.

- GPCC precipitation data not reliable (few number of stations) or available after 2010.
- Satellite precipitation data are available.
- Since 1998 relatively stable meteorological conditions (moderately wet compared to last 100 years).

Based on these considerations the following decisions were made:

- Period 1961-1990: Calibration of parameters of the water balance model.
- Period 1998-2014: Adopted as reference period for final results.

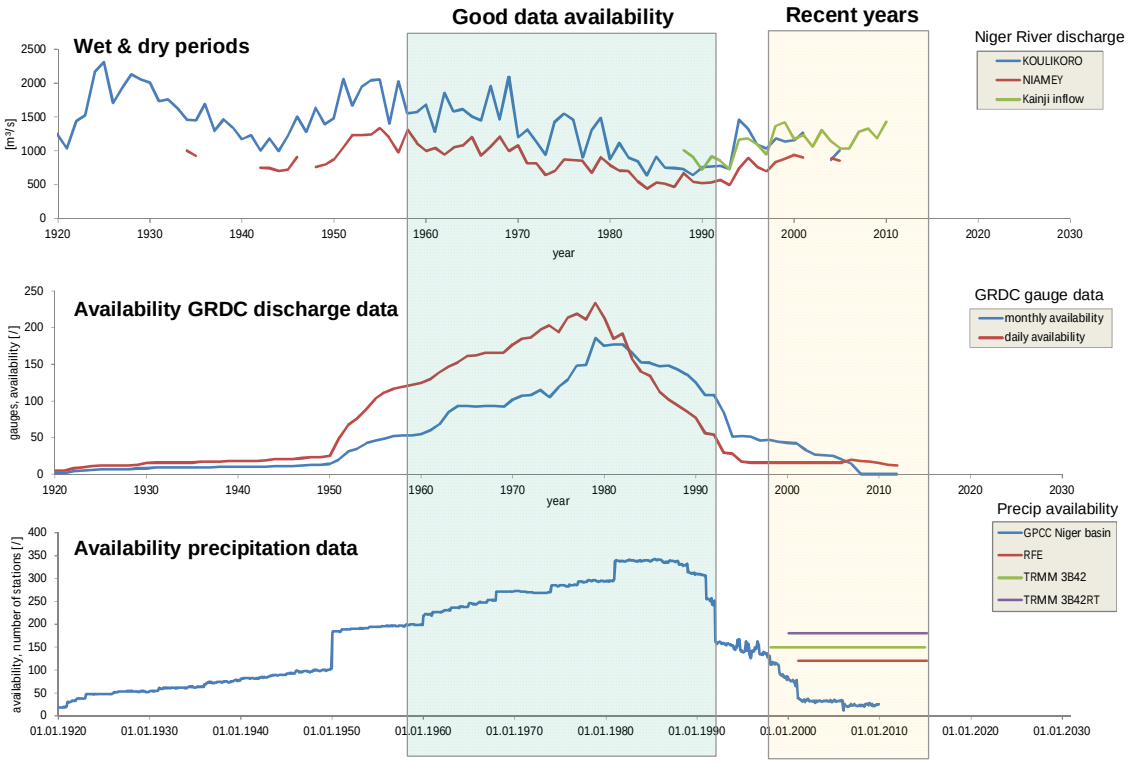


**Figure 25: Summary of data availability to define a reference period for the hydropower potential assessment.**

### 5.3.3 Delineation of river network

Initial tests with the original river network (~100,000 river reaches) available from Hydrosheds showed that the river network does not include small streams in humid regions (e.g. Guinea, south-eastern part of Nigeria, etc.). However, such small streams might be attractive for pico/micro/mini hydropower plants. Hence, the original Hydrosheds river network is too coarse. Therefore, a new, finer river network was created.

The following method was used to create the river network for West Africa:

- Start with 15s Hydrosheds flow direction grid.
- Compute flow accumulation grid.
- Use a threshold of 2 km² upstream catchment area to convert flow accumulation (GIS grid layer) into river network (GIS line layer). This results in more than 1 Mio river reaches for West Africa.
- Use basic water balance model (uncalibrated model parameters) to compute a rough estimate of mean annual discharge for all river reaches.
- Eliminate reaches with zero discharge (three decimal places). This mainly applies to arid regions.
- Merge adjacent reaches with no lateral tributaries (pseudo nodes due to previous step).
- Final river network includes about 500,000 river reaches for West Africa.

Thus, the final river network includes about five times as many reaches as the original river network of Hydrosheds. A regional comparison with the original river network of Hydrosheds shows that in arid regions the new river network includes a significantly smaller number of river reaches, whereas in humid regions the new river network includes a significantly higher number of reaches.

River names were assigned to reaches by use of the following data sources:

- Information from gauges (GRDC, etc.)
- SIEREM GIS line layer
- Michelin map (online)
- Google map (online)
- OpenStreetMap (online)
- Bing map (online)
- Travelmag map (hardcopy)

In the river network a reach is defined as the river section between a confluence of a tributary and the next downstream tributary. Two GIS point shape files were created representing the start- and end-points of river reaches. Reach start-points were delineated by identifying the 15s cell points where two reaches join. Reach end-points were delineated by identifying the last 15s cell point before the confluence with the next downstream reach. (The cell points directly at the confluence with the next downstream reach cannot be used as this would also include inflow from the other tributary.) For very short reaches (that flow only from one cell to the next downstream cell) the reach

start-point and end-point are identical. The start- and end-points can be used in various GIS analyses to query grid values for reaches.

The upstream catchment area for each reach was computed with the following method:

- Analyze the area covered by the 15s grid cells over the study domain. In the southern part of the study domain the grid cells have a size of 0.213 km², whereas in the northern part the cell size is 0.200 km². Thus, the grid cells in the south are by 6.5% larger than in the north.
- Produce a grid that shows the regional variation of the 15s grid cell area.
- Accumulate the grid area with the flow direction grid to compute a grid showing upstream catchment area.
- Query the value of the "upstream catchment area" grid with the reach end-points to assign upstream catchment areas to each reach of the river network. Here, it is crucial that reach end-points are defined as the last 15s cell before a confluence with a tributary (see explanation above).

The topology between reaches was determined with GIS analysis of nodes. The topology defines the upstream/downstream relationship of reaches. Therefore, each reach contains the following information:

- ARCID: ID number of reach
- TOARCID: ID number of next downstream reach
- FROMARCID: ID number of dominant upstream reach (largest inflow)

The last attribute above required to compute mean annual discharge for each reach (see section further below). Most reaches have two upstream reaches. Several hundred reaches have three upstream reaches. And there are individual cases of up to five upstream reaches. The ARCID number of the reach with the largest discharge is stored in the attribute FROMARCID. For headwater reaches FROMARCID is set to zero. Similarly, for reaches discharging into the ocean (or local sinks) TOARCID is set to zero.

The topology described above enables to create longitudinal river profiles by data-base queries. The longitudinal river profiles show the channel elevation along the river course. Different methods were tested using various digital elevation models. The final method uses the Hydrosheds unconditioned DEM and consists of two steps:

- Step 1: Assign initial elevation at end of reach with neighborhood statistics
    - Use reach end-points for geo-processing
    - Analyze 3s elevation data in 15s box around end-point node (25 values)
    - Assign 10% percentile of 3s elevation distribution around the end-point node

- Step 2: Ensure continuous downward slope along river network
    - Carve through barriers in downstream direction
    - Fill sinks in upstream direction
    - Compute average elevation from above two steps
    - Use smoothing algorithm to remove artificial elevation drops (e.g. at flat rivers 1m drops due to integer data are averaged out with smoothing algorithm, resulting in a continuous, gentle slope). The smoothing algorithm prioritizes the smoothing of elevation along main rivers. This means that main rivers are smoothed first, and tributaries of decreasing size are smoothed in subsequent steps in a tree-like manner.
    - Keep fixed water level elevation at major existing reservoirs

In the method outlined above, step 1 was tested with three different elevation models and different percentiles for the neighborhood analysis. Figure 26 shows an example longitudinal profile after testing different DEMs for step 1. In this example the minimum elevation (0% percentile) is used in the neighborhood analysis. Figure 26 shows that the most plausible elevation data is obtained from Hydrosheds unconditioned DEM. The conditioned DEM of Hydrosheds ensures continuous downstream slopes, but this DEM results in too low elevation due to stream-burning (see Figure 27), whereas the ASTER DEM includes problematic spikes in the elevation data. A more detailed analysis of ASTER DEM stacking data revealed that in large areas over West Africa (e.g. parts of Liberia, Côte d'Ivoire and Nigeria) clouds appear to decrease the quality of the ASTER elevation data (due to low stacking number of satellite observations). Even though Hydrosheds unconditioned DEM yields the most plausible results in Figure 26, it is also clear that step 2 is required to ensure continuous downward slope along the river network.

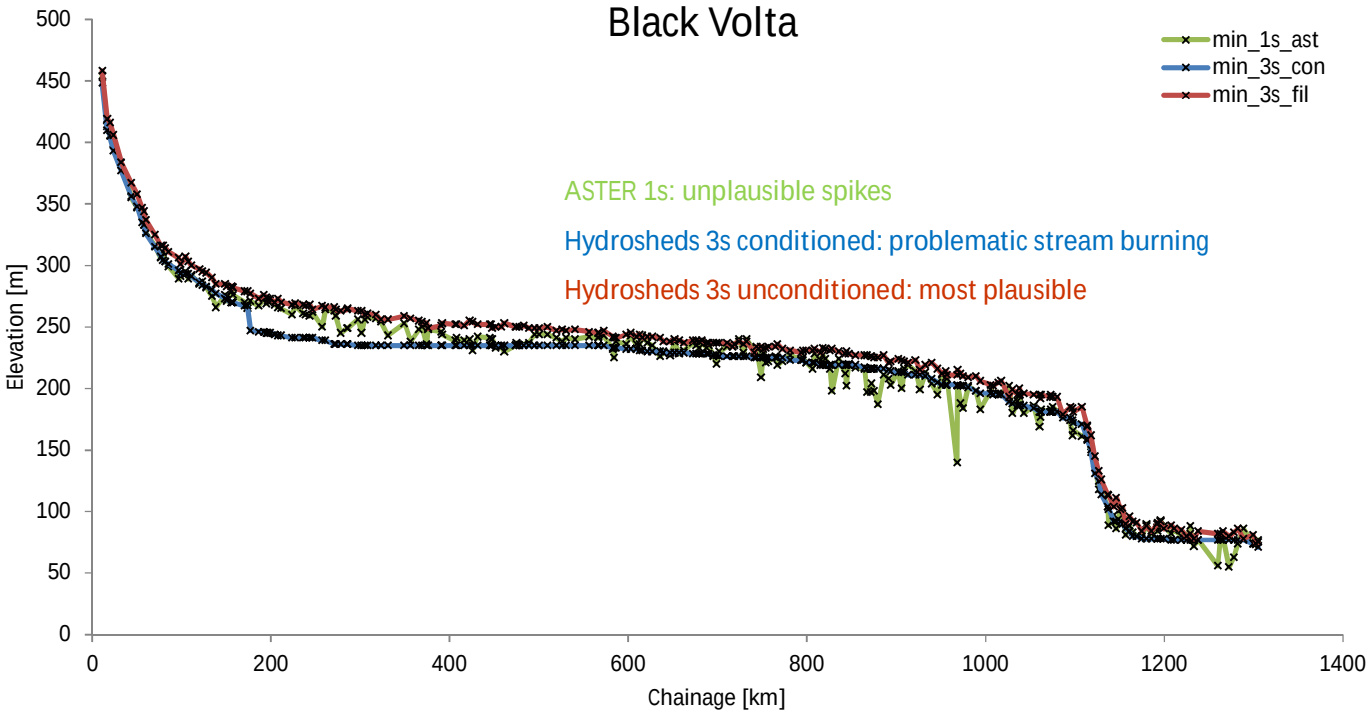


**Figure 26: Comparison of longitudinal river profiles with raw data of three different DEMs for the Black Volta. Result before application of step 2 (smoothing; see text for detailed explanation).**

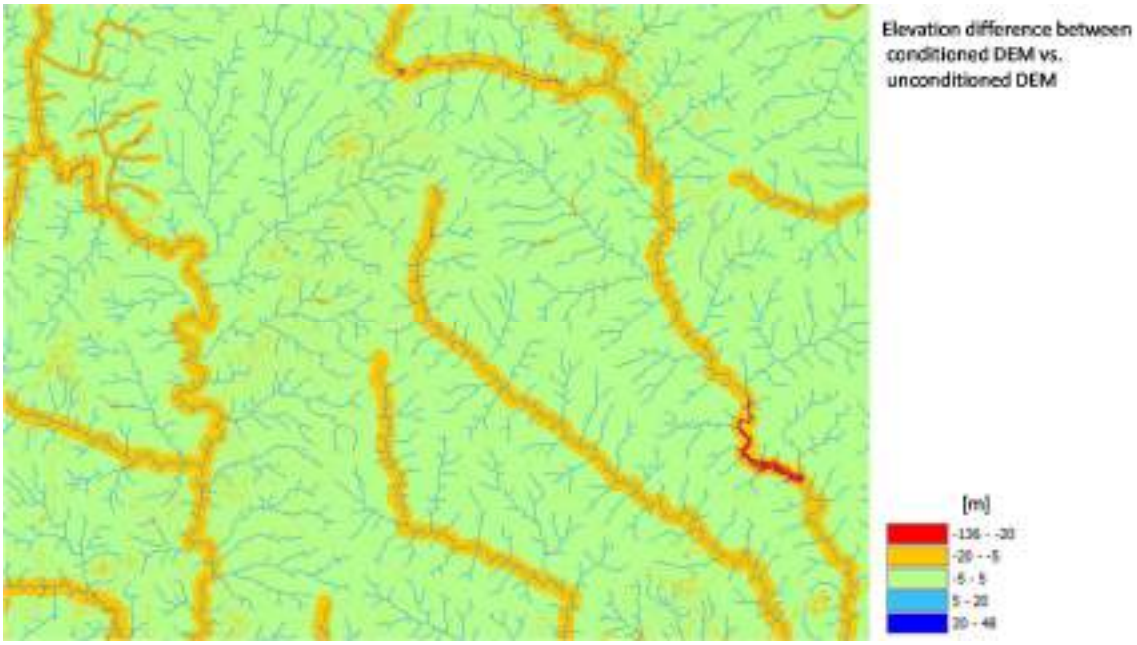


**Figure 27: Comparison of elevation data from Hydrosheds conditioned and unconditioned 3s DEMs. Example for region in Burkina Faso. Yellow areas indicate stream burning by 5 to 20 m. Red area shows extensive stream burning (more than 20 m) at an existing reservoir (Bagre reservoir).**

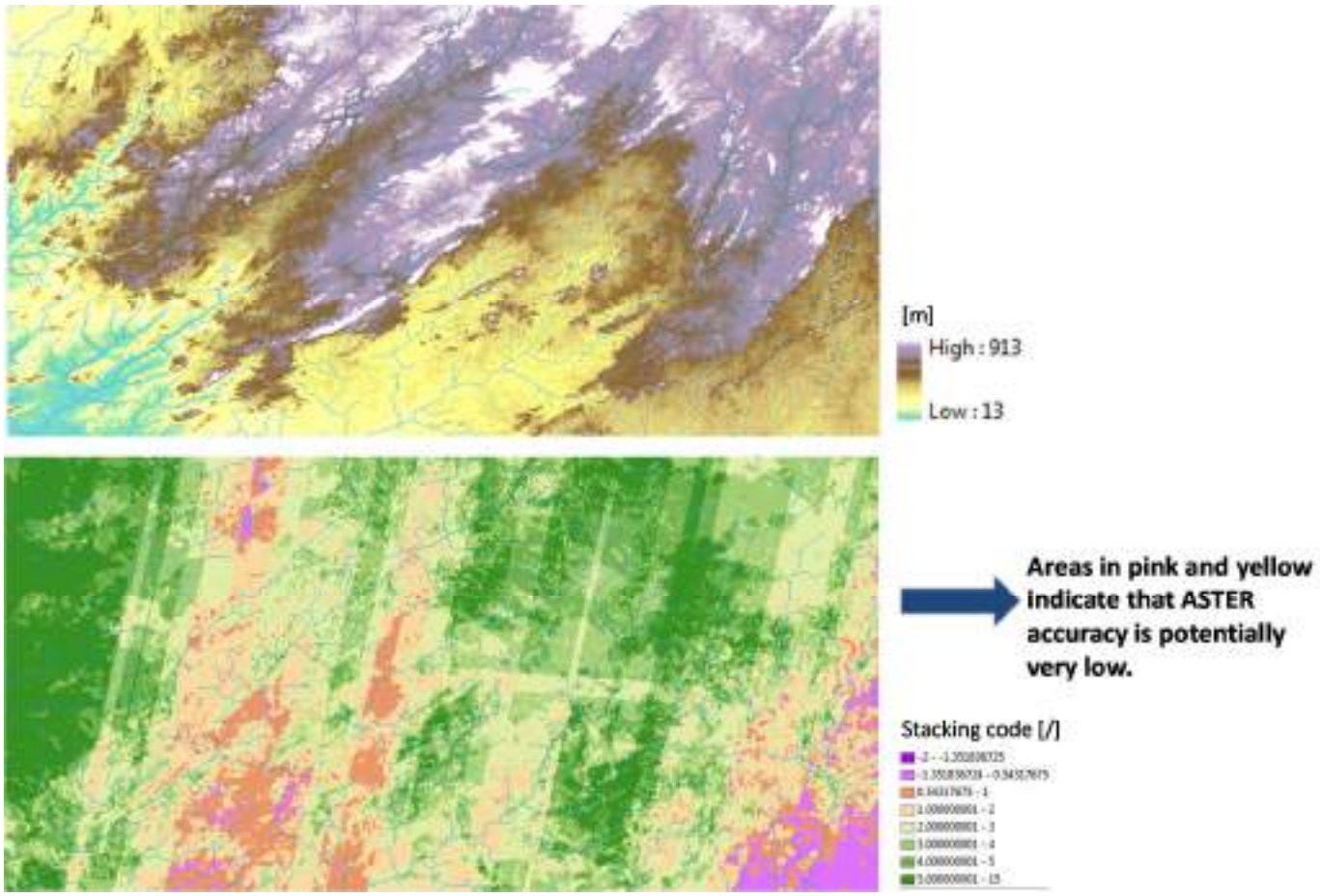


**Figure 28: Analysis of stacking number of ASTER DEM. Example for an area in northern Liberia. Top: Elevation. Bottom: Stacking number (counting number of ASTER satellite observations). Green areas indicate sufficient number of stacking for ASTER data assimilation scheme, whereas pink and yellow colors indicate insufficient stacking number with potentially low accuracy of ASTER elevation data.**

### 5.3.4 Delineation of sub-areas

Sub-areas were defined as sub-catchments of river basins. The following method was used:

- Topology of the river-network was analyzed to define sub-catchment outlets were the sub-catchment area exceeds 3000 km². This method was applied from upstream to downstream reaches.

- In coastal regions, where thousands of small streams discharge directly to the ocean, the threshold for delineating sub-catchments was reduced from 3000 to 1000 km².

- Manual adjustments of sub-catchments were made at existing major reservoirs to ensure that the whole reservoir lake is included solely in one sub-catchment.

The method outlined above resulted in 1060 sub-catchments. An example is shown in Figure 29.

**Figure 29: Example for sub-catchments delineated in Sierra Leone.**

### 5.3.5 Mean annual discharge

A simple annual water balance model based on the Budyko method (Budyko 1974, Figure 30) is applied to estimate annual runoff in West Africa. Different formulations of the Budyko method have been proposed (see e.g. Milly and Dunne 2002, Zhang et al. 2011, Gerrits et al. 2009) and we use the equation proposed by Choudhury (1999).

**Budyko annual water balance relationship:**

$$\frac{ETA}{P} = \left[1 + \left(\frac{ETP}{P}\right)^{-c}\right]^{-1/c}$$

ETA: annual actual evapotranspiration [mm]
ETP: annual potential evapotranspiration [mm]
P: annual precipitation [mm]
c: model parameter

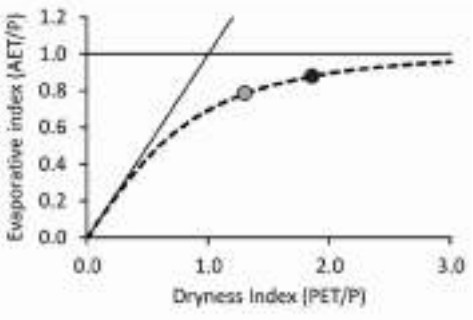


**Figure 30: Annual water balance model using the Budyko method.**

The inputs to the water balance model are annual values of precipitation and potential evapotranspiration. A model parameter c is used to control the model sensitivity. The output of the Budyko method is the ratio of annual precipitation that is lost via actual evapotranspiration. From this value annual runoff is computed by applying the basic water balance equation (Runoff = Precipitation – Actual Evapotranspiration). Here, it is assumed that storage change is negligible for the mean annual time-scale.

The model outlined above is applied to compute the local runoff for each reach of the river network (500,000 river reaches). Discharge is computed by aggregating runoff along the river network.

At some rivers there are major losses due to floodplain evaporation (Inner Niger Delta, Sokoto floodplain, Yobe floodplains) and diversion of water for irrigation schemes (e.g. Markala barrage, Mali). This has to be considered in the model, otherwise discharge is over-estimated for these rivers. Therefore, in the water balance model 32 major losses are considered for rivers in West Africa (Figure 31).

The Budyko method was originally developed to estimate long-term mean annual water balance. The result of the Budyko model can be controlled by the model parameter c. The objective is a regional estimation of this model parameter by comparison with observed discharge data at 410 gauges. As each gauge covers a different observational period the water balance model was applied for each individual year between 1950 and 2010 with GPCC precipitation data. The resulting simulated discharge time-series was compared to observed discharge in those years where observed data were available. This allowed to compute bias statistics and visual checks of simulated vs. observed annual discharge to guide the manual calibration of the model parameter. The regional distribution of the final model parameter is displayed in Figure 32. The parameter values implicitly account for the catchment response, which is influenced by soils, geology, vegetation, topography (slope) and climate.

During calibration it was found that CRU potential evapotranspiration data are too low in Côte d'Ivoire and coastal regions. This was confirmed by comparison with other data products (Climwat, H2O). Therefore, the potential evapotranspiration data of CRU were adjusted by correction factors shown in Figure 33.

The calibrated water balance model is able to reproduce the available observations with reasonable accuracy. Figure 34 shows a comparison of long-term mean annual discharge at 410 gauges (each gauge covers a different observation period).

Also annual discharge in individual years is simulated with reasonable accuracy, with plots shown for all main rivers in West Africa in Figure 35 to Figure 47. In the plots the horizontal lines give the long-term mean annual discharge, blue colour indicating observed value, red colour indicating simulated value (average computed for exactly the same years where observations are available), and green colour showing the average computed with TRMM precipitation data for the reference period 1998-2014. For all gauges the simulated discharge corresponds well with the observed discharge. Deviations in individual years should not be overrated, as only the average of the period 1998-2014 is used in the final results.

The comparison of simulated and observed annual discharge allows the following conclusions:

- The sensitivity of discharge to changes in precipitation is captured well by the model. This is an important pre-condition for the subsequent climate change analysis (with projected future changes in precipitation).

- The carry-over effect of soil moisture states is not strong enough to strongly impact the water balance from year to year. Therefore, the Budyko method also yields plausible results in individual years.

- Individual tests analysing the non-linearity in the Budyko annual water balance showed that the explicit consideration of spatial variability in precipitation is important to simulate discharge in larger river basins (spatial lumping of precipitation would yield biased results), whereas the explicit consideration of temporal variability in precipitation can be neglected (the results are almost identical with temporal lumping).

The last point above enabled to apply the water balance model calibrated on individual years with long-term mean annual precipitation data of TRMM for the reference period 1998-2014.

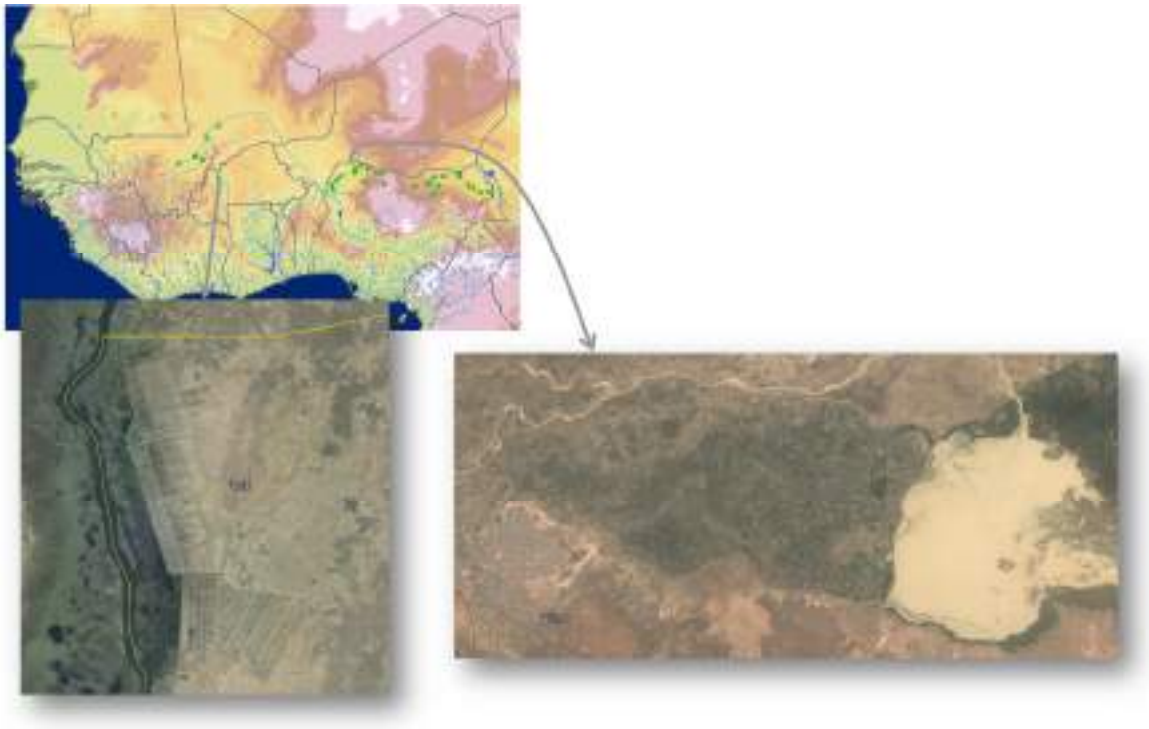

**Figure 31: Consideration of losses (floodplains, irrigation diversions) at West African rivers. Top: Green dots show 32 points where losses are considered in the model. Bottom left: Irrigation scheme near Oue at the Black Volta (Burkina Faso). Bottom right: Irrigation scheme near Wurno (Nigeria).**

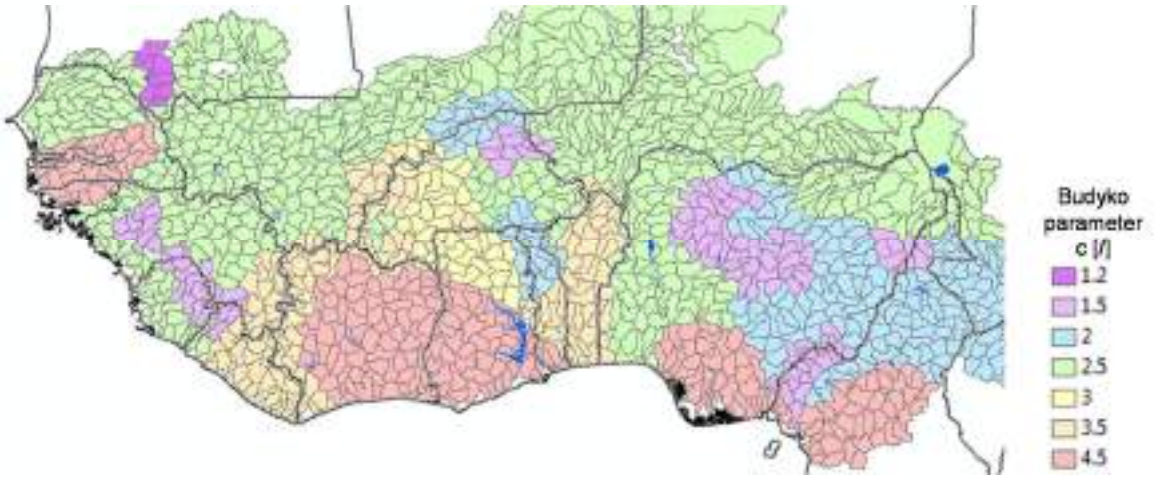


**Figure 32: Regional calibration result of the Budyko model parameter.**

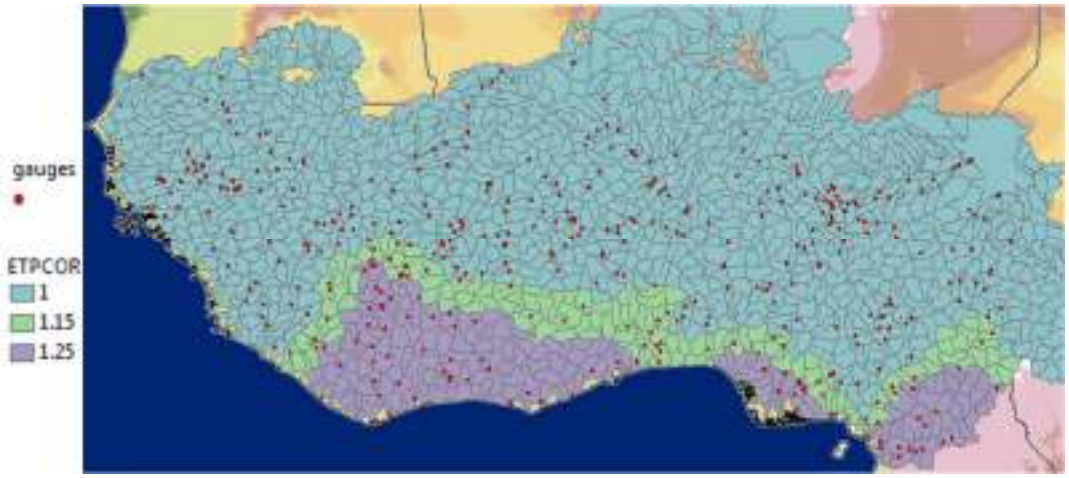


**Figure 33: Regional distribution of the factor to correct potential evapotranspiration data of CRU.**

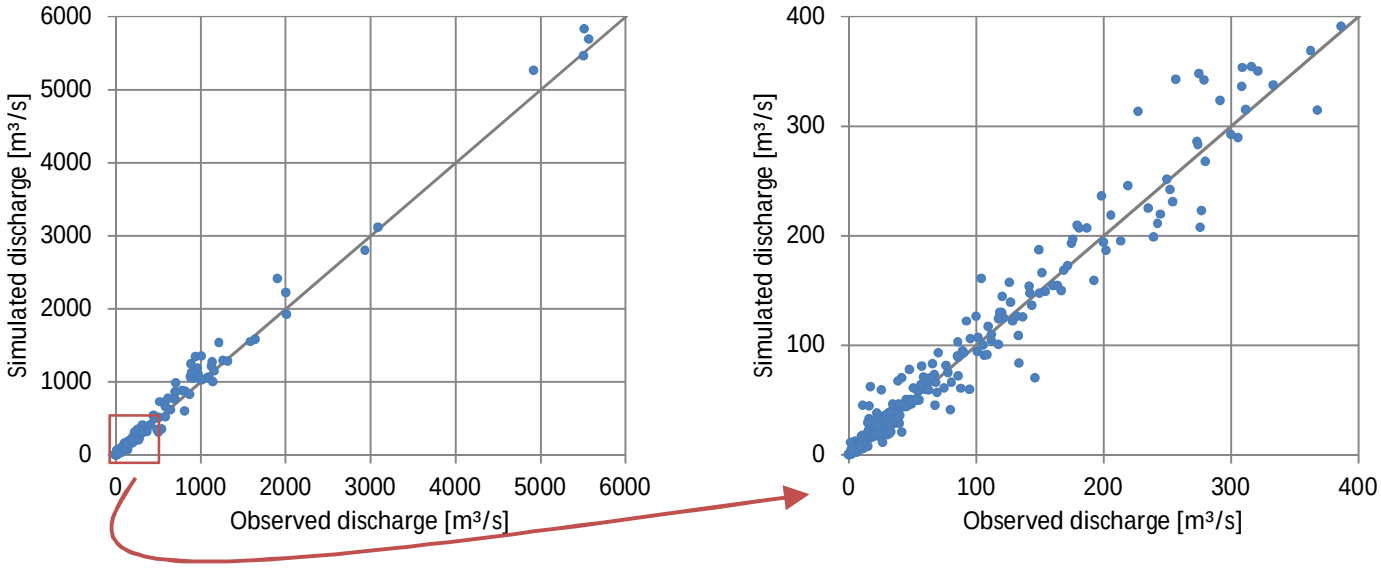


**Figure 34: Comparison of simulated and observed long-term mean annual discharge data for 410 gauges. Left: All gauges. Right: Zoom-in on gauges for medium and small rivers.**

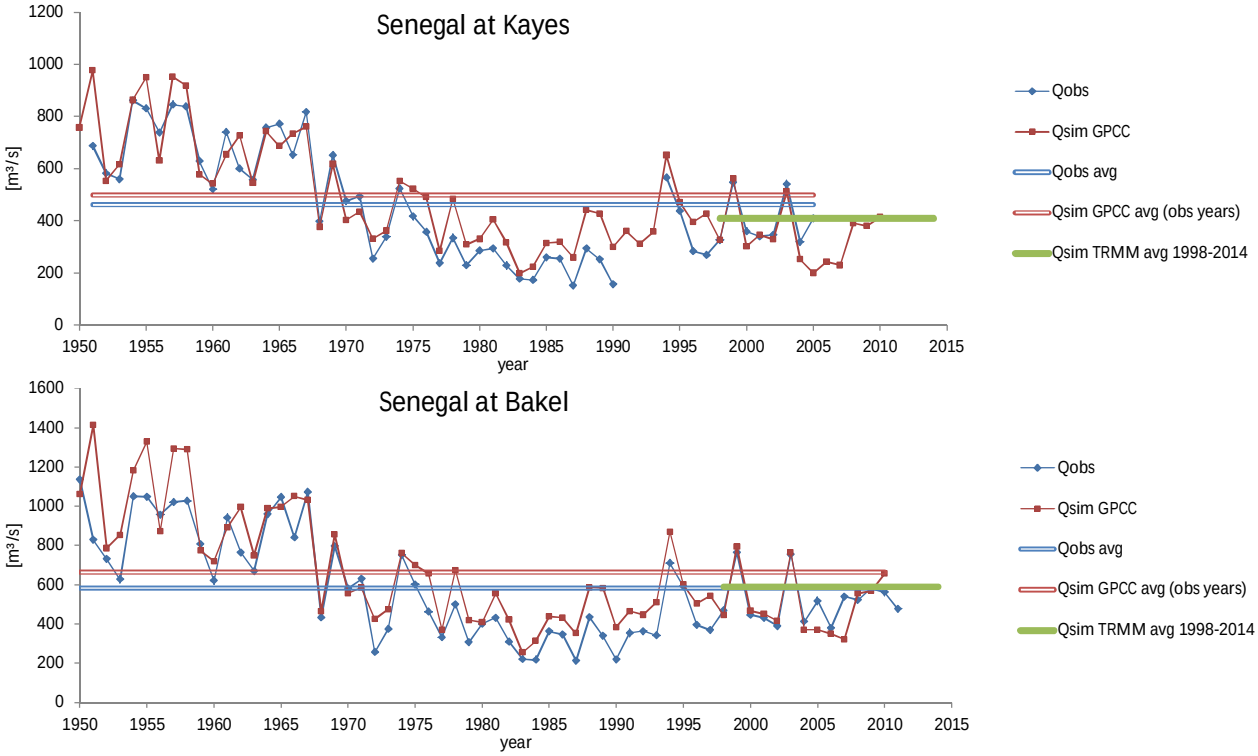


**Figure 35: Simulated and observed annual discharge at the Senegal River.**

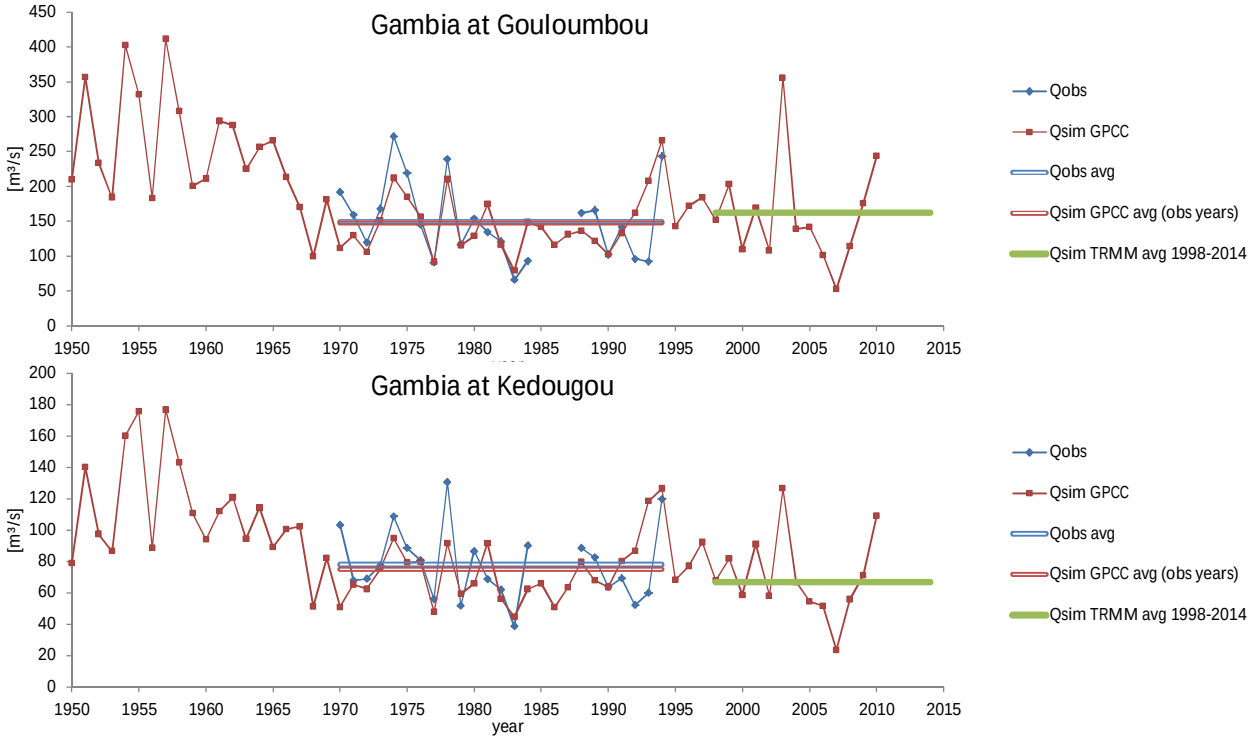


**Figure 36: Simulated and observed annual discharge at the Gambia River.**

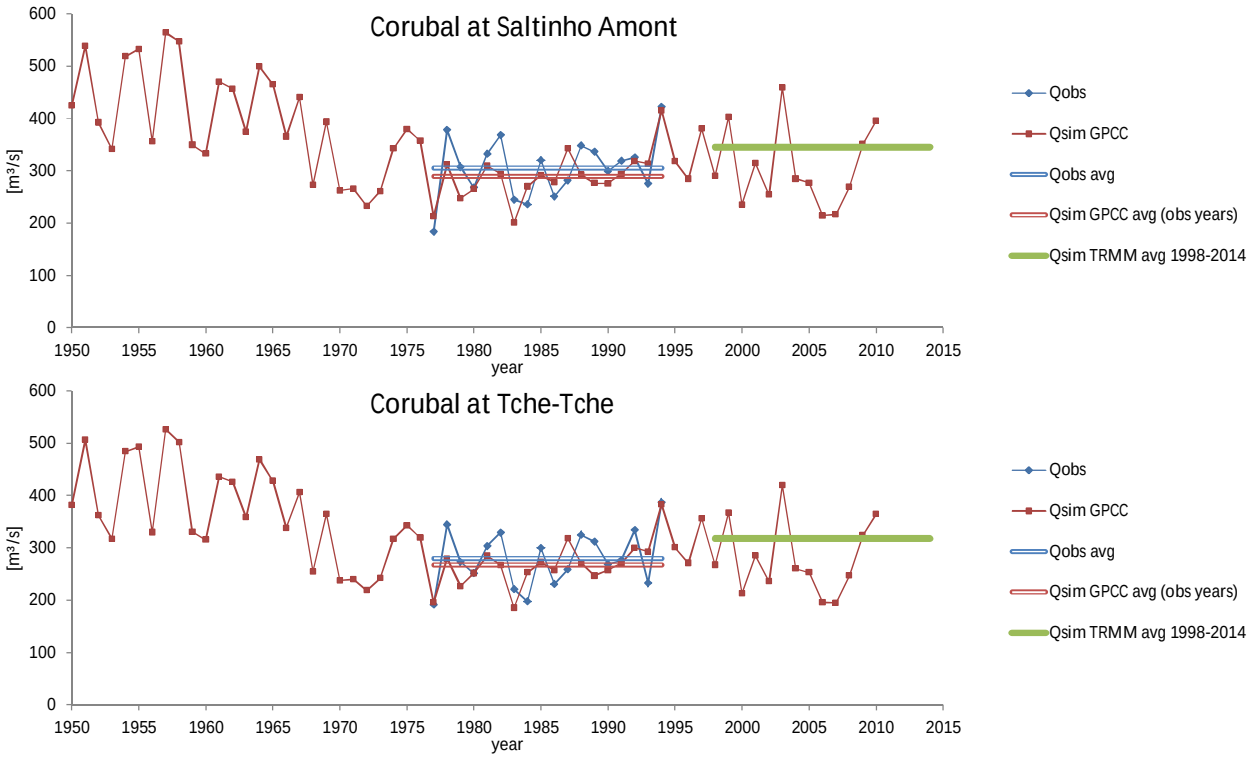


**Figure 37: Simulated and observed annual discharge at the Corubal River.**

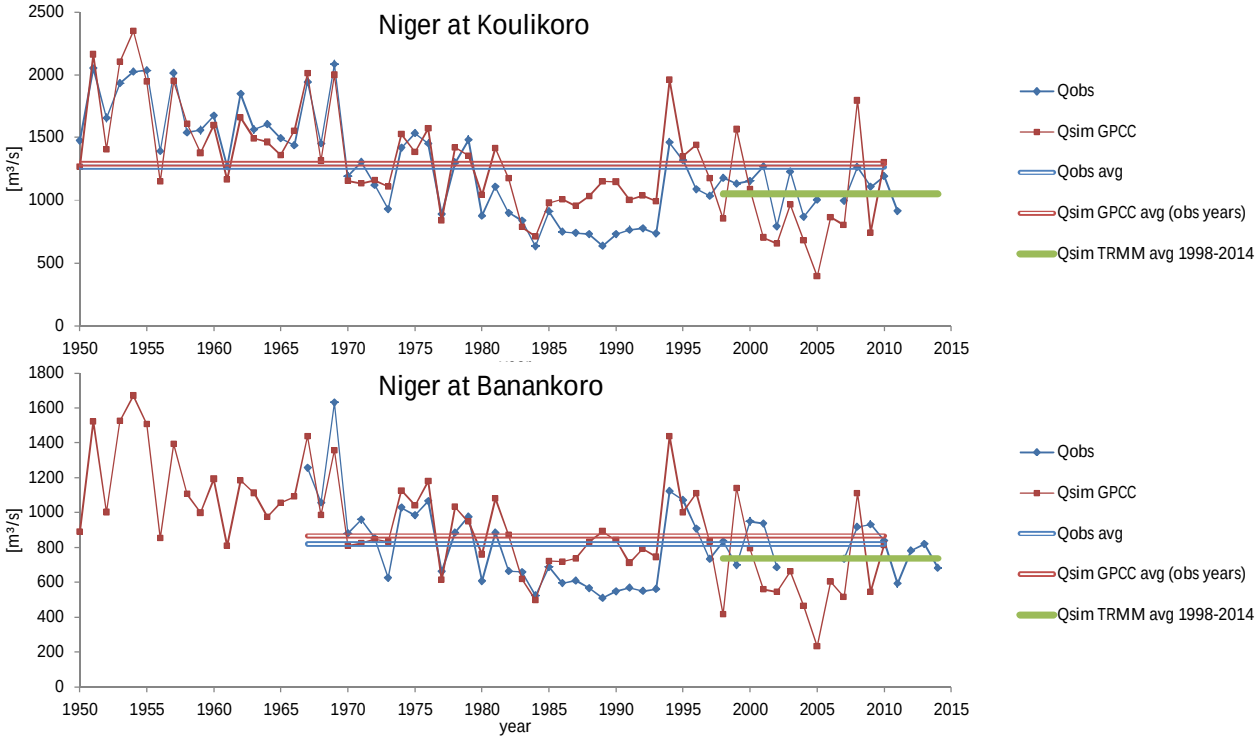


**Figure 38: Simulated and observed annual discharge at the Niger River.**

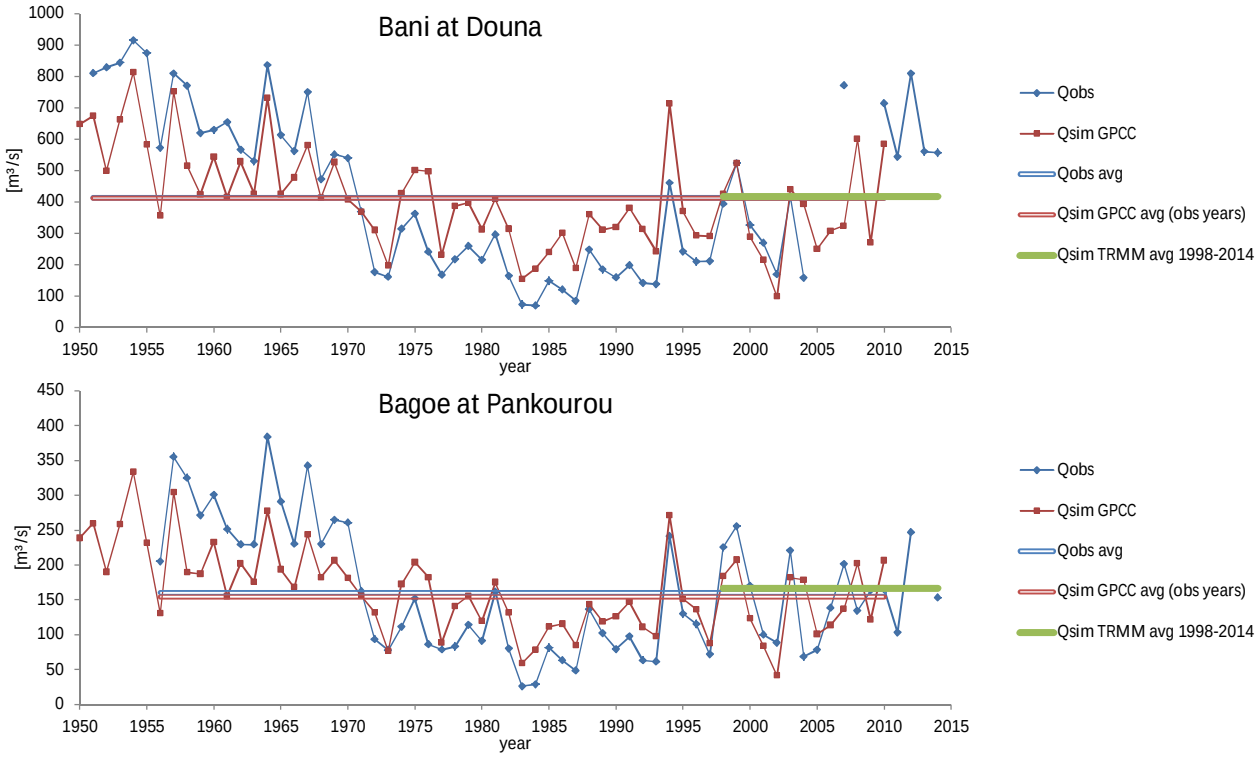


**Figure 39: Simulated and observed annual discharge at the Bani and Bagoe rivers.**

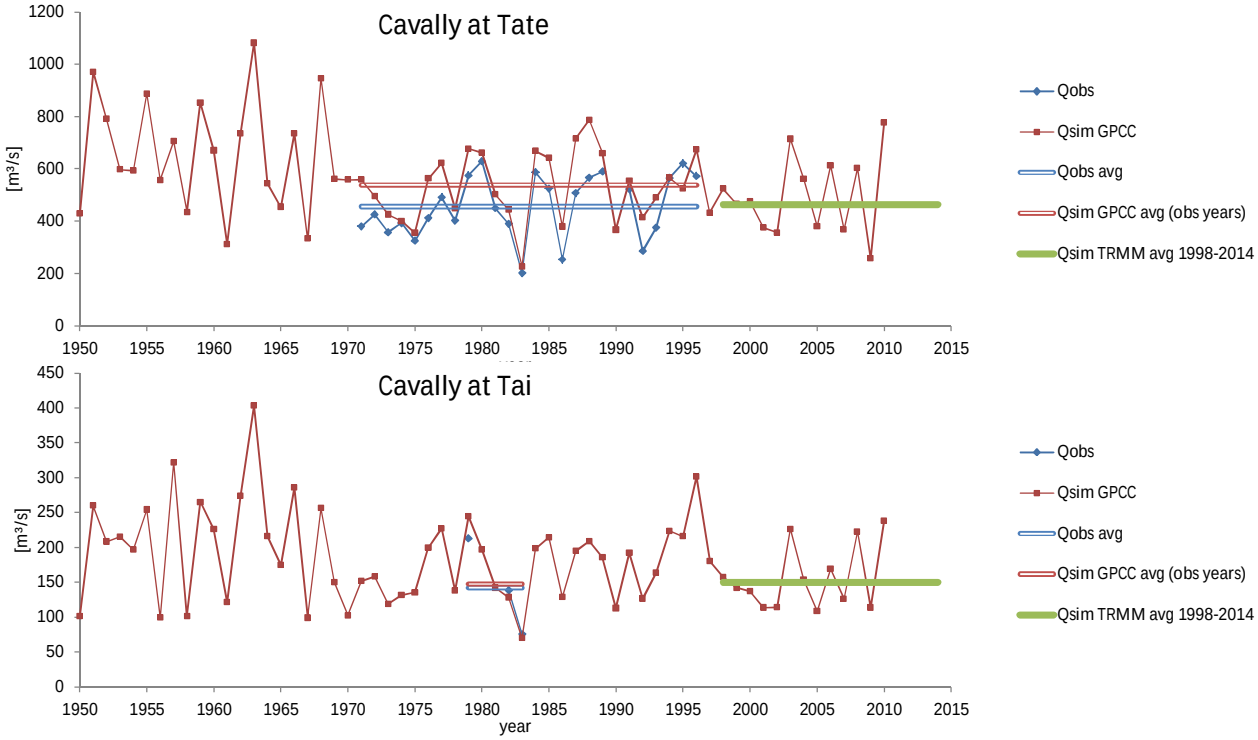


**Figure 40: Simulated and observed annual discharge at the Cavally River.**

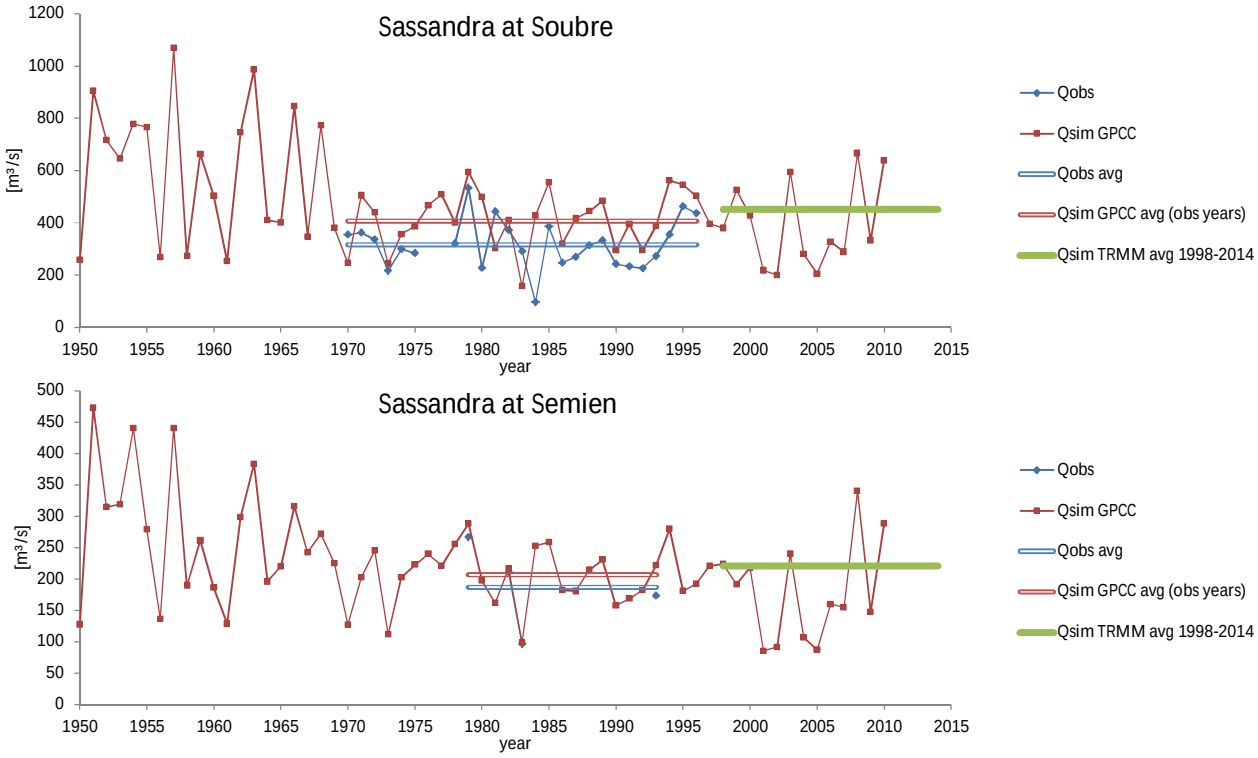


**Figure 41: Simulated and observed annual discharge at the Sassandra River.**

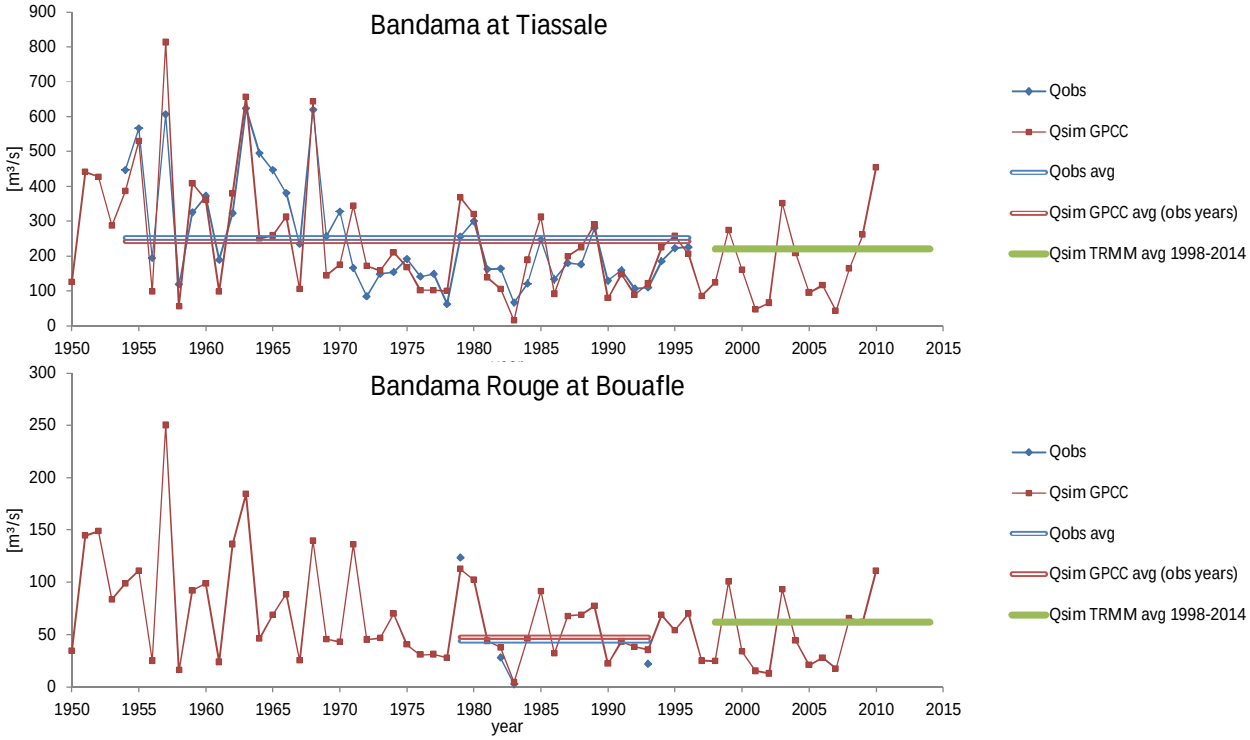


**Figure 42: Simulated and observed annual discharge at the Bandama River.**

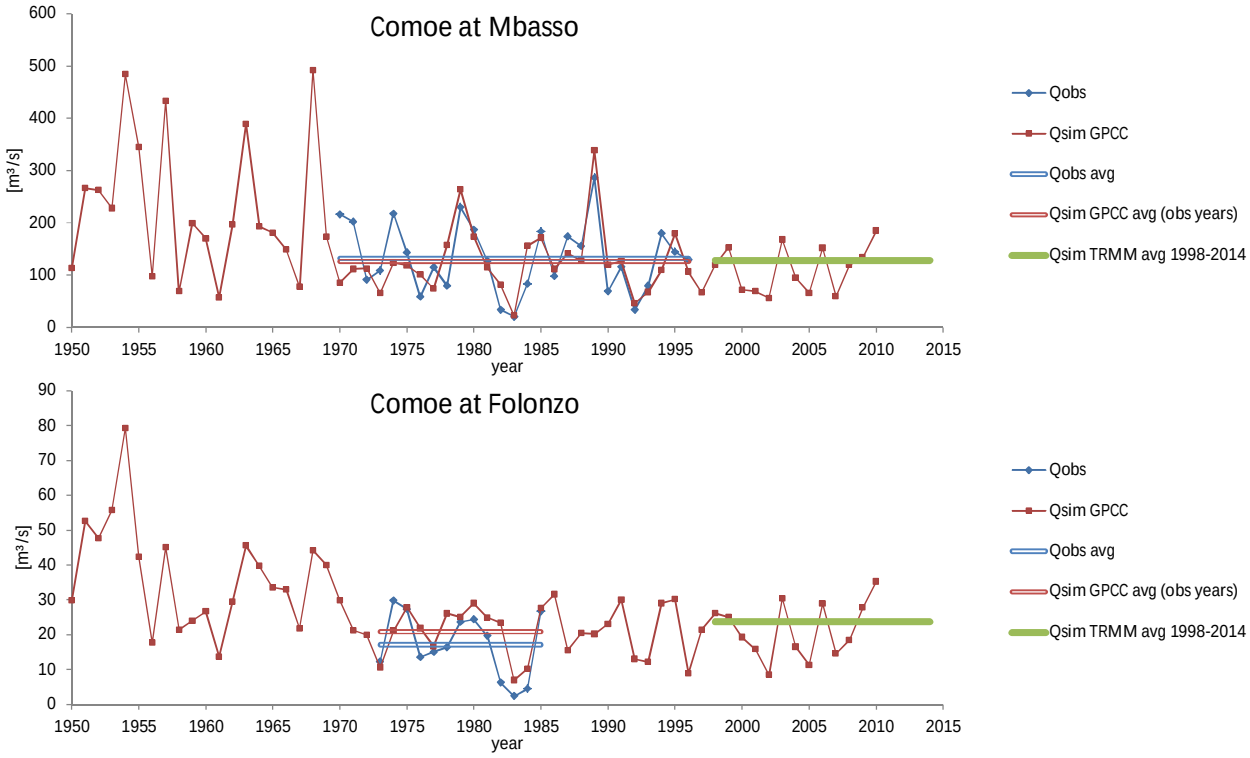


**Figure 43: Simulated and observed annual discharge at the Comoe River.**

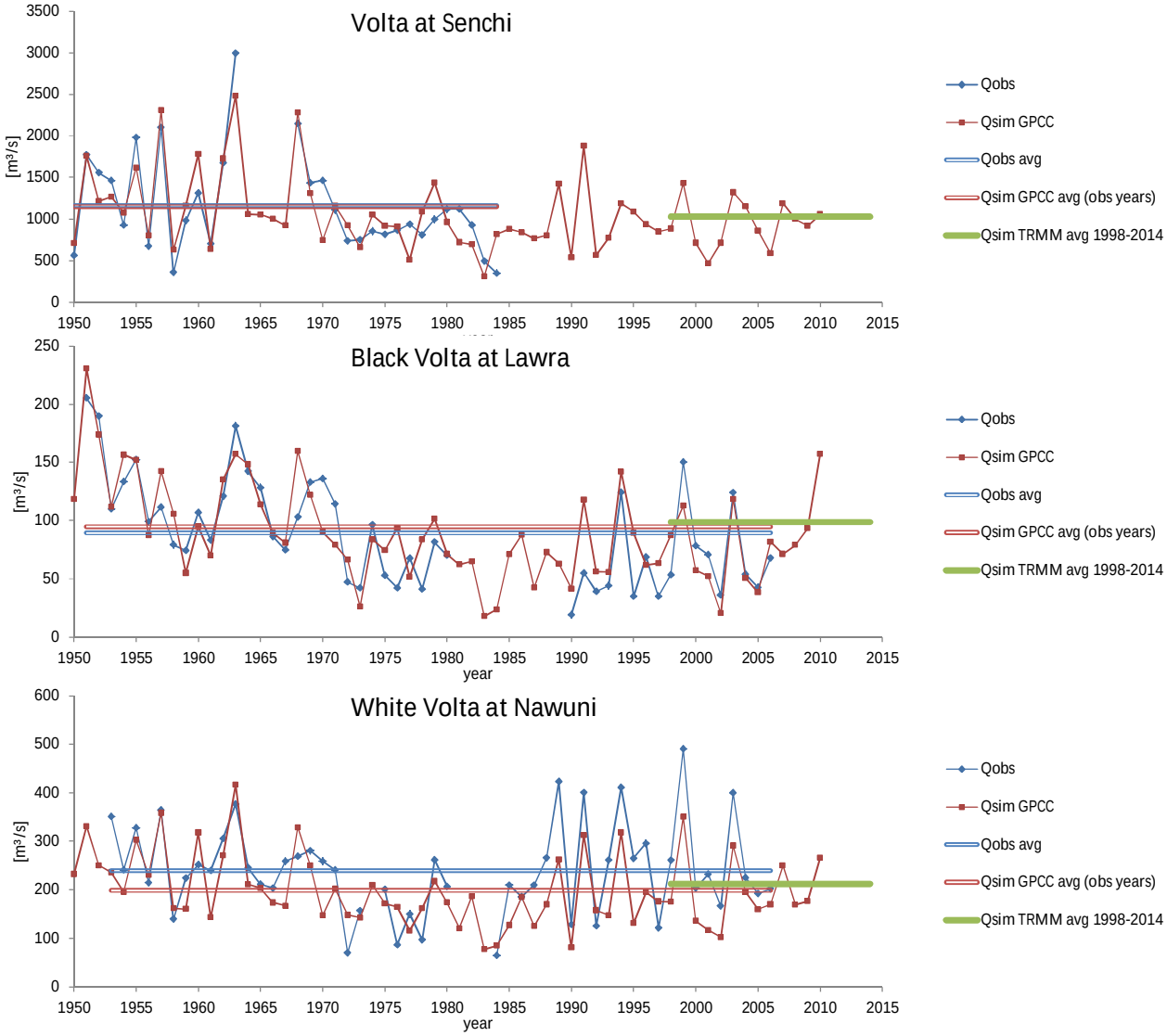


**Figure 44: Simulated and observed annual discharge at the Volta River and its main tributaries.**

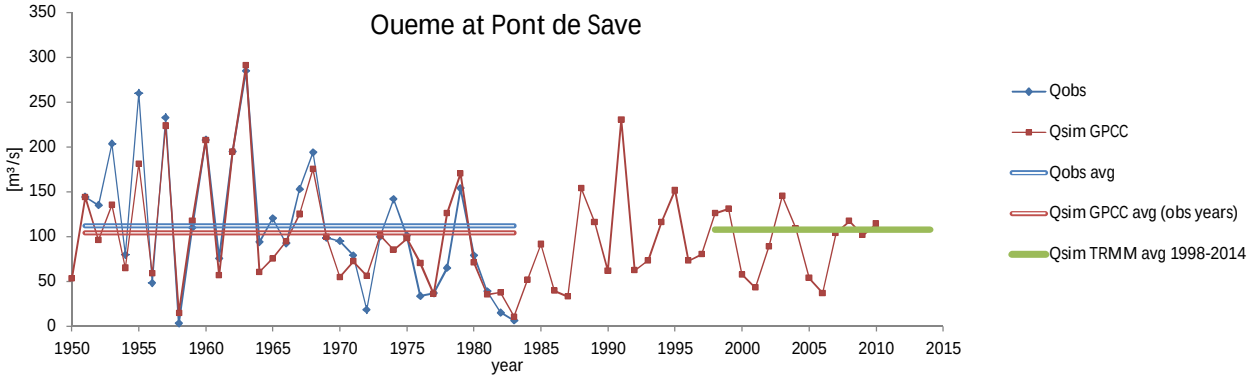


**Figure 45: Simulated and observed annual discharge at the Oueme River.**

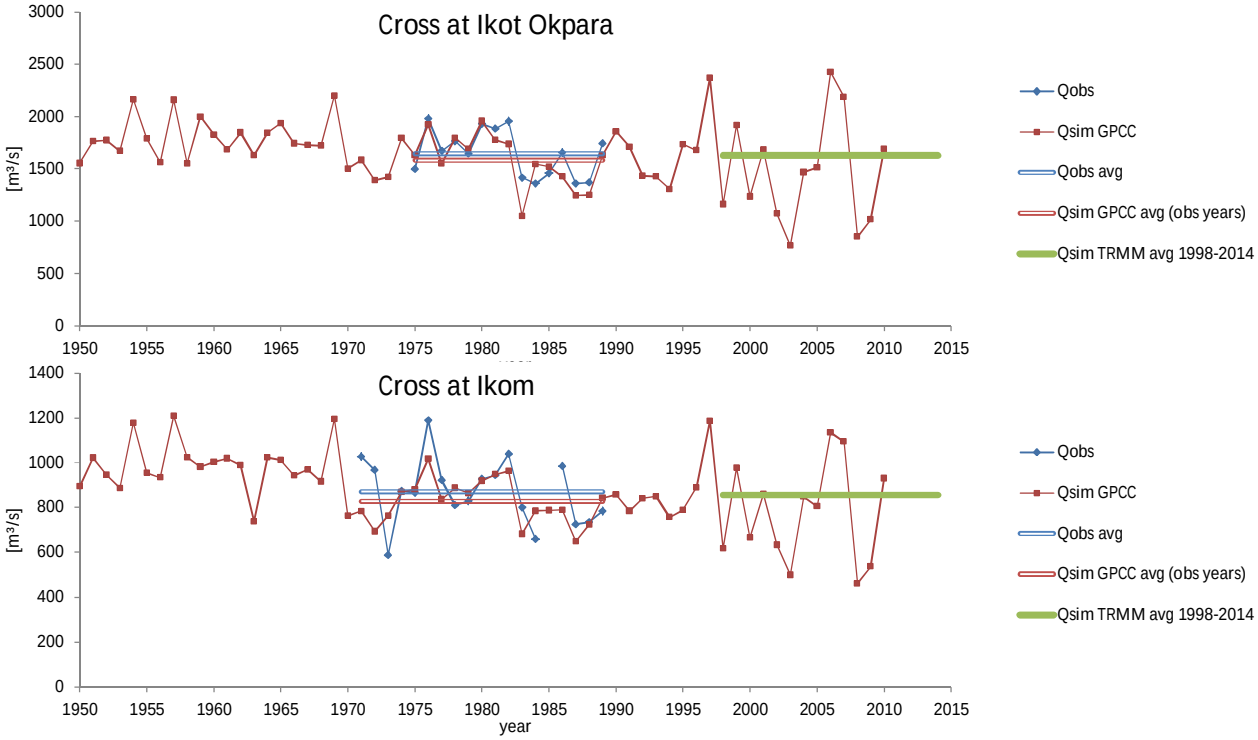


**Figure 46: Simulated and observed annual discharge at the Cross River.**

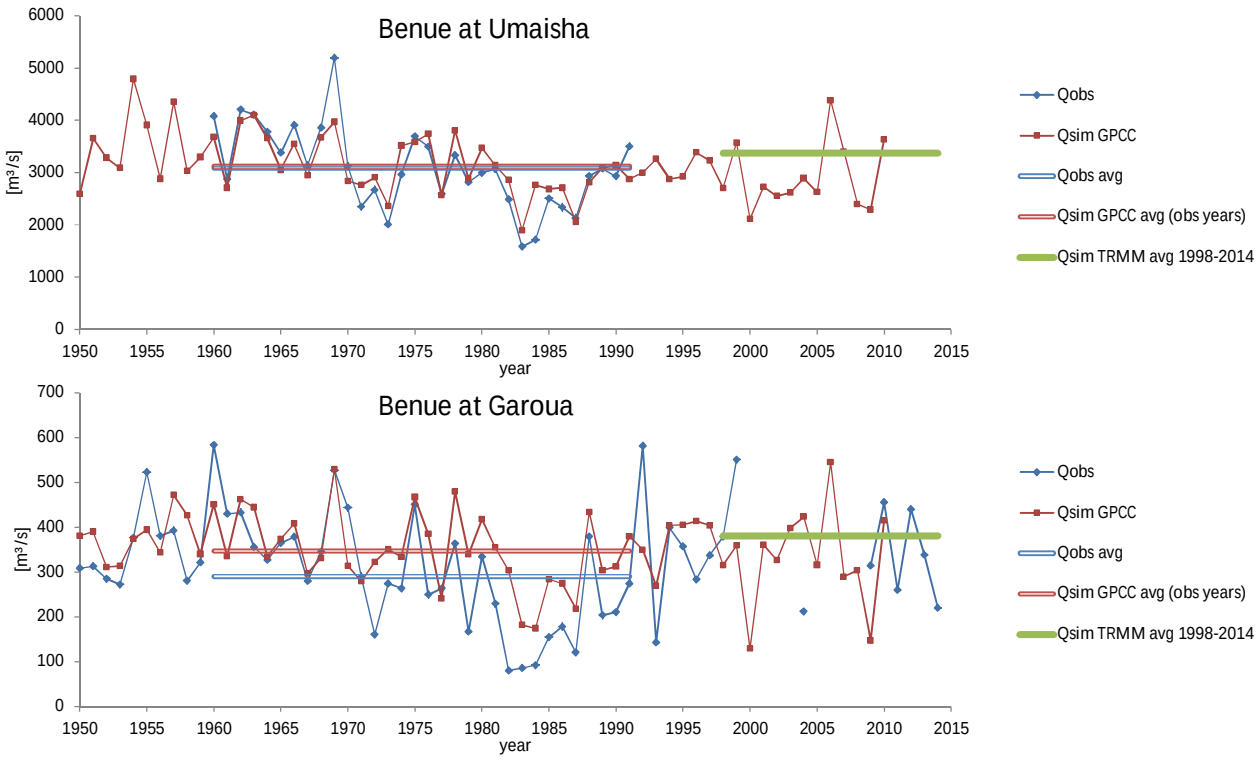


**Figure 47: Simulated and observed annual discharge at the Benue River.**

### 5.3.6 Seasonality in discharge

The seasonality in discharge describes how the long-term mean annual flow is distributed between the twelve months of the year. Obviously, in West Africa during the dry season low flows occur and during the Monsoon season high flows occur. However, the timing and magnitude of the seasonal variation differ between regions. In the coastal regions along the Gulf of Guinea there are two rainy seasons and therefore also two seasonal peaks in flow. The observed discharge data of 410 gauges were analyzed to define 9 typical seasonal flow regimes (Figure 48).

The map in Figure 49 displays the spatial clustering of the observed seasonal flow regimes at gauges. This information was used to assign seasonal runoff regimes to the 1060 sub-catchments (Figure 50). Here, it has to be noted that a seasonal runoff regime describes the local generation of runoff (units of mm), whereas a flow regime describes the seasonality of discharge (units of $m^3/s$) in the river, which may be the result of a superposition of various different seasonal runoff regimes in the upstream basin.

The annual water balance model was extended to simulate long-term mean monthly discharge (flow seasonality) for each reach (500,000) with the following method:

1. Seasonal runoff regime: Distribute the annual runoff onto individual months by using the seasonal runoff regime shown in Figure 50.

2. Compute monthly discharge: Computed from monthly local flow and upstream monthly inflow.

3. Routing: Rough consideration of flow times along the river network (flow velocity estimated from channel slope). Routing is important to consider the flow time of several months at large (long) rivers.

4. Modification of flow seasonality:

    a. Consider reservoir operation at large dams (Kainji, Lake Volta, etc.)

    b. Consider impact of floodplains (Inner Niger Delta, upper Black Volta, etc.)

Thus, the final monthly flows at each reach are a superposition of:

- Upstream seasonality: In many basins the headwater regions show a different seasonality in flow than downstream regions.

- Flow times: Routing of flow along the river network, in some basins it takes one month and longer until the flood from the upstream headwater region arrives at downstream river sections.

- Reservoir and floodplain impacts: These modify (dampen) the flow seasonality. At many reservoirs there is also significant outflow during the dry season, which alters the seasonal flow regime in downstream river sections.

The simulated flow regime was compared to observed flow regime at selected gauges. In general, there is a good concordance between the simulated and observed values

(Figure 51). In the graphs, simulated flows represent average conditions for 1998-2014, whereas observed flows represent average conditions for the observational record (e.g. 1960-1990). The graphs also visualize the strong impact of reservoir operation on discharge. For example, the graphs in row 5 columns 3 and 4 show the observed seasonal flow regime of the Sassandra River downstream of the Soubre dam. In the period 1970-1975 (pre-construction) there is strong seasonality in the observational flow records, whereas in the period 1985-1996 (post-construction) dry season flows are much higher and peak flow is lower. A similar seasonal flow regime is also simulated for 1998-2014.

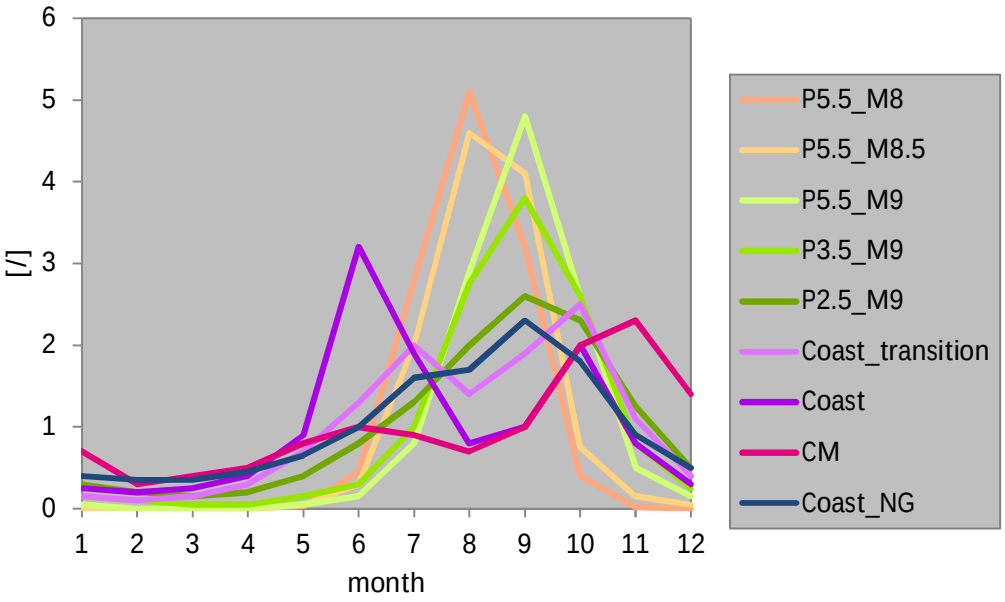


**Figure 48: Definition of nine typical seasonal flow regimes. Flow regimes were normalized with mean annual flow. Thus, a value of e.g. 3.0 means that in this month the flow is three times larger than the mean annual flow.**

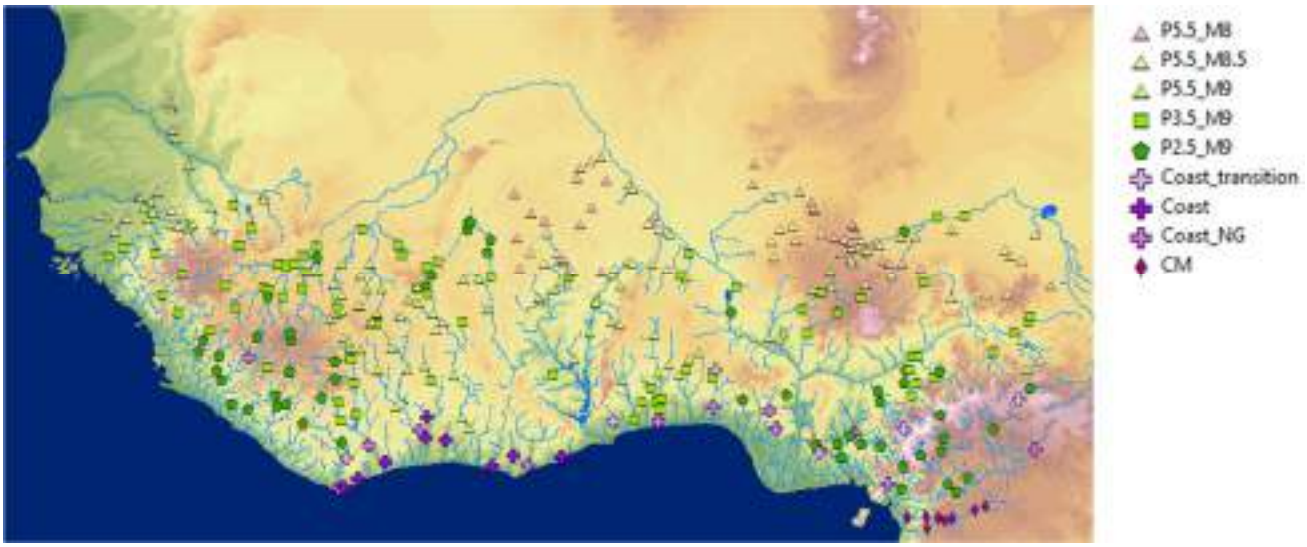


**Figure 49: Classification of the observed long-term mean monthly discharge into nine typical seasonal flow regimes. Downstream gauges were removed from the map, due to superposition of various flow regimes from upstream regions.**

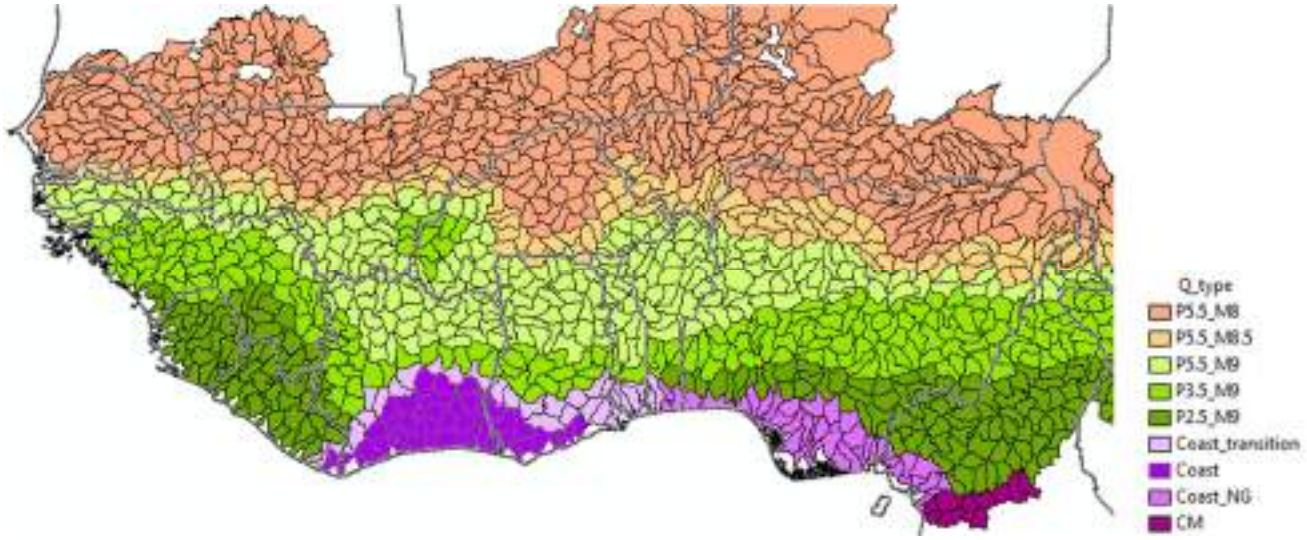


**Figure 50: Nine typical seasonal runoff regimes assigned to sub-catchments.**

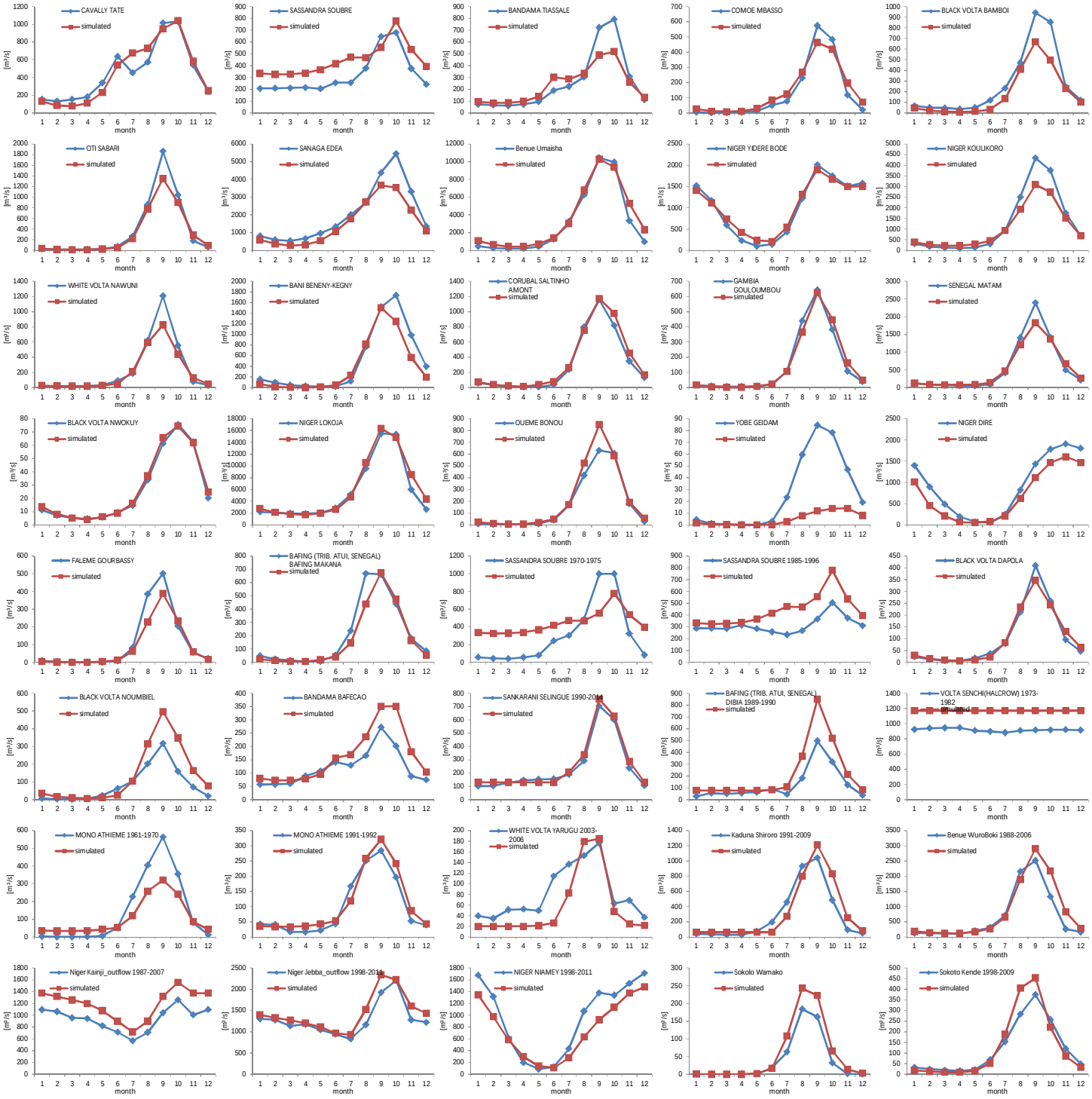


**Figure 51: Simulated (red) and observed (blue) seasonality in discharge at selected gauges. Simulated flows represent average conditions for 1998-2014, whereas observed flows represent average conditions for the observational record (e.g. 1960-1990).**

### 5.3.7 Hydropower potential

There are different definitions of hydropower potential, as listed below:

- Gross theoretical hydropower potential: Hydropower generation if all natural water flows would be utilized by 100% efficient turbines.
- Theoretical hydropower potential: Rough consideration of energy losses due to turbine efficiency and hydraulic losses (penstock, etc.)
- Technical hydropower potential: Also considering spillway losses due to limited design flow of turbines. Excluding sites with unsuitable geologic and topographic settings.
- Economic hydropower potential: Also considering economic restrictions (investment costs, energy prices)
- Exploitable hydropower potential: Also considering environmental and social restrictions (protected areas)

This study focuses only on the theoretical hydropower potential which is computed as follows:

***Power*** [MW] = ***Flow*** [m³/s] * ***Height*** [m] * ***C***

where

***Power*** is the theoretical hydropower potential [MW]

***Flow*** is the long-term mean annual discharge [m³/s]

***Height*** is the elevation difference from start to end of a river reach [m]

***C*** is a constant for considering unit conversion and efficiency/hydraulic losses. In this study the following value is assumed: c = 8.5/1000

The above equation is applied to all river reaches (500,000) to compute the theoretical hydropower potential from mean annual flow and elevation data for each reach. The chosen value of the constant C represents an overall plant efficiency (turbines, generator, transformer, hydraulic losses) of about 87% (C = 8.5/1000 = 0.87 * 9.81 /1000).

The theoretical hydropower potential gives the upper limit of mean power that could be produced in the river reach under the following assumptions:

- The full head (elevation difference from start to end) of the reach is utilized.
- The full river discharge is turbinated (no spillway losses).
- Efficiency of turbines, generator and transformer as well as hydraulic losses (penstock, etc.) are already roughly considered.

The theoretical hydropower potential is by definition higher than the technical, economic or exploitable potential, which were not assessed in this study.

### 5.3.8 Hydropower classification

A classification scheme was applied to determine the:

- Preferred hydropower plant size
- Preferred hydropower plant type
- Preferred hydropower turbine type

#### Classification of preferred hydropower plant size

Four classes are considered for the preferred plant size (installed capacity, see Table 7). The classification scheme is based on mean annual discharge (m³/s) and specific hydropower potential (MW/km) as shown in Figure 52. This classification scheme is applied for each river reach. The classification scheme includes "No attractive potential" for river reaches with too low specific hydropower potential. In some cases it may still be worthwhile to utilize this potential in e.g. multi-purpose schemes.

The classification scheme shown in Figure 52 combines an analysis of existing hydropower plants in West Africa as well as expert judgement, based on the following considerations:

**Boundary between small and medium/large HPP (Boundary 1 in** Figure 52**)**

Derived from empirical data: Q-P plot for existing hydropower plants in West Africa shows clear boundary between medium/large and small HPP.

Boundary is not vertical. For river sections with given mean annual flow (e.g. 10 m³/s) a high specific potential (e.g. 10 MW/km) is more likely to be developed by a large scheme, whereas a moderate potential (e.g. 1 MW km) would probably be developed by a small scheme.

Example for a scheme with length of reservoir or power water way L = 5 km and rated discharge (Qr) is 200% of mean annual flow Q (plant factor ≈ 0.5)
P = 10 MW/km: P x L = 10 x 5 = 50 MW 50 MW x 200% = 100 MW
P = 1 MW/km: P x L = 1 x 5 = 5 MW 5 MW x 200% = 10 MW

Boundary is also not horizontal. Larger rivers generally have a higher specific potential. (With increasing river size the increase in Q is generally stronger than the decrease in slope). A hydropower development in large rivers is therefore typically dealing with a large specific potential. Construction of a weir or dam in a large river is costly. Therefore a minimum plant size is required in order to make the scheme economic. As a consequence in such rivers hydropower development would always require a substantial length of the reservoir or the power water way, thereby preferring large hydro.

**Boundary between small and pico/micro/mini HPP (Boundary 2 in** Figure 52**)**

Also derived from empirical data. Boundary is not very distinct. Proposed boundary crosses vertical Q = 1 m³/s at P = 0.1 MW/km, which is consistent with 1 MW capacity if a length L of 5 km is assumed.

Example:
P = 0.1 MW/km: P x L = 0.1 x 5 = 0.5 MW 5 MW x 200% = 1 MW

Again the boundary line is declined (neither horizontal nor vertical). Smaller rivers (with Q < 1 m³/s) have been considered more suitable for mini hydro development, as they typically do not have a

specific potential higher than 0.1 MW/km. Boundary small vs. pico/micro/mini hydro (boundary 2) was assumed to be parallel to boundary small vs. medium/large hydro (boundary 1).

The analyses of existing hydropower plants shows that in fact a number of small hydropower plants have been built in the mini hydro domain. A closer look at these plants reveals that they are reservoir schemes with daily or weekly storage and a rather low plant factor. Such kind of peaking plants might be an attractive solution if combined with solar or wind. They might become more common in the future, with boundary small vs. pico/micro/mini hydro moving leftwards.

**Lower bound for pico/micro/mini HPP (Lower bound 1 in** Figure 52**)**

It was assumed that a specific potential below 0.05 MW/km in most cases would not be attractive, as this requires 1 km river length to be developed in order to exploit 100 kW (at a plant factor of 0.5).

Example:
P = 0.05 MW/km: P x L = 0.05 x 1 = 0.05 MW 0.05 MW x 200% = 0.1 MW

From the experience of the Consultant in most cases such schemes are economically not feasible. In the pico/micro scale hydro development below 0.05 MW/km might however be feasible. This scale is however not fully represented by the spatial resolution of the study. The boundary therefore probably is conservative (underestimating potential) for pico/micro hydro at rivers with Q < 0.1 m³/s. It is probably less conservative (overestimating potential) for mini hydro at rivers with Q > 0.1 m³/s.

**Lower bound for small and medium/large HPP (Lower bound 2 in** Figure 52**)**

This boundary is rather uncertain, mainly due to the fact that especially in the range P = 0.1 – 1 MW/km small, medium, and large hydro typically goes with multi-purpose project. In this range single-purpose hydropower projects would socio-economically not be feasible.

Multi-purpose projects with a strong irrigation component are characteristic for the small and medium hydro range. Typically these are rivers with mean annual flow being in the range from 10 to several 100 m³/s mean annual flow. The main purpose of developments on large rivers with Q > 1000 m³/s is always hydropower, with irrigation being secondary purpose or not relevant.

Therefore it was assumed that the lower bound 2 would connect lower bound 1 with the Q/P point 1000/1. This means that for large hydro at rivers with Q > 1000 m³/s a specific potential of 1 MW/km is required, which seems to be a reasonable number, also confirmed by existing plants. A reservoir with a length of 100 km would allow developing a capacity of 200 MW, if a plant factor of 0.5 is assumed.

Example:
P = 1 MW/km: P x L = 1 x 100 = 100 MW 100 MW x 200% = 200 MW

The above classification scheme is applied for each river reach. In a second step, the results are aggregated for sub-areas, by computing the sum of all river reaches within a sub-area for each plant size.

**Table 7: Classification of preferred hydropower plant size.**

| Class | Description of preferred hydropower plant size |
|---|---|
| 0 | None. No attractive theoretical potential for hydropower. |
| 1 | Attractive theoretical potential for pico/micro/mini HPP with installed capacity < 1 MW. |
| 2 | Attractive theoretical potential for small HPP with installed capacity 1-30 MW. |
| 3 | Attractive theoretical potential for medium/large HPP with installed capacity > 30 MW. |

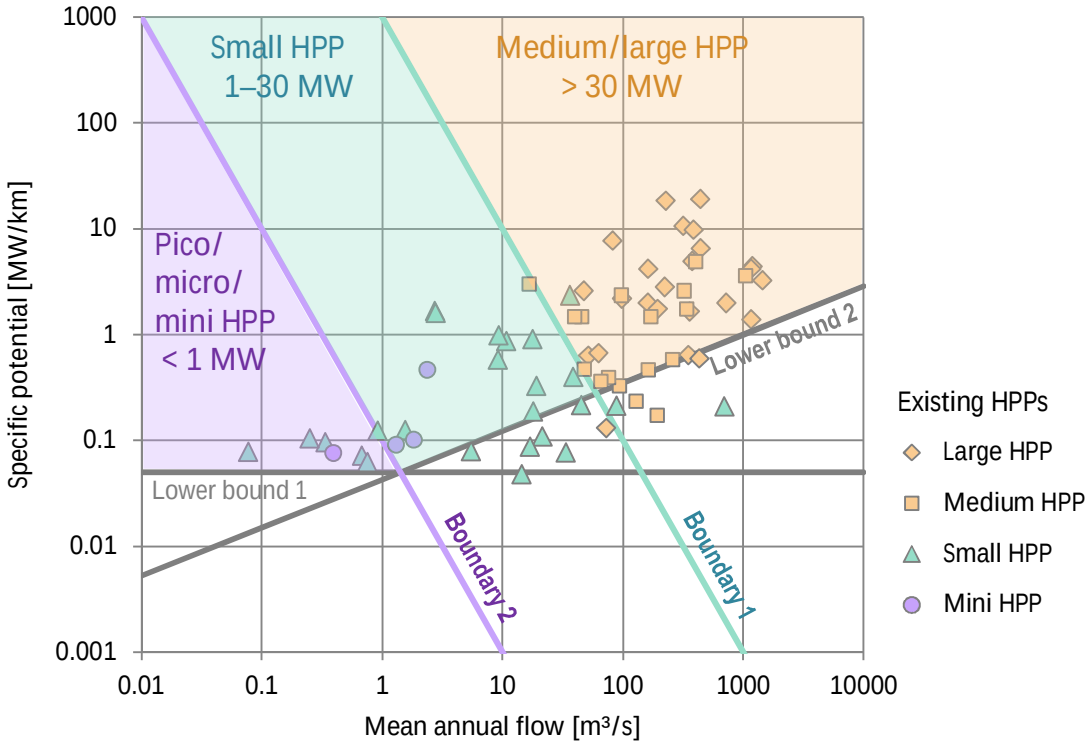


**Figure 52: Classification scheme to determine preferred plant size (installed capacity) from mean annual flow and specific hydropower potential. The points show existing hydropower plants in West Africa.**

## Classification of preferred hydropower plant type

The plant type describes the general layout of the hydropower plant, either with or without a reservoir, as well as either with or without diversion of water. Table 8 lists the four plant types considered in this study (see also Figure 53). An analysis of existing hydropower plants shows that all four plant types are found in West Africa (see examples in Figure 54 to Figure 57). A fifth type that is sometimes found in West Africa, where a quite small hydropower plant diverts a small share of water from a large river (e.g. Yele HPP in Sierra Leone), is not considered in the plant type classification.

The plant type classification is first done for each river reach. This information is then used for a general classification of plant type for sub-areas. The plant type classification is based on expert judgement and uses general considerations about slope of river (e.g. high slope is attractive for hydropower plant with diversion), mean annual discharge (e.g. run-of-river hydropower plants without diversion are usually not built at small rivers), and seasonality in flow (dry season flow is critical for run-of-river plants, whereas reservoirs can buffer seasonality in flows). The following procedure was used for classification of river reaches (where Q_YEAR is mean annual discharge in m³/s, RATIO_MIN is ratio of flow in dry season to Q_YEAR, SLOPE is slope of river channel in m/m, PLANT_SIZE indicates plant size class as defined in Table 7,

PLANT_TYPX indicates if reach is suitable (0=no, 1=yes) for plant type class X as listed in Table 8):

1. Initial definition
    a. Exclude reaches where PLANT_SIZE=0
    b. For reaches where Q_YEAR>=10 & RATIO_MIN>=0.14 set PLANT_TYP1=1
    c. For reaches where SLOPE>=0.01 & RATIO_MIN>=0.15 set PLANT_TYP2=1
    d. For reaches where SLOPE>=0.0003 & SLOPE<=0.05 & Q_YEAR>=5 set PLANT_TYP3=1
    e. For reaches where SLOPE>=0.02 & Q_YEAR>=2 set PLANT_TYP4=1
2. Assign plant types to remaining reaches that have no plant type assigned yet (overall 15942 reaches)
    a. Select from remaining reaches where PLANT_SIZE=1 and set PLANT_TYP2=1
    b. Select from remaining reaches where SLOPE>=0.01 & RATIO_MIN>=0.09 and set PLANT_TYP2=1
    c. Select from remaining reaches where SLOPE>=0.015 & Q_YEAR>=1.5 and set PLANT_TYP4=1
    d. Select from remaining reaches where SLOPE>=0.0003 & Q_YEAR>=2 and set PLANT_TYP3=1
    e. Select from remaining reaches where Q_YEAR>=100 (mainly Benue River) and set PLANT_TYP3=1
    f. Select from remaining reaches where SLOPE>=0.015 and set PLANT_TYP2=1
    g. Select remaining reaches and set PLANT_TYP3=1
3. Manually set hydropower plant type for river reaches located at existing hydropower plants with large reservoirs (overall 18 HPPs)
    a. PLANT_TYP3=1
    b. PLANT_TYP1=0
    c. PLANT_TYP2=0
    d. PLANT_TYP4=0

In the above classification scheme the first step is used to assign a hydropower plant type based on general considerations. A river reach can be suitable for multiple different plant types. After the first step about 16,000 river reaches remained, that have an attractive theoretical hydropower potential (plant size class > 0, according to Table 7), but no plant type is assigned to the reach, yet. Therefore, in the second step the rules for assigning plant types are continuously relaxed, until all reaches have at least one plant type assigned. In the third step the plant type is manually set for river reaches located at existing hydropower plants with large reservoirs. Note that the classification for PLANT_TYP2 includes rivers where the hydropower plant cannot operate during the

dry season due to limited flow. This could be compensated by a combination with solar power (as there are no clouds during the dry season).

In a final step the plant types of river reaches are assigned to sub-areas. The results for the river network are not published, but only the results for sub-areas.

**Table 8: Classification of suitability for various plant types.**

| Class | Description of hydropower plant type |
|---|---|
| 1 | Run-of-river hydropower plant without diversion. |
| 2 | Run-of-river hydropower plant with diversion. |
| 3 | Storage (reservoir) hydropower plant without diversion. |
| 4 | Storage (reservoir) hydropower plant with diversion. |

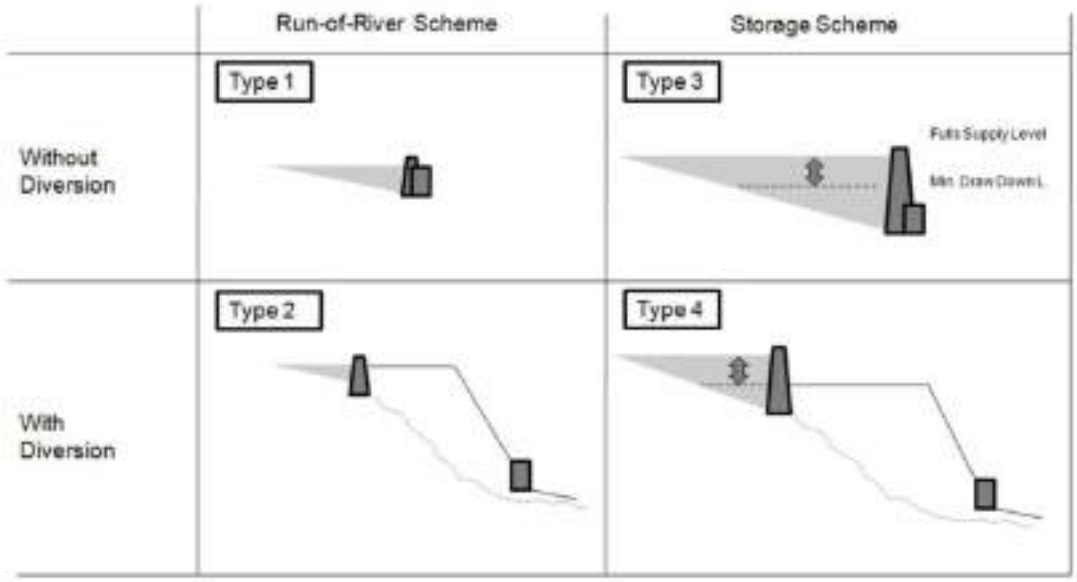


**Figure 53: Schematic visualization of classification of different hydropower plant types.**


**Figure 54: Hydropower plant type "Run-of-river scheme without diversion". Example Tourni HPP in Burkina Faso.**


**Figure 55: Hydropower plant type "Run-of-river scheme with diversion". Example Jekko 1 HPP in Nigeria.**

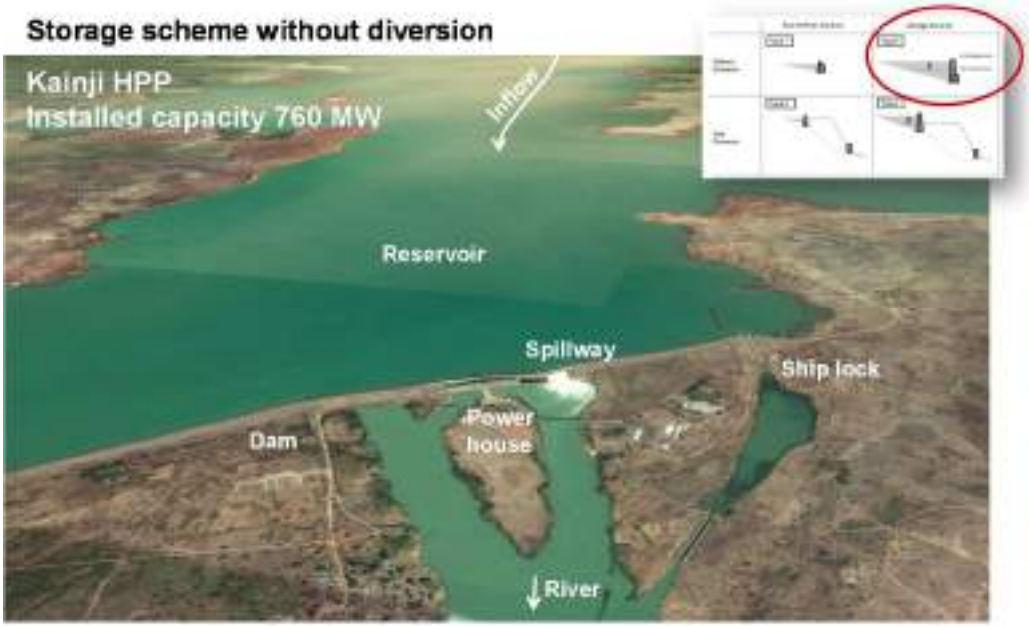


**Figure 56: Hydropower plant type "Storage scheme without diversion". Example Kainji HPP, Nigeria.**


**Figure 57: Hydropower plant type "Storage scheme with diversion". Example Kurra HPP in Nigeria.**

## Classification of preferred turbine type

For classification of turbine type three different classes are considered, as listed in Table 9. The following rules are used for classification of river reaches:

1. Assign Kaplan turbine type to reaches where PLANT_TYP1=1 (see description of plant type) and channel slope is smaller than 0.01 m/m.

2. Assign Pelton turbine type to reaches where channel slope is greater than 0.05 m/m.

3. Assign Francis turbine type to all reaches.

The above classification scheme is only applied to river reaches that have an attractive theoretical hydropower potential (see Table 7). In a second step the results are assigned to sub-areas. The results for river reaches are not published.

**Table 9: Classification of suitability for various turbine types.**

| Class | Description of turbine type |
|---|---|
| 1 | Kaplan turbine |
| 2 | Pelton turbine |
| 3 | Francis turbine |

### 5.3.9 Discussion of accuracy

The results of this study are heavily based on models. As every model is a simplification of reality there will always be differences between simulated and observed variables. One of the main objectives of this study was to give a regional overview about the hydropower potential in West Africa and to identify regions and rivers that have an attractive theoretical hydropower potential for different plant sizes of installed capacities. As the hydropower potential is controlled by (a) mean annual discharge and (b) elevation of longitudinal river profile these are also the key variables for assessing the accuracy of the results, as discussed below. Obviously, once an attractive region or river is identified field measurements are required for more detailed analysis of the hydropower potential.

The accuracy of the elevation data is discussed first. Here, only the elevation difference from start to end of a river reach (or channel slope) is of interest, not the absolute elevation values. The general shape of longitudinal river profiles (i.e. steep and flat stretches of a river) should be identified well in hydropower resource mapping results. However, a difficult task was to differentiate between noise in the DEM (resulting in spikes in elevation) and actual sudden change in channel slope. A quite advanced smoothing technique was applied after extensive testing and visual inspection of results. It was decided to apply a rather strong smoothing to be on the conservative side to avoid identifying attractive hydropower sites that are actually only artefacts of noise in the DEM data. On the other hand, strong smoothing also means that for some natural sites with sudden change in channel slope the hydropower potential is under-estimated.

A related problem to the one discussed above is that the river reaches in the GIS layer have a length of e.g. 10km, and only the average channel slope is computed for the whole river reach. For pico/micro/mini HPPs very short sections (e.g. 1km) may be interesting, but this cannot be identified when the river reach is too long (averaging of channel slope over longer distances). Therefore, for pico/micro/mini HPP field

campaigns are required to establish the exact location of interesting sites along the river network (and also to compute the hydropower potential for these sites).

In contrast to elevation measurements, which can be done quite easily in the field, the estimation of long-term mean flow conditions by field measurements is a more difficult task. This requires to build a flow gauge, to establish a rating curve (conversion of water level to discharge data), to regularly update the rating curve for different flow conditions (high and low flow), and to secure funding and personnel for continuous measurements over many years. Therefore, it is understandable that flow gauges are only built at strategic locations of high interest.

The mean annual flow estimated in this study represents a long-term average for the period 1998-2014. Of course, flow in individual years may differ considerably from this long-term average, but they should be on similar magnitude. The accuracy of the simulation results depends on the observed discharge data that were available during calibration of the water balance model. In some regions there were hardly any long-term observations available (Guinea, Sierra Leone, Liberia, Côte d'Ivoire). Unfortunately, these are also the regions that show a high theoretical hydropower potential. In addition, the rainfall inputs (GPCC, TRMM) show less accuracy in mountainous region due to the high spatial variability of rainfall (and technical issues for satellite-based data retrieval). Therefore, the accuracy of results is expected to be lower in those regions.

The available discharge observations were used for a comparison with simulated discharge. The simulation results in general show a good agreement with the observations (see also Figure 58), with the following caveats:

- The gauges are only located at larger river basins, but not a small streams. Due to the high spatial variability of rainfall in mountainous terrain it is expected that the simulation results are less accurate for small streams than for large rivers.

- Some of the gauges may be affected by systematic bias in discharge observation (e.g. due to outdated rating curve). It was tried to eliminate the most obvious measurement errors (e.g. comparison upstream vs. downstream gauges), but certainly not all errors could be corrected. In case of biased discharge observations, this bias was incorporated in the water balance model during model calibration.

- Old discharge data (e.g. from the 1960s) appear to be of higher quality than more recent observations. Again, this may be related to outdated discharge rating curves (as confirmed by discussions with hydrologist from the region).

Thus, the discussion of accuracy above shows that the simulation results should not be taken for granted, but always put into context. In some regions the accuracy will be higher, in other regions it will be lower. The main objective should not be forgotten, i.e. to give a regional overview and to identify regions and rivers that have an attractive hydropower potential. Once an interesting region or river is identified, field measurements are required for more detailed analysis.

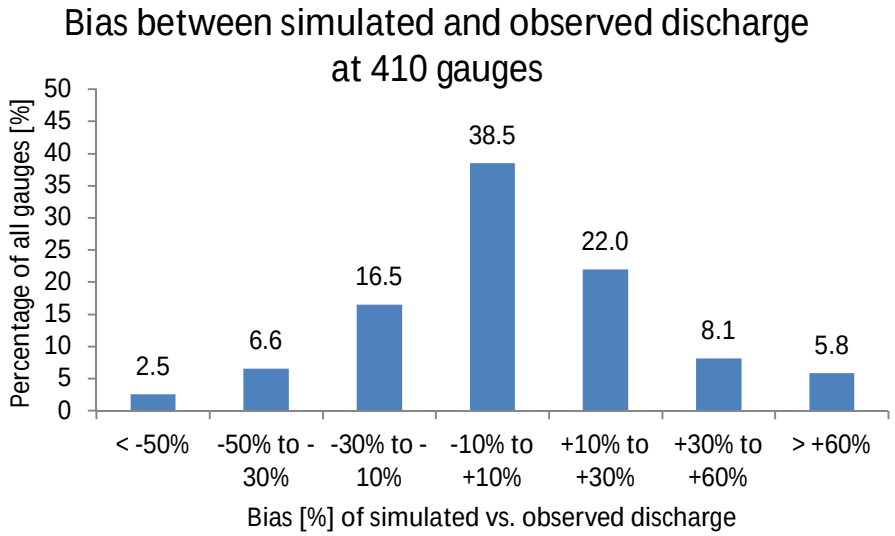


**Figure 58: Histogram showing the bias between simulated and observed long-term mean annual discharge at 410 gauges. Evaluation period differs between gauges because of different observational records.**

In addition to the accuracy of the hydrological simulation results, also the accuracy of correct river names has to be discussed. The most reliable sources for river names proved to be the GRDC gauges and the SIEREM data set. However, only a limited number of rivers are identifiable from these sources. Therefore, various online maps were used to identify additional river names. For the online maps the Michelin map proved to be the most useful one. In a few cases also the other online maps provided useful information (here mainly Google map, but rarely Bing or OpenStreetMap). Unfortunately, there are many examples where the river names in the online maps are inconsistent and sometimes misplaced. Especially in remote areas and in headwater regions the online maps often do not show any river names. In some parts of West Africa (e.g. Liberia) the hardcopy Travelmag map was a useful source.

The most difficult part (and probably the most error-prone part) was to find the correct branch of the river in the headwater region. This is exemplified by several errors in the headwater river course in the SIEREM data base. In downstream regions the course of the river to be named is quite obvious, whereas in the headwater region there are many tributaries of similar size and identification of the river to be named can be a tedious and error-prone task. Therefore, a conservative approach was chosen, where rivers were not named if the correct branch was not clear.

## 5.4 Results

The results of the hydropower resource mapping are published in two separate GIS layers, which are described in the following two chapters.

### 5.4.1 Layer D2 river network

The results for the river network are published in a GIS line shape file named “Layer D2 River Network”. The shape file consists of more than 500,000 river reaches with a typical length of 1 to 10 km (see example in Figure 59).

Each river reach in the GIS layer contains 39 attributes (Table 10). These attributes allow creating different maps in the ECOWREX system of ECREEE. For example, named rivers in the GIS layer can be displayed to get a regional overview about the general course of main rivers in the region (Figure 60). For the GIS layer 272 different river names were identified, and about 35,000 reaches have an assigned river name. The remaining reaches are mainly unnamed tributaries, but also some smaller rivers are included where the river name was not readily available from maps.

Different maps can be created from the GIS attributes showing the hydropower potential and classification results. Figure 61 and Figure 62 show example maps for preferred hydropower plant size along the river network.

The data in the GIS attribute table also allow to automatically create longitudinal river profiles by clicking on a river reach. Figure 63 and Figure 64 show two examples for such longitudinal river profiles, plotting elevation (red) and mean annual discharge (blue) from the source to the mouth of the river. Inflow from tributaries is clearly identifiable as sudden increase in river discharge. The background color indicates if a river reach has an attractive theoretical hydropower potential for pico/micro/mini HPP (< 1 MW installed capacity), small HPP (1-30 MW installed capacity), or medium/large HPP (> 30 MW installed capacity).

In addition to longitudinal river profiles, which show mean annual discharge along the river course, also seasonality in discharge can be plotted for each river reach from the data included in the GIS data table. Figure 65 displays three examples for mean monthly discharge.

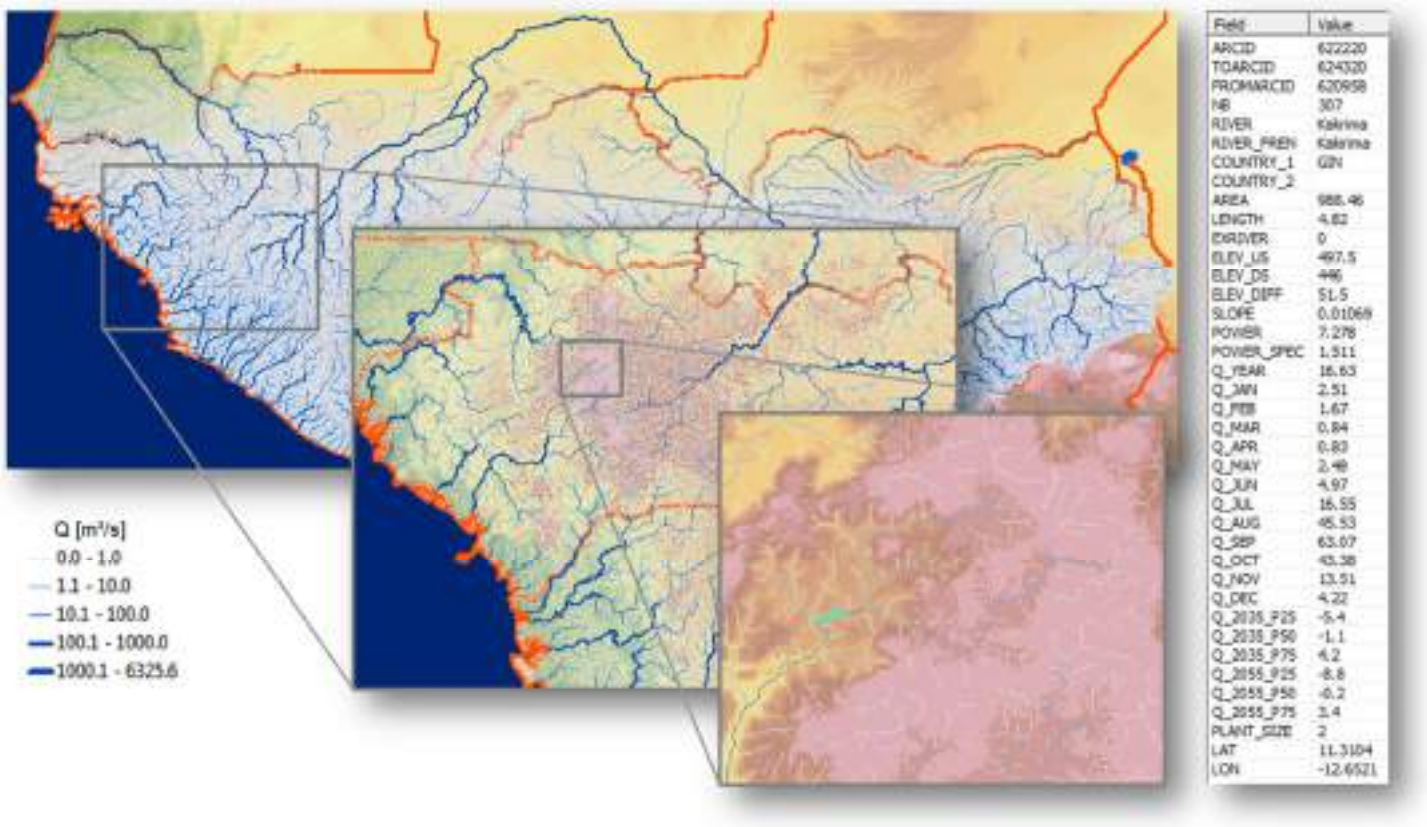


**Figure 59: Map showing Layer D2 River Network. Example for zoom-in on a selected river reach (highlighted in cyan color) and display of GIS attribute table.**

**Table 10: Attributes of the GIS shape file "Layer D2 River Network".**

| Attribute | Units | Description |
|---|---|---|
| ARCID | / | ID number of reach |
| TOARCID | / | ID number of next downstream reach |
| FROMARCID | / | ID number of dominant upstream reach (largest inflow) |
| NB | / | ID number of sub-area |
| RIVER | text | River name (English) |
| RIVER_FREN | text | River name (French) |
| COUNTRY_1 | text | Country (ISO code) |
| COUNTRY_2 | text | Second country (ISO code) if reach forms international border |
| AREA | km² | Total upstream catchment area (km²) of reach |
| LENGTH | km | Length (km) of reach |
| EXRIVER | / | Flag indicating external river originating from another sub-area (0: local river, 1: external river) |
| ELEV_US | m | Elevation (m) at upstream end of reach |
| ELEV_DS | m | Elevation (m) at downstream end of reach |
| ELEV_DIFF | m | Elevation difference (m) in reach |
| SLOPE | m/m | Slope (m/m) of reach |
| POWER | MW | Theoretical hydropower potential (MW) for the period 1998-2014 |
| POWER_SPEC | MW/km | Specific hydropower potential (MW/km) for the period 1998-2014 |
| Q_YEAR | m³/s | Mean annual discharge (m³/s) simulated for the period 1998-2014 |
| Q_JAN | m³/s | Mean monthly discharge (m³/s) 1998-2014 in January |
| Q_FEB | m³/s | Mean monthly discharge (m³/s) 1998-2014 in February |
| Q_MAR | m³/s | Mean monthly discharge (m³/s) 1998-2014 in March |
| Q_APR | m³/s | Mean monthly discharge (m³/s) 1998-2014 in April |
| Q_MAY | m³/s | Mean monthly discharge (m³/s) 1998-2014 in May |
| Q_JUN | m³/s | Mean monthly discharge (m³/s) 1998-2014 in June |
| Q_JUL | m³/s | Mean monthly discharge (m³/s) 1998-2014 in July |
| Q_AUG | m³/s | Mean monthly discharge (m³/s) 1998-2014 in August |
| Q_SEP | m³/s | Mean monthly discharge (m³/s) 1998-2014 in September |
| Q_OCT | m³/s | Mean monthly discharge (m³/s) 1998-2014 in October |
| Q_NOV | m³/s | Mean monthly discharge (m³/s) 1998-2014 in November |
| Q_DEC | m³/s | Mean monthly discharge (m³/s) 1998-2014 in December |
| Q_2035_P25 | % | Change in future mean annual discharge in % (2026-2045 vs. 1998-2014) for the lower quartile simulation using 30 climate model runs of the CORDEX-Africa ensemble (RCP4.5 and RCP8.5) |
| Q_2035_P50 | % | Change in future mean annual discharge in % (2026-2045 vs. 1998-2014) for the median simulation using 30 climate model runs of the CORDEX-Africa ensemble (RCP4.5 and RCP8.5) |
| Q_2035_P75 | % | Change in future mean annual discharge in % (2026-2045 vs. 1998-2014) for the upper quartile simulation using 30 climate model runs of the CORDEX-Africa ensemble (RCP4.5 and RCP8.5) |
| Q_2055_P25 | % | Change in future mean annual discharge in % (2046-2065 vs. 1998-2014) for the lower quartile simulation using 30 climate model runs of the CORDEX-Africa ensemble (RCP4.5 and RCP8.5) |
| Q_2055_P50 | % | Change in future mean annual discharge in % (2046-2065 vs. 1998-2014) for the median simulation using 30 climate model runs of the CORDEX-Africa ensemble (RCP4.5 and RCP8.5) |
| Q_2055_P75 | % | Change in future mean annual discharge in % (2046-2065 vs. 1998-2014) for the upper quartile simulation using 30 climate model runs of the CORDEX-Africa ensemble (RCP4.5 and RCP8.5) |
| PLANT_SIZE | / | Preferred hydropower plant size (0: none, 1: <1MW, 2: 1-30MW, 3: >30MW installed capacity) |
| LAT | deg | Latitude (decimal degrees North) at end of reach |
| LON | deg | Longitude (decimal degrees East) at end of reach |

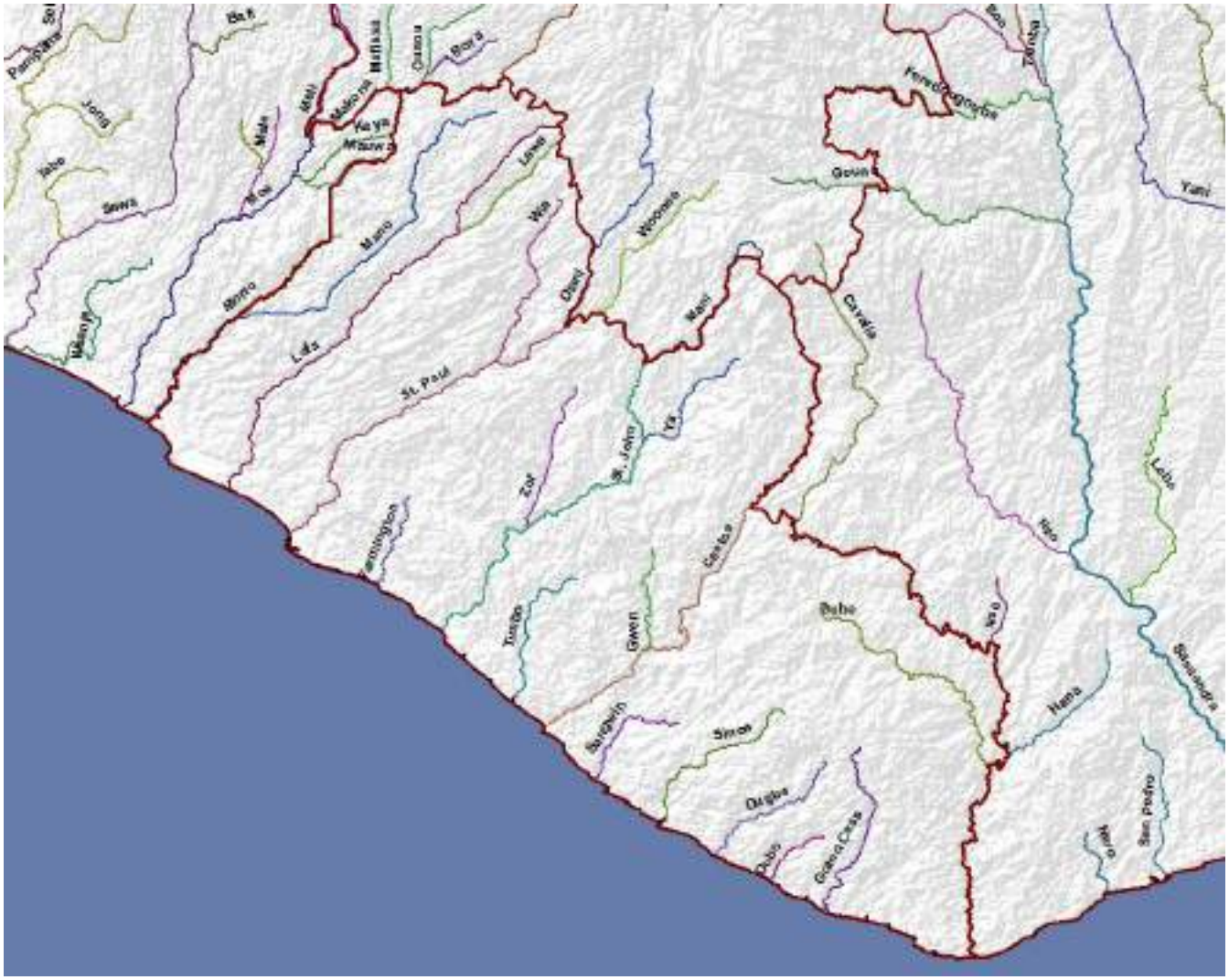


**Figure 60: Named rivers of the GIS river network layer in Liberia.**

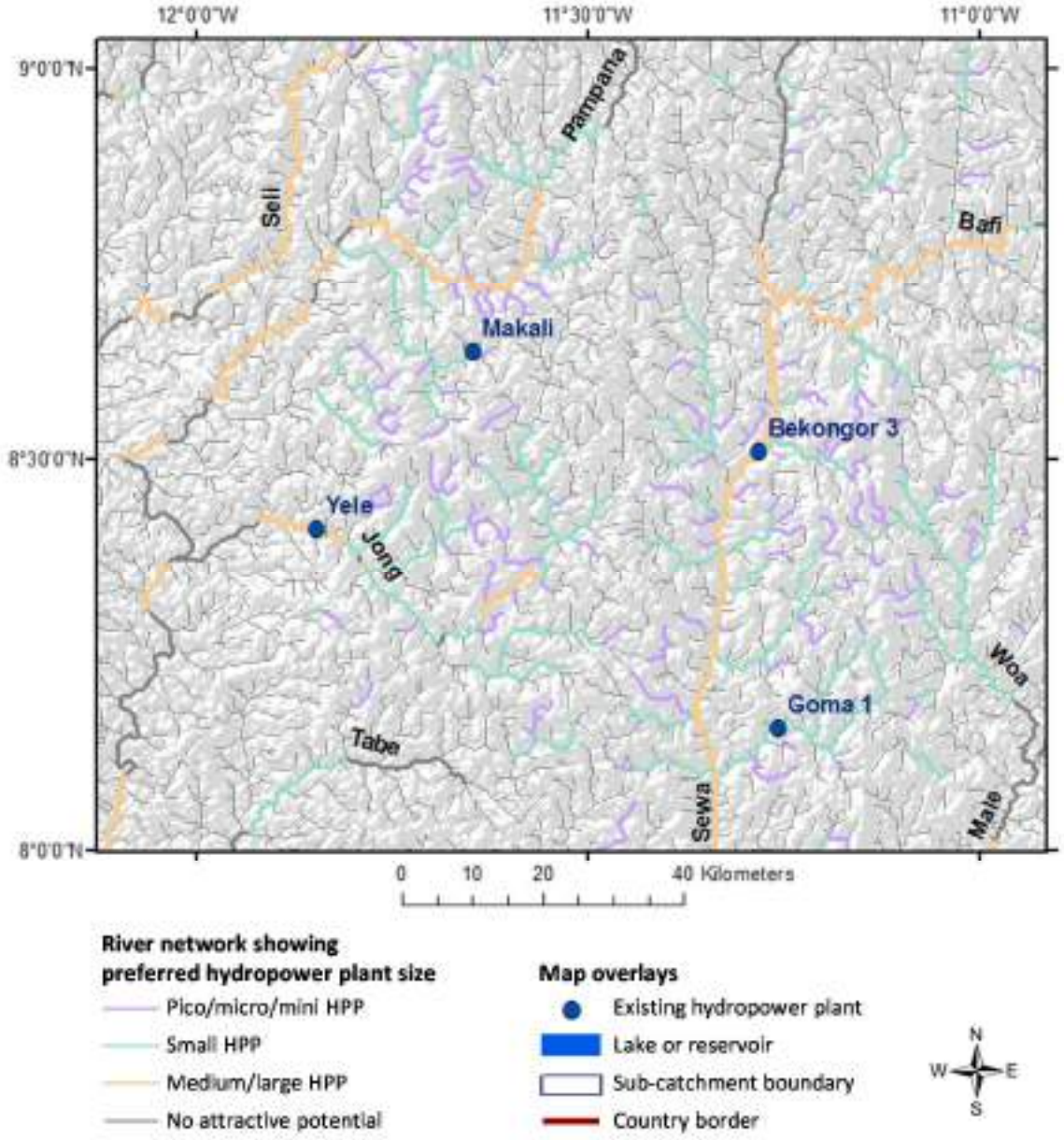


**Figure 61: Example map showing preferred hydropower plant size for the river network in central Sierra Leone.**

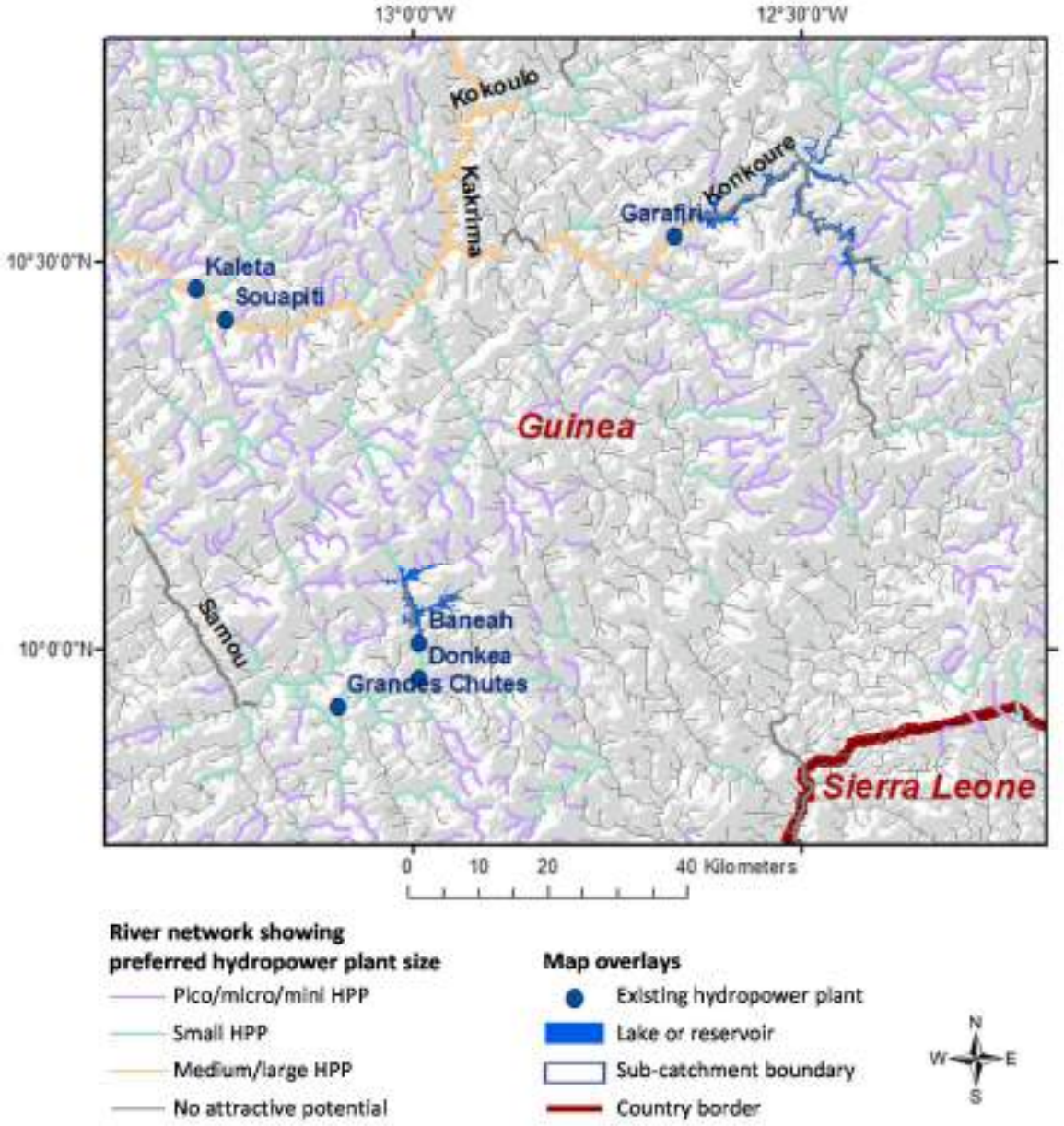


**Figure 62: Example map showing preferred hydropower plant size for the river network in central southern Guinea.**

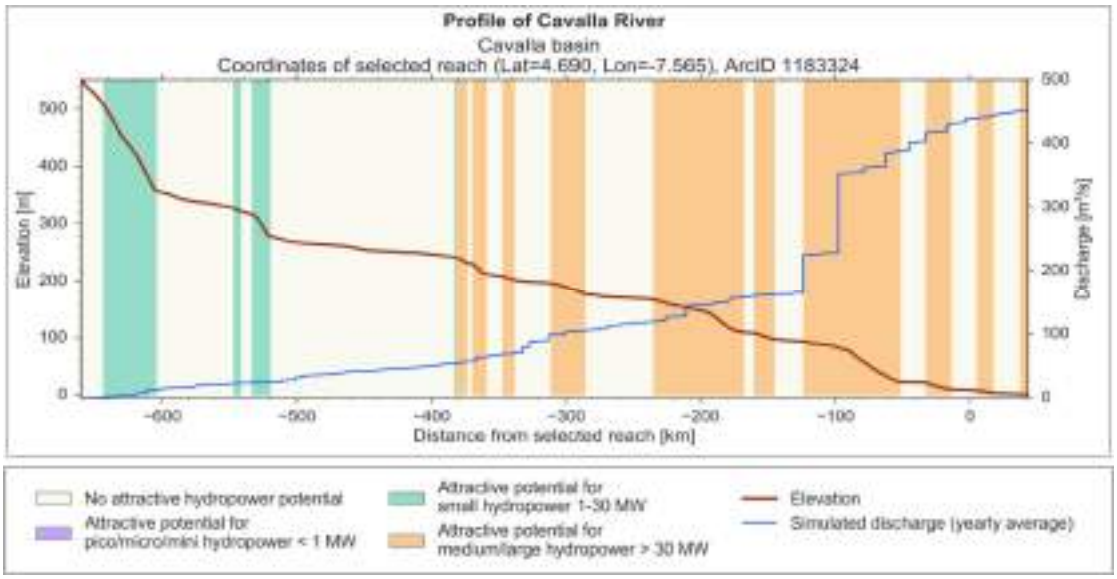


**Figure 63: Longitudinal river profile. Example for the Cavalla River.**

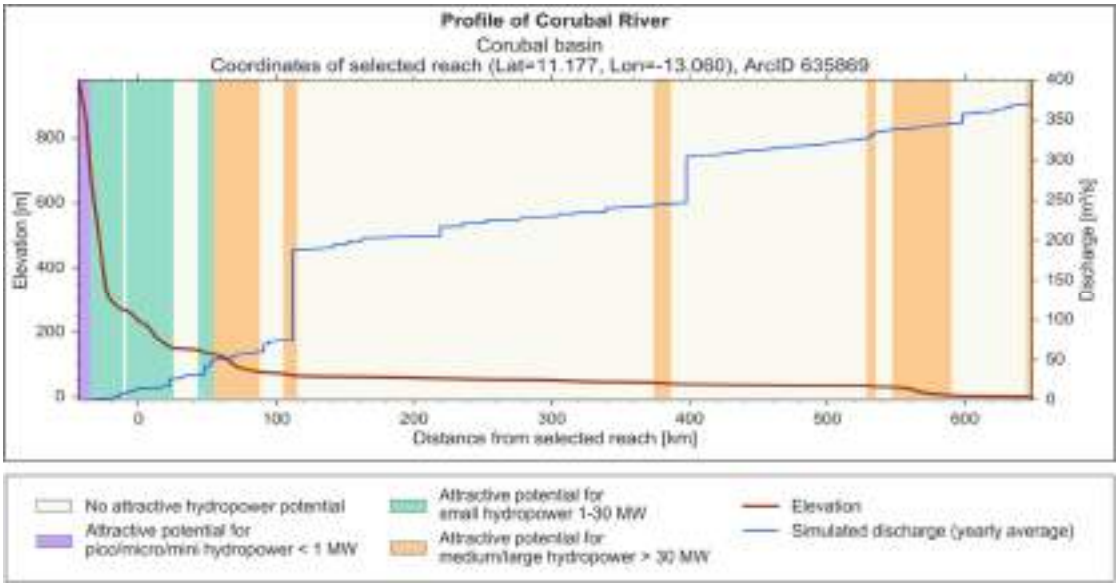


**Figure 64: Longitudinal river profile. Example for the Corubal River.**

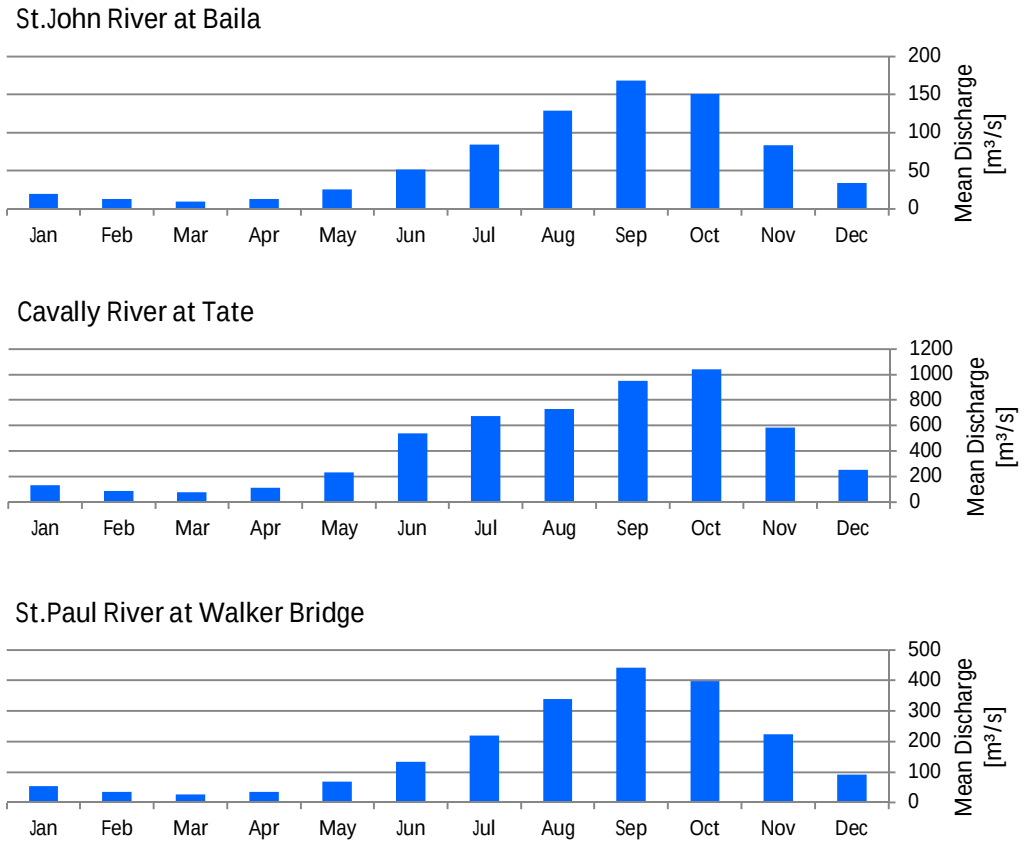


**Figure 65: Examples for simulated mean monthly discharge for three selected locations.**

### 5.4.2 Layer D3 sub-areas

The results of the sub-catchments are published in a GIS polygon shape file named "Layer D3 sub-areas". The shape file consists of 1060 sub-catchments with a typical size of about 3000 km² (Figure 66).

Each sub-catchment in the GIS layer contains 54 attributes (Table 11 to Table 12). These attributes allow creating different maps in the ECOWREX system of ECREEE.

Figure 67 displays example maps for the mean annual water balance of the period 1998-2014. The maps show the spatial distribution of precipitation, actual evapotranspiration and runoff.

Figure 68 to Figure 70 display example maps showing the location of sub-catchments with attractive theoretical hydropower potential for pico/micro/mini HPP, small HPP and medium/large HPP.

The sub-catchments also include an extensive list of attributes detailing the results of the climate change impact assessment (see chapter 6).

**Figure 66: Layer D3 sub-areas consisting of 1060 sub-catchments. Red: country borders. Black: sub-catchment borders.**

**Table 11: Attributes of the GIS shape file "Layer D3 Sub-areas", part 1 of 2.**

| Attribute | Units | Description |
|---|---|---|
| NB | / | ID number of sub-area |
| AREA | km² | Local size (km²) of sub-area |
| PRECIP_Y | mm | Mean annual precipitation (mm) in the period 1998-2014 |
| ETA_Y | mm | Mean annual actual evapotranspiration (mm) simulated for the period 1998-2014 |
| RUNOFF_Y | mm | Mean annual runoff (mm) simulated for the period 1998-2014 |
| TEMP_Y | °C | Mean annual air temperature (°C) in the period 1998-2014 |
| P_2035_P25 | % | Change in future mean annual precipitation in % (2026-2045 vs. 1998-2014) for the lower quartile projection of 30 climate model runs in the CORDEX-Africa ensemble (RCP4.5 and RCP8.5) |
| P_2035_P50 | % | Change in future mean annual precipitation in % (2026-2045 vs. 1998-2014) for the median projection of 30 climate model runs in the CORDEX-Africa ensemble (RCP4.5 and RCP8.5) |
| P_2035_P75 | % | Change in future mean annual precipitation in % (2026-2045 vs. 1998-2014) for the upper quartile projection of 30 climate model runs in the CORDEX-Africa ensemble (RCP4.5 and RCP8.5) |
| P_2055_P25 | % | Change in future mean annual precipitation in % (2046-2065 vs. 1998-2014) for the lower quartile projection of 30 climate model runs in the CORDEX-Africa ensemble (RCP4.5 and RCP8.5) |
| P_2055_P50 | % | Change in future mean annual precipitation in % (2046-2065 vs. 1998-2014) for the median projection of 30 climate model runs in the CORDEX-Africa ensemble (RCP4.5 and RCP8.5) |
| P_2055_P75 | % | Change in future mean annual precipitation in % (2046-2065 vs. 1998-2014) for the upper quartile projection of 30 climate model runs in the CORDEX-Africa ensemble (RCP4.5 and RCP8.5) |
| E_2035_P25 | % | Change in future mean annual actual evapotranspiration in % (2026-2045 vs. 1998-2014) for the lower quartile simulation using 30 climate model runs of the CORDEX-Africa ensemble (RCP4.5 and RCP8.5) |
| E_2035_P50 | % | Change in future mean annual actual evapotranspiration in % (2026-2045 vs. 1998-2014) for the median simulation using 30 climate model runs of the CORDEX-Africa ensemble (RCP4.5 and RCP8.5) |
| E_2035_P75 | % | Change in future mean annual actual evapotranspiration in % (2026-2045 vs. 1998-2014) for the upper quartile simulation using 30 climate model runs of the CORDEX-Africa ensemble (RCP4.5 and RCP8.5) |
| E_2055_P25 | % | Change in future mean annual actual evapotranspiration in % (2046-2065 vs. 1998-2014) for the lower quartile simulation using 30 climate model runs of the CORDEX-Africa ensemble (RCP4.5 and RCP8.5) |
| E_2055_P50 | % | Change in future mean annual actual evapotranspiration in % (2046-2065 vs. 1998-2014) for the median simulation using 30 climate model runs of the CORDEX-Africa ensemble (RCP4.5 and RCP8.5) |
| E_2055_P75 | % | Change in future mean annual actual evapotranspiration in % (2046-2065 vs. 1998-2014) for the upper quartile simulation using 30 climate model runs of the CORDEX-Africa ensemble (RCP4.5 and RCP8.5) |
| R_2035_P25 | % | Change in future mean annual runoff in % (2026-2045 vs. 1998-2014) for the lower quartile simulation using 30 climate model runs of the CORDEX-Africa ensemble (RCP4.5 and RCP8.5) |
| R_2035_P50 | % | Change in future mean annual runoff in % (2026-2045 vs. 1998-2014) for the median simulation using 30 climate model runs of the CORDEX-Africa ensemble (RCP4.5 and RCP8.5) |
| R_2035_P75 | % | Change in future mean annual runoff in % (2026-2045 vs. 1998-2014) for the upper quartile simulation using 30 climate model runs of the CORDEX-Africa ensemble (RCP4.5 and RCP8.5) |
| R_2055_P25 | % | Change in future mean annual runoff in % (2046-2065 vs. 1998-2014) for the lower quartile simulation using 30 climate model runs of the CORDEX-Africa ensemble (RCP4.5 and RCP8.5) |
| R_2055_P50 | % | Change in future mean annual runoff in % (2046-2065 vs. 1998-2014) for the median simulation using 30 climate model runs of the CORDEX-Africa ensemble (RCP4.5 and RCP8.5) |
| R_2055_P75 | % | Change in future mean annual runoff in % (2046-2065 vs. 1998-2014) for the upper quartile simulation using 30 climate model runs of the CORDEX-Africa ensemble (RCP4.5 and RCP8.5) |
| T_2035_P25 | °C | Change in future mean annual air temperature in °C (2026-2045 vs. 1998-2014) for the lower quartile projection of 30 climate model runs in the CORDEX-Africa ensemble (RCP4.5 and RCP8.5) |
| T_2035_P50 | °C | Change in future mean annual air temperature in °C (2026-2045 vs. 1998-2014) for the median projection of 30 climate model runs in the CORDEX-Africa ensemble (RCP4.5 and RCP8.5) |
| T_2035_P75 | °C | Change in future mean annual air temperature in °C (2026-2045 vs. 1998-2014) for the upper quartile projection of 30 climate model runs in the CORDEX-Africa ensemble (RCP4.5 and RCP8.5) |
| T_2055_P25 | °C | Change in future mean annual air temperature in °C (2046-2065 vs. 1998-2014) for the lower quartile projection of 30 climate model runs in the CORDEX-Africa ensemble (RCP4.5 and RCP8.5) |
| T_2055_P50 | °C | Change in future mean annual air temperature in °C (2046-2065 vs. 1998-2014) for the median projection of 30 climate model runs in the CORDEX-Africa ensemble (RCP4.5 and RCP8.5) |
| T_2055_P75 | °C | Change in future mean annual air temperature in °C (2046-2065 vs. 1998-2014) for the upper quartile projection of 30 climate model runs in the CORDEX-Africa ensemble (RCP4.5 and RCP8.5) |

**Table 12: Attributes of the GIS shape file "Layer D3 Sub-areas", part 2 of 2.**

| Attribute | Units | Description |
|---|---|---|
| POWER | MW | Theoretical hydropower potential (MW) for the period 1998-2014 (total of all river reaches located in the sub-area) |
| POW_MINI | MW | Theoretical hydropower potential (MW) for pico/micro/mini hydropower plants (< 1 MW installed capacity) for the period 1998-2014 |
| POW_SMALL | MW | Theoretical hydropower potential (MW) for small hydropower plants (1-30 MW installed capacity) for the period 1998-2014 |
| POW_MEDIUM | MW | Theoretical hydropower potential (MW) for medium/large hydropower plants (>30 MW installed capacity) for the period 1998-2014 |
| ATT_MINI | / | Region with theoretical hydropower potential that is attractive (0: no, 1: yes) for pico/micro/mini hydropower plants (< 1 MW installed capacity) |
| ATT_SMALL | / | Region with theoretical hydropower potential that is attractive (0: no, 1: yes) for small hydropower plants (1-30 MW installed capacity) |
| ATT_MEDIUM | / | Region with theoretical hydropower potential that is attractive (0: no, 1: yes) for medium/large hydropower plants (> 30 MW installed capacity) |
| PLANT_TYP1 | / | Region suitable (0: no, 1: yes) for hydropower plant type 1 (run-of-river without diversion) |
| PLANT_TYP2 | / | Region suitable (0: no, 1: yes) for hydropower plant type 2 (run-of-river with diversion) |
| PLANT_TYP3 | / | Region suitable (0: no, 1: yes) for hydropower plant type 3 (storage without diversion) |
| PLANT_TYP4 | / | Region suitable (0: no, 1: yes) for hydropower plant type 4 (storage with diversion) |
| TURBINE | text | Preferred turbine type |
| PT_2035_25 | % | Change in future hydropower potential in % (2026-2045 vs. 1998-2014) for the lower quartile simulation using 30 climate model runs of the CORDEX-Africa ensemble (RCP4.5 and RCP8.5) |
| PT_2035_50 | % | Change in future hydropower potential in % (2026-2045 vs. 1998-2014) for the median simulation using 30 climate model runs of the CORDEX-Africa ensemble (RCP4.5 and RCP8.5) |
| PT_2035_75 | % | Change in future hydropower potential in % (2026-2045 vs. 1998-2014) for the upper quartile simulation using 30 climate model runs of the CORDEX-Africa ensemble (RCP4.5 and RCP8.5) |
| PT_2055_25 | % | Change in future hydropower potential in % (2046-2065 vs. 1998-2014) for the lower quartile simulation using 30 climate model runs of the CORDEX-Africa ensemble (RCP4.5 and RCP8.5) |
| PT_2055_50 | % | Change in future hydropower potential in % (2046-2065 vs. 1998-2014) for the median simulation using 30 climate model runs of the CORDEX-Africa ensemble (RCP4.5 and RCP8.5) |
| PT_2055_75 | % | Change in future hydropower potential in % (2046-2065 vs. 1998-2014) for the upper quartile simulation using 30 climate model runs of the CORDEX-Africa ensemble (RCP4.5 and RCP8.5) |
| PL_2035_25 | % | Change in future hydropower potential in % (2026-2045 vs. 1998-2014) of local rivers (having their source in the same sub-area) for the lower quartile simulation using 30 climate model runs of the CORDEX-Africa ensemble (RCP4.5 and RCP8.5) |
| PL_2035_50 | % | Change in future hydropower potential in % (2026-2045 vs. 1998-2014) of local rivers (having their source in the same sub-area) for the median simulation using 30 climate model runs of the CORDEX-Africa ensemble (RCP4.5 and RCP8.5) |
| PL_2035_75 | % | Change in future hydropower potential in % (2026-2045 vs. 1998-2014) of local rivers (having their source in the same sub-area) for the upper quartile simulation using 30 climate model runs of the CORDEX-Africa ensemble (RCP4.5 and RCP8.5) |
| PL_2055_25 | % | Change in future hydropower potential in % (2046-2065 vs. 1998-2014) of local rivers (having their source in the same sub-area) for the lower quartile simulation using 30 climate model runs of the CORDEX-Africa ensemble (RCP4.5 and RCP8.5) |
| PL_2055_50 | % | Change in future hydropower potential in % (2046-2065 vs. 1998-2014) of local rivers (having their source in the same sub-area) for the median simulation using 30 climate model runs of the CORDEX-Africa ensemble (RCP4.5 and RCP8.5) |
| PL_2055_75 | % | Change in future hydropower potential in % (2046-2065 vs. 1998-2014) of local rivers (having their source in the same sub-area) for the upper quartile simulation using 30 climate model runs of the CORDEX-Africa ensemble (RCP4.5 and RCP8.5) |

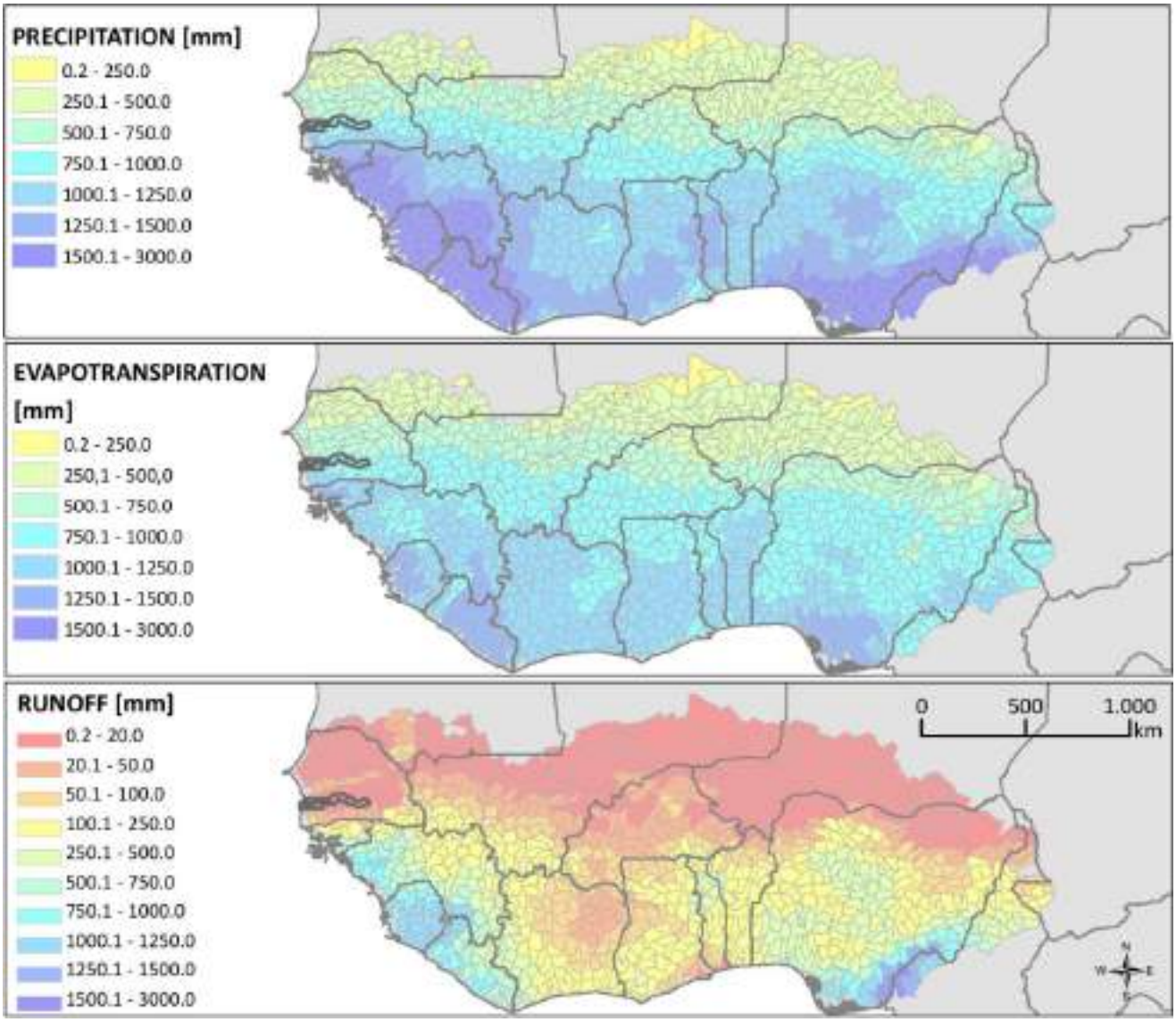


**Figure 67: Mean annual water balance for the period 1998-2014 displayed for 1060 sub-catchments.**

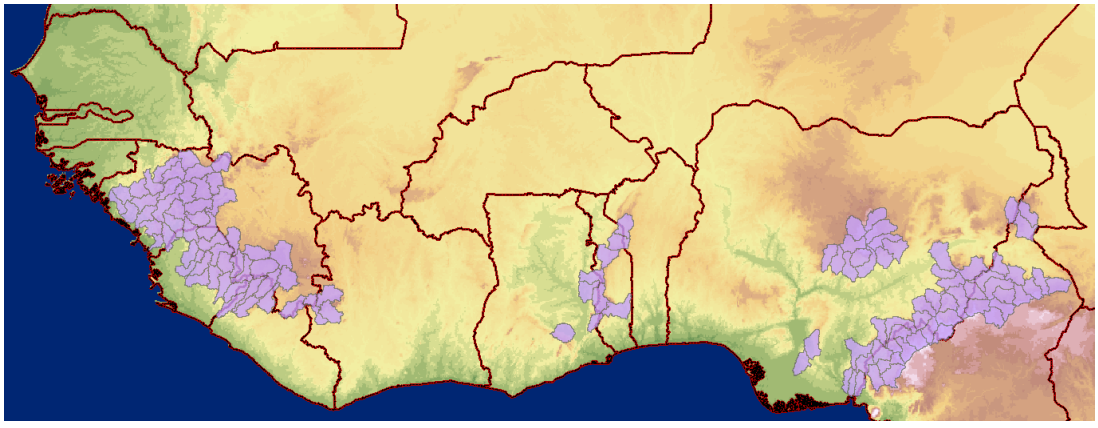

**Figure 68: Sub-catchments (purple) with attractive theoretical hydropower potential for pico/micro/mini HPP.**

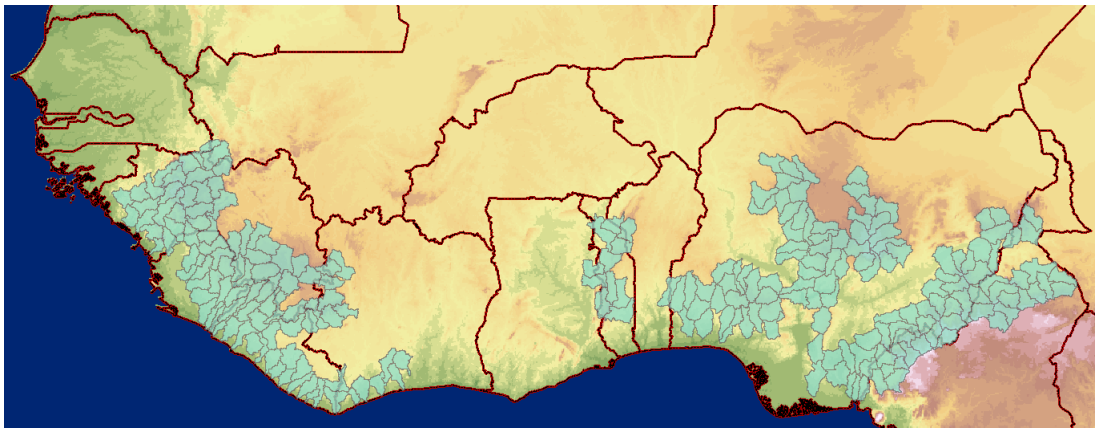

**Figure 69: Sub-catchments (green) with attractive theoretical hydropower potential for small HPP.**

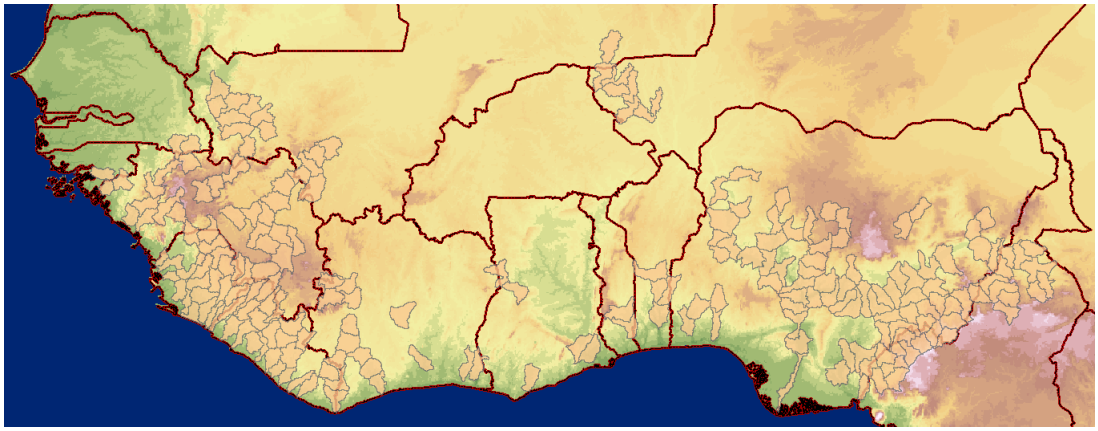

**Figure 70: Sub-catchments (orange) with attractive theoretical hydropower potential for medium/large HPP.**

## 5.5 Lessons learned

Several lessons were learned during the hydropower resource mapping, as summarized below:

- **Digital elevation models (DEM):** Various DEMs with different spatial resolution were analyzed in this study. It was found that the DEM with the finest spatial resolution (ASTER 30m) gave inconsistent results for elevation along the river network. This may be related to low stacking due to cloudy conditions during satellite overpasses, which is the reason why ASTER data include a considerable share of gap filling with SRTM data. In contrast, the unconditioned DEM of Hydrosheds (90m) gave quite consistent elevation results.

- **Data availability:** The best data availability was between 1960 and 1990, whereas the number of available precipitation stations and operational flow gauges is much smaller in the 2000s. This lack of observations is partially offset

by new satellite rainfall products, but field observations are still the most reliable source of information (see also Fekete et al., 2015). In some countries (Guinea, Sierra Leone, Liberia, Côte d'Ivoire) there are hardly any long-term discharge observations available (or the data could not be identified in this study even though considerable effort was invested by ECREEE to obtain discharge data).

- **Data quality:** The quality of data differs greatly between countries and products:
  - Rainfall data: GPCC data was found to be the most reliable rainfall product (at least for the period 1960-1990 with high number of rainfall gauges). TRMM satellite rainfall data proved to be reliable, whereas RFE satellite rainfall data has the finest spatial resolution, but is severely biased in some years in Guinea, Sierra Leone, and Liberia.
  - Potential evapotranspiration data: In most parts of West Africa the CRU and Climwat data sets (both use Penman-Monteith method) are consistent with each other. However, in Côte d'Ivoire and surrounding regions there is a systematic difference, which had to be corrected before applied as input to water balance modelling.
  - Discharge data: A major effort was required for correct geo-referencing of gauges provided by GRDC, as many gauges were misplaced by 10 km or more (showing an erroneous location at the wrong river). Other issues were filling of numerous and extensive gaps in the time-series records, to enable computation of annual means. Visual checks were required to identify and remove obvious errors in the data provided by river basin authorities.
- **Diversions for irrigation:** In those parts of West Africa that are potentially attractive for hydropower development diversions for irrigation are not significant. However, at some rivers (e.g. Niger River, Black Volta) diversions had to be considered as otherwise the downstream hydropower potential would have been over-estimated.
- **Water balance modelling:** A simple, well calibrated water balance model proved to be sufficient to reproduce the available observations (i.e. simulated and observed discharge corresponds well at numerous gauges). However, discharge can be simulated more accurately (a) in the period 1960-1990 than in later periods and (b) in large basins than in small basins. Both of this may be explained by the spatial and temporal accuracy of the rainfall inputs.

## 5.6 Conclusions and recommendations

Extensive GIS data sets have been prepared within this study. These datasets will be available to the general public via the ECOWREX system of ECREEE. Experts can use the ECOWREX system to identify regions and rivers that have a promising theoretical hydropower potential, as well as climate change projections for future river discharge.

Based on the study results we give the following recommendations:

- Provide extensive training for stakeholders from ECOWAS countries using the ECOWREX system. Such training should present the main results of the hydropower potential mapping, as well as how the data can be used for additional/follow-up analysis. The training should mainly focus on Guinea, Sierra Leone and Liberia due to the lack of previous studies in those countries.

- Several countries with high theoretical hydropower potential (Guinea, Sierra Leone, Liberia) have a lack of up-to-date discharge observations. Most of the gauging stations were abandoned in the 1980s and 1990s. We recommend starting targeted flow measurement campaigns in such countries. The hydropower resource mapping can help to select which rivers shall be targeted in the flow measurement campaigns.

In addition to the GIS layers the study results are also available in 14 country reports (see chapter 7). Furthermore, the methodology and study results are also published in Kling et al. (2016) and Kling et al. (2017).

# 6 CLIMATE CHANGE SCENARIOS

## 6.1 Objective

Hydropower plants are investments with a lifetime of several decades. Regional hydropower development needs to be based on long-term strategic planning, with planning horizons of many decades. Anticipation of long-term trends in the climate system due to global warming, and the related impact on hydropower potential, can therefore be essential for sound planning of hydropower development.

The objective of the climate change scenario analyses is therefore to assess possible future climate trends and their impact on future discharge and hydropower potential. The assessment is based on climate projections for the 21st century from 15 Regional Climate Models of the CORDEX-Africa ensemble, representing the most detailed climate simulations currently available for Africa.

## 6.2 Data sources

Climate change projections are available for West Africa based on Global Climate Models (GCMs) and Regional Climate Models (RCMs). RCMs provide climate simulations in higher spatial resolution than GCMs, with better representation of regional climate peculiarities. Application of RCM data in climate change impact studies therefore yields more precise regional analyses.

GCMs and RCMs use greenhouse gas emission scenarios that affect their climate change projections. As of the latest IPCC report (Fifth Assessment Report published in December 2013) the previously used emission scenarios (e.g. A2, A1B, etc.) are now replaced by Representative Concentration Pathways (RCPs).

RCM simulations for limited areas need GCM simulations for the entire global climate system as boundary conditions. With one RCM, several RCM runs can be produced by applying different driving GCMs.

For the climate change scenario analyses RCM data of the Coordinated Regional Downscaling Experiment in Africa (CORDEX, see Giorgi et al., 2009) are used, which are the result of the most recent research with RCMs for West Africa. The CORDEX Africa data were published in 2015 and this study is one of the first to use CORDEX Africa data. Data of two different greenhouse gas emission scenarios, the moderate-low RCP4.5 and the high RCP8.5 are considered. Table 13 lists the analysed climate model runs, which include four different RCMs from four different climate modelling institutions, applied with different driving GCMs. The total number of RCM runs for each emission scenario is 15, resulting in 30 different regional climate change projections.

**Table 13: CORDEX Africa climate model runs**

| Climate modelling institution | Acronym | Country | RCM | Driving GCMs |
|---|---|---|---|---|
| Koninklijk Nederlands Meteorologisch Instituut | KNMI | Netherlands | RACMO22T | ICHEC-EC-EARTH |
| Danmarks Meteorologiske Institut | DMI | Denmark | HIRHAM5 | ICHEC-EC-EARTH |
| Climate Limited-area Modelling-Community | CLMcom | Germany | CCLM4-8-17 | CNRM-CERFACS-CNRM-CM5 |
| | | | | ICHEC-EC-EARTH |
| | | | | MOHC-HadGEM2-ES |
| | | | | MPI-M-MPI-ESM-LR |
| Sveriges Meteorologiska och Hydrologiska Institut | SMHI | Sweden | RCA4 | CCCma-CanESM2 |
| | | | | CNRM-CERFACS-CNRM-CM5 |
| | | | | ICHEC-EC-EARTH |
| | | | | MIROC-MIROC5 |
| | | | | MOHC-HadGEM2-ES |
| | | | | MPI-M-MPI-ESM-LR |
| | | | | NCC-NorESM1-M |
| | | | | NOAA-GFDL-GFDL-ESM2M |
| | | | | IPSL-IPSL-CM5A-MR |

## 6.3 Methodology

Precipitation and air temperature data from the 30 available RCM runs were processed for the 1060 sub-catchments derived for Layer D3 (see chapter 5.3.4). Time-series of annual precipitation and air temperature were calculated from the gridded monthly RCM data for each sub-catchment. The annual time-series data 1950-2100 were smoothed with 11-year moving average to enable more robust calculation of long-term trends. Climate change signals in each RCM run were computed between the long-term mean values for the reference period 1998-2014 and for two future periods (2026-2045, 2046-2065). Figure 71 exemplarily shows the smoothed time-series of annual temperature (for sub-area 359, in southern Guinea) and the reference and future periods, demonstrating the range of climate simulations.

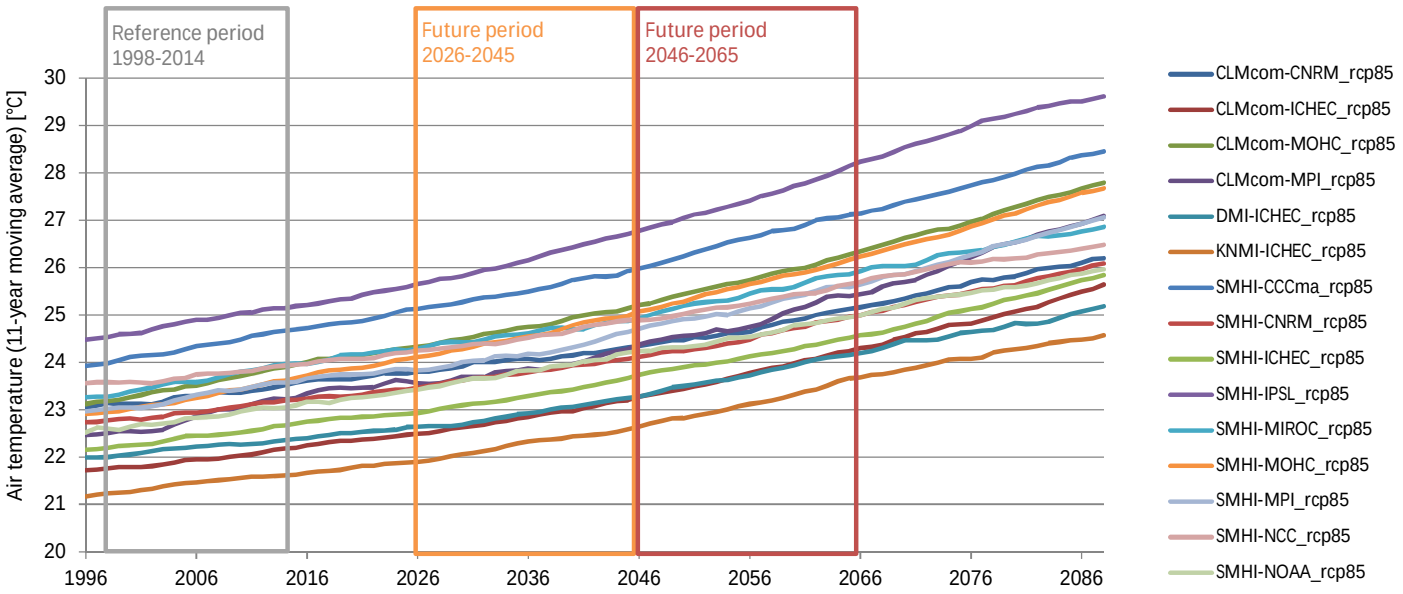


**Figure 71: Smoothed (moving average) time-series of air temperature (example for sub-area 359 and RCP8.5), with boxes showing reference period and future periods for calculation of climate change signals**

The large range of simulation results for the historic period shows that many simulations deviate considerably from the observed climate. This is the reason why climate model data usually is not directly applied, but either corrected (bias correction) or used to derive climate change signals (delta change method, Hay et al., 2000). Figure 72 shows the climate change signals derived from the time-series shown in Figure 71 (but including both emission scenarios, demonstrating the larger increase in temperature with higher greenhouse gas emissions in RCP8.5).

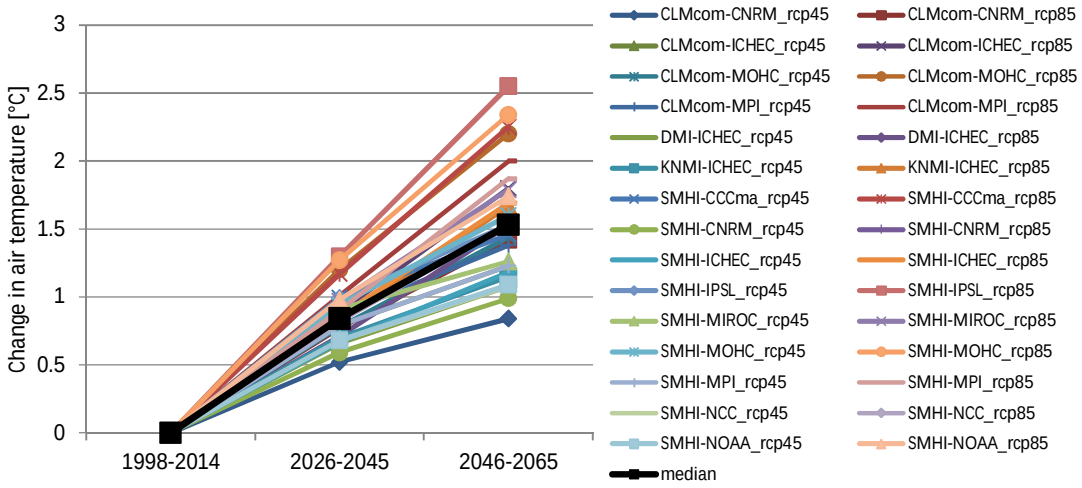


**Figure 72: Temperature change signals (example for subbasin 359 and both, RCP4.5 and RCP8.5)**

The climate change signals of the two future periods were used to drive the water balance model under climate change scenarios with the delta change method. For this method, future precipitation and temperature are derived by applying the climate change signals in the RCM data to the original observational data of the reference period (additive in the case of temperature, multiplicative in the case of precipitation). The increase in future potential evapotranspiration is computed from the increase in future temperature based on sensitivity tests with the CROPWAT model of FAO (based on the Penman-Monteith method). The derived factor was found to be well in line with scaling factors obtained in climate modelling experiments by Scheff and Frierson (2014).

With 30 RCM runs and two future periods, the water balance model was run 60 times. For each river reach (500,000) the 30 results of future discharge were summarized by computing the median and upper and lower quartiles (from 30 RCM runs) in the two future periods. The median value of 30 projections divides the range of 30 results into 15 values that are higher than the median and 15 values that are lower. Upper and lower quartiles represent the values that are exceeded by 25% or 75% of the results, respectively

## 6.4 Results overview

The results of the climate change study are incorporated into the other GIS layers:

- Layer D1 Climatic Zones
- Layer D2 River Network
- Layer D3 Sub-areas
- Layer D4 Country Reports

Table 14 to Table 17 list the attributes of the above layers that are the result of the climate change study. The following naming conventions are used in the GIS attribute tables:

- P: Change in future mean annual precipitation in %.
- T: Change in future mean annual air temperature in °C.
- E: Change in future mean annual evapotranspiration in %.
- R: Change in future mean annual runoff in %.
- Q: Change in future mean annual discharge in %.
- PT: Change in future hydropower potential in %
- PL: Change in future hydropower potential in % of local rivers having their source in the same sub-area (as opposed to rivers having their source in a different sub-area)
- 2035: Period 2026-2045 vs. 1998-2014.

- 2055: Period 2046-2065 vs. 1998-2014.

- P25: Lower quartile simulation (25% percentile) using 30 climate model runs of the CORDEX-Africa ensemble (RCP4.5 and RCP8.5).

- P50: Median simulation (50% percentile) using 30 climate model runs of the CORDEX-Africa ensemble (RCP4.5 and RCP8.5).

- P75: Upper quartile simulation (75% percentile) using 30 climate model runs of the CORDEX-Africa ensemble (RCP4.5 and RCP8.5).

Using data of the sub-areas and river network GIS layers, the maps in Figure 73 and Figure 74 show the expected impact of climate change on future mean annual water resources. From the 30 climate model runs the median result (50% percentile, P50) was used to generate the maps, which show change signals comparing the future periods 2026-2045 (Figure 73) and 2046-2065 (Figure 74) vs. the reference period 1998-2014.

The maps in Figure 73 and Figure 74 are examples for visualization of the results of the climate change study. The full results are available via the GIS layers published in the ECOWREX system of ECREEE. In addition, a summary of the results is available in the country reports.

In addition to the median result (P50) of the 30 climate model runs, also the lower quartile (25% percentile, P25) and upper quartile (75% percentile, P75) are available in the GIS layers to estimate the uncertainty in the projection. Figure 75 shows examples for projected changes in discharge using the P25, P50 and P75 data of the GIS table. In the example plots for the St. John, Cavally and St. Paul rivers in Liberia, the projections with individual climate models consistently show an increase in future. Only a few outliers project a decrease in future discharge, whereas if the median result of 30 climate model runs is considered then discharge is expected to increase by +5 % to +10 % in the far future. This would be beneficial for hydropower development in Liberia.

**Table 14: Climate change results included in the attributes of the GIS shape file "Layer D1 Climatic Zones".**

| Attribute | Units | Description |
|---|---|---|
| P_2035_P25 | % | Change in future mean annual precipitation in % (2026-2045 vs. 1998-2014) for the lower quartile projection of 30 climate model runs in the CORDEX-Africa ensemble (RCP4.5 and RCP8.5) |
| P_2035_P50 | % | Change in future mean annual precipitation in % (2026-2045 vs. 1998-2014) for the median projection of 30 climate model runs in the CORDEX-Africa ensemble (RCP4.5 and RCP8.5) |
| P_2035_P75 | % | Change in future mean annual precipitation in % (2026-2045 vs. 1998-2014) for the upper quartile projection of 30 climate model runs in the CORDEX-Africa ensemble (RCP4.5 and RCP8.5) |
| P_2055_P25 | % | Change in future mean annual precipitation in % (2046-2065 vs. 1998-2014) for the lower quartile projection of 30 climate model runs in the CORDEX-Africa ensemble (RCP4.5 and RCP8.5) |
| P_2055_P50 | % | Change in future mean annual precipitation in % (2046-2065 vs. 1998-2014) for the median projection of 30 climate model runs in the CORDEX-Africa ensemble (RCP4.5 and RCP8.5) |
| P_2055_P75 | % | Change in future mean annual precipitation in % (2046-2065 vs. 1998-2014) for the upper quartile projection of 30 climate model runs in the CORDEX-Africa ensemble (RCP4.5 and RCP8.5) |
| T_2035_P25 | °C | Change in future mean annual air temperature in °C (2026-2045 vs. 1998-2014) for the lower quartile projection of 30 climate model runs in the CORDEX-Africa ensemble (RCP4.5 and RCP8.5) |
| T_2035_P50 | °C | Change in future mean annual air temperature in °C (2026-2045 vs. 1998-2014) for the median projection of 30 climate model runs in the CORDEX-Africa ensemble (RCP4.5 and RCP8.5) |
| T_2035_P75 | °C | Change in future mean annual air temperature in °C (2026-2045 vs. 1998-2014) for the upper quartile projection of 30 climate model runs in the CORDEX-Africa ensemble (RCP4.5 and RCP8.5) |
| T_2055_P25 | °C | Change in future mean annual air temperature in °C (2046-2065 vs. 1998-2014) for the lower quartile projection of 30 climate model runs in the CORDEX-Africa ensemble (RCP4.5 and RCP8.5) |
| T_2055_P50 | °C | Change in future mean annual air temperature in °C (2046-2065 vs. 1998-2014) for the median projection of 30 climate model runs in the CORDEX-Africa ensemble (RCP4.5 and RCP8.5) |
| T_2055_P75 | °C | Change in future mean annual air temperature in °C (2046-2065 vs. 1998-2014) for the upper quartile projection of 30 climate model runs in the CORDEX-Africa ensemble (RCP4.5 and RCP8.5) |
| E_2035_P25 | % | Change in future mean annual potential evapotranspiration in % (2026-2045 vs. 1998-2014) for the lower quartile simulation using 30 climate model runs of the CORDEX-Africa ensemble (RCP4.5 and RCP8.5) |
| E_2035_P50 | % | Change in future mean annual potential evapotranspiration in % (2026-2045 vs. 1998-2014) for the median simulation using 30 climate model runs of the CORDEX-Africa ensemble (RCP4.5 and RCP8.5) |
| E_2035_P75 | % | Change in future mean annual potential evapotranspiration in % (2026-2045 vs. 1998-2014) for the upper quartile simulation using 30 climate model runs of the CORDEX-Africa ensemble (RCP4.5 and RCP8.5) |
| E_2055_P25 | % | Change in future mean annual potential evapotranspiration in % (2046-2065 vs. 1998-2014) for the lower quartile simulation using 30 climate model runs of the CORDEX-Africa ensemble (RCP4.5 and RCP8.5) |
| E_2055_P50 | % | Change in future mean annual potential evapotranspiration in % (2046-2065 vs. 1998-2014) for the median simulation using 30 climate model runs of the CORDEX-Africa ensemble (RCP4.5 and RCP8.5) |
| E_2055_P75 | % | Change in future mean annual potential evapotranspiration in % (2046-2065 vs. 1998-2014) for the upper quartile simulation using 30 climate model runs of the CORDEX-Africa ensemble (RCP4.5 and RCP8.5) |

**Table 15: Climate change results included in the attributes of the GIS shape file "Layer D2 River Network".**

| Attribute | Units | Description |
|---|---|---|
| Q_2035_P25 | % | Change in future mean annual discharge in % (2026-2045 vs. 1998-2014) for the lower quartile simulation using 30 climate model runs of the CORDEX-Africa ensemble (RCP4.5 and RCP8.5) |
| Q_2035_P50 | % | Change in future mean annual discharge in % (2026-2045 vs. 1998-2014) for the median simulation using 30 climate model runs of the CORDEX-Africa ensemble (RCP4.5 and RCP8.5) |
| Q_2035_P75 | % | Change in future mean annual discharge in % (2026-2045 vs. 1998-2014) for the upper quartile simulation using 30 climate model runs of the CORDEX-Africa ensemble (RCP4.5 and RCP8.5) |
| Q_2055_P25 | % | Change in future mean annual discharge in % (2046-2065 vs. 1998-2014) for the lower quartile simulation using 30 climate model runs of the CORDEX-Africa ensemble (RCP4.5 and RCP8.5) |
| Q_2055_P50 | % | Change in future mean annual discharge in % (2046-2065 vs. 1998-2014) for the median simulation using 30 climate model runs of the CORDEX-Africa ensemble (RCP4.5 and RCP8.5) |
| Q_2055_P75 | % | Change in future mean annual discharge in % (2046-2065 vs. 1998-2014) for the upper quartile simulation using 30 climate model runs of the CORDEX-Africa ensemble (RCP4.5 and RCP8.5) |

**Table 16: Climate change results included in the attributes of the GIS shape file "Layer D3 Sub-areas", part 1 of 2.**

| Attribute | Units | Description |
|---|---|---|
| P_2035_P25 | % | Change in future mean annual precipitation in % (2026-2045 vs. 1998-2014) for the lower quartile projection of 30 climate model runs in the CORDEX-Africa ensemble (RCP4.5 and RCP8.5) |
| P_2035_P50 | % | Change in future mean annual precipitation in % (2026-2045 vs. 1998-2014) for the median projection of 30 climate model runs in the CORDEX-Africa ensemble (RCP4.5 and RCP8.5) |
| P_2035_P75 | % | Change in future mean annual precipitation in % (2026-2045 vs. 1998-2014) for the upper quartile projection of 30 climate model runs in the CORDEX-Africa ensemble (RCP4.5 and RCP8.5) |
| P_2055_P25 | % | Change in future mean annual precipitation in % (2046-2065 vs. 1998-2014) for the lower quartile projection of 30 climate model runs in the CORDEX-Africa ensemble (RCP4.5 and RCP8.5) |
| P_2055_P50 | % | Change in future mean annual precipitation in % (2046-2065 vs. 1998-2014) for the median projection of 30 climate model runs in the CORDEX-Africa ensemble (RCP4.5 and RCP8.5) |
| P_2055_P75 | % | Change in future mean annual precipitation in % (2046-2065 vs. 1998-2014) for the upper quartile projection of 30 climate model runs in the CORDEX-Africa ensemble (RCP4.5 and RCP8.5) |
| E_2035_P25 | % | Change in future mean annual actual evapotranspiration in % (2026-2045 vs. 1998-2014) for the lower quartile simulation using 30 climate model runs of the CORDEX-Africa ensemble (RCP4.5 and RCP8.5) |
| E_2035_P50 | % | Change in future mean annual actual evapotranspiration in % (2026-2045 vs. 1998-2014) for the median simulation using 30 climate model runs of the CORDEX-Africa ensemble (RCP4.5 and RCP8.5) |
| E_2035_P75 | % | Change in future mean annual actual evapotranspiration in % (2026-2045 vs. 1998-2014) for the upper quartile simulation using 30 climate model runs of the CORDEX-Africa ensemble (RCP4.5 and RCP8.5) |
| E_2055_P25 | % | Change in future mean annual actual evapotranspiration in % (2046-2065 vs. 1998-2014) for the lower quartile simulation using 30 climate model runs of the CORDEX-Africa ensemble (RCP4.5 and RCP8.5) |
| E_2055_P50 | % | Change in future mean annual actual evapotranspiration in % (2046-2065 vs. 1998-2014) for the median simulation using 30 climate model runs of the CORDEX-Africa ensemble (RCP4.5 and RCP8.5) |
| E_2055_P75 | % | Change in future mean annual actual evapotranspiration in % (2046-2065 vs. 1998-2014) for the upper quartile simulation using 30 climate model runs of the CORDEX-Africa ensemble (RCP4.5 and RCP8.5) |
| R_2035_P25 | % | Change in future mean annual runoff in % (2026-2045 vs. 1998-2014) for the lower quartile simulation using 30 climate model runs of the CORDEX-Africa ensemble (RCP4.5 and RCP8.5) |
| R_2035_P50 | % | Change in future mean annual runoff in % (2026-2045 vs. 1998-2014) for the median simulation using 30 climate model runs of the CORDEX-Africa ensemble (RCP4.5 and RCP8.5) |
| R_2035_P75 | % | Change in future mean annual runoff in % (2026-2045 vs. 1998-2014) for the upper quartile simulation using 30 climate model runs of the CORDEX-Africa ensemble (RCP4.5 and RCP8.5) |
| R_2055_P25 | % | Change in future mean annual runoff in % (2046-2065 vs. 1998-2014) for the lower quartile simulation using 30 climate model runs of the CORDEX-Africa ensemble (RCP4.5 and RCP8.5) |
| R_2055_P50 | % | Change in future mean annual runoff in % (2046-2065 vs. 1998-2014) for the median simulation using 30 climate model runs of the CORDEX-Africa ensemble (RCP4.5 and RCP8.5) |
| R_2055_P75 | % | Change in future mean annual runoff in % (2046-2065 vs. 1998-2014) for the upper quartile simulation using 30 climate model runs of the CORDEX-Africa ensemble (RCP4.5 and RCP8.5) |
| T_2035_P25 | °C | Change in future mean annual air temperature in °C (2026-2045 vs. 1998-2014) for the lower quartile projection of 30 climate model runs in the CORDEX-Africa ensemble (RCP4.5 and RCP8.5) |
| T_2035_P50 | °C | Change in future mean annual air temperature in °C (2026-2045 vs. 1998-2014) for the median projection of 30 climate model runs in the CORDEX-Africa ensemble (RCP4.5 and RCP8.5) |
| T_2035_P75 | °C | Change in future mean annual air temperature in °C (2026-2045 vs. 1998-2014) for the upper quartile projection of 30 climate model runs in the CORDEX-Africa ensemble (RCP4.5 and RCP8.5) |
| T_2055_P25 | °C | Change in future mean annual air temperature in °C (2046-2065 vs. 1998-2014) for the lower quartile projection of 30 climate model runs in the CORDEX-Africa ensemble (RCP4.5 and RCP8.5) |
| T_2055_P50 | °C | Change in future mean annual air temperature in °C (2046-2065 vs. 1998-2014) for the median projection of 30 climate model runs in the CORDEX-Africa ensemble (RCP4.5 and RCP8.5) |
| T_2055_P75 | °C | Change in future mean annual air temperature in °C (2046-2065 vs. 1998-2014) for the upper quartile projection of 30 climate model runs in the CORDEX-Africa ensemble (RCP4.5 and RCP8.5) |

**Table 17: Climate change results included in the attributes of the GIS shape file "Layer D3 Sub-areas", part 2 of 2.**

| Attribute | Units | Description |
|---|---|---|
| PT_2035_25 | % | Change in future hydropower potential in % (2026-2045 vs. 1998-2014) for the lower quartile simulation using 30 climate model runs of the CORDEX-Africa ensemble (RCP4.5 and RCP8.5) |
| PT_2035_50 | % | Change in future hydropower potential in % (2026-2045 vs. 1998-2014) for the median simulation using 30 climate model runs of the CORDEX-Africa ensemble (RCP4.5 and RCP8.5) |
| PT_2035_75 | % | Change in future hydropower potential in % (2026-2045 vs. 1998-2014) for the upper quartile simulation using 30 climate model runs of the CORDEX-Africa ensemble (RCP4.5 and RCP8.5) |
| PT_2055_25 | % | Change in future hydropower potential in % (2046-2065 vs. 1998-2014) for the lower quartile simulation using 30 climate model runs of the CORDEX-Africa ensemble (RCP4.5 and RCP8.5) |
| PT_2055_50 | % | Change in future hydropower potential in % (2046-2065 vs. 1998-2014) for the median simulation using 30 climate model runs of the CORDEX-Africa ensemble (RCP4.5 and RCP8.5) |
| PT_2055_75 | % | Change in future hydropower potential in % (2046-2065 vs. 1998-2014) for the upper quartile simulation using 30 climate model runs of the CORDEX-Africa ensemble (RCP4.5 and RCP8.5) |
| PL_2035_25 | % | Change in future hydropower potential in % (2026-2045 vs. 1998-2014) of local rivers (having their source in the same sub-area) for the lower quartile simulation using 30 climate model runs of the CORDEX-Africa ensemble (RCP4.5 and RCP8.5) |
| PL_2035_50 | % | Change in future hydropower potential in % (2026-2045 vs. 1998-2014) of local rivers (having their source in the same sub-area) for the median simulation using 30 climate model runs of the CORDEX-Africa ensemble (RCP4.5 and RCP8.5) |
| PL_2035_75 | % | Change in future hydropower potential in % (2026-2045 vs. 1998-2014) of local rivers (having their source in the same sub-area) for the upper quartile simulation using 30 climate model runs of the CORDEX-Africa ensemble (RCP4.5 and RCP8.5) |
| PL_2055_25 | % | Change in future hydropower potential in % (2046-2065 vs. 1998-2014) of local rivers (having their source in the same sub-area) for the lower quartile simulation using 30 climate model runs of the CORDEX-Africa ensemble (RCP4.5 and RCP8.5) |
| PL_2055_50 | % | Change in future hydropower potential in % (2046-2065 vs. 1998-2014) of local rivers (having their source in the same sub-area) for the median simulation using 30 climate model runs of the CORDEX-Africa ensemble (RCP4.5 and RCP8.5) |
| PL_2055_75 | % | Change in future hydropower potential in % (2046-2065 vs. 1998-2014) of local rivers (having their source in the same sub-area) for the upper quartile simulation using 30 climate model runs of the CORDEX-Africa ensemble (RCP4.5 and RCP8.5) |

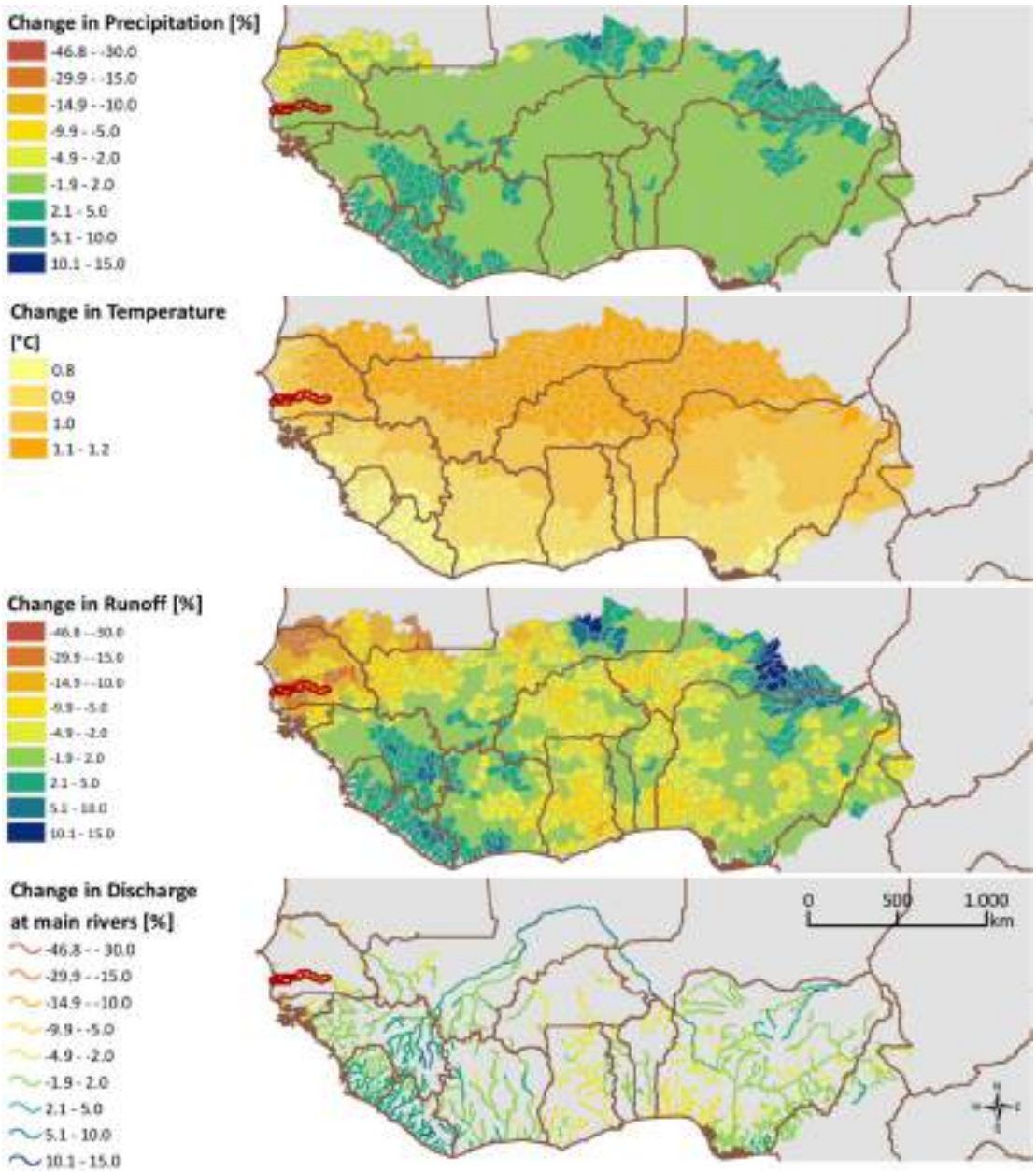


**Figure 73: Climate change projections for the near future 2026-2045 vs. 1998-2014.**

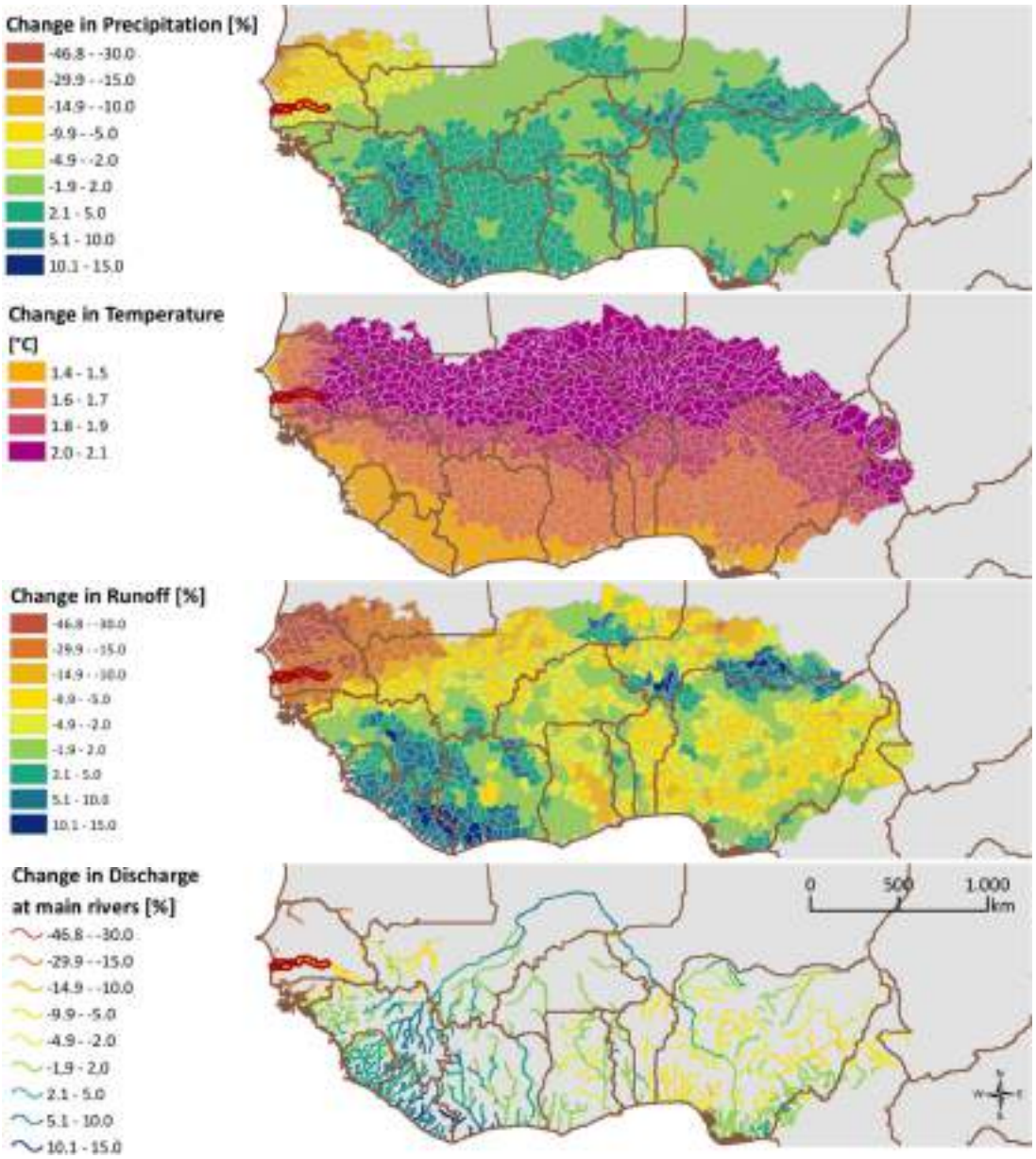


**Figure 74: Cliamte change projections for the far future 2046-2065 vs. 1998-2014.**

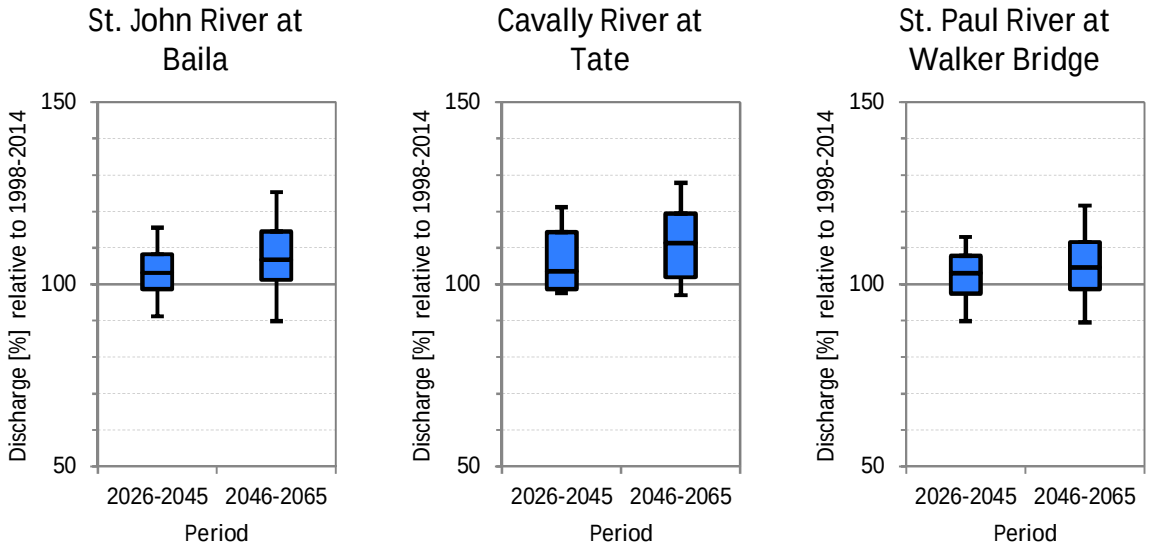


**Figure 75: Example box-plots visualizing the spread in individual climate model projections for changes in future discharge. The box shows the inner quartile range (25% to 75% percentile), whereas the whiskers show outliers (10% and 90% percentiles).**

## 6.5 Discussion of uncertainty

Climate change projections always include a certain degree of uncertainty. Therefore, in this study we used an ensemble modelling approach based on the projections of 30 RCM runs. The results of these projections were summarized by the median and lower and upper quartile projections to give an indication of the uncertainty. These data can be used to create box-plots (as shown e.g. in Figure 75).

When working with projections of climate models, one has to consider that there are various different sources of uncertainty, which are due to:

- emission scenario (or RCP)
- natural climate variability (i.e. climate cycles and random realization of climate)
- simulation errors in GCM
- simulation errors in RCM

The future emissions depend on political decisions as well as technological development, population growth and economic growth. In this study we used the two most commonly used emission scenarios – RCP4.5 (moderate emissions) and RCP8.5 (high emissions). Therefore, uncertainty due to emission scenario is already included in the results (box-plots). We decided to present just one set of final results (based on both RCPs) instead of presenting the results separately for RCP4.5 and RCP8.5. This reflects the notion that for hydropower assessments the uncertainty about future emissions should be treated in a similar way as the uncertainty due to e.g. simulation errors in GCM/RCMs.

RCMs provide more detailed projections than GCMs. However, even though we used the outputs of RCMs (CORDEX-Africa RCM ensemble), these data are also affected by biases in the driving GCMs and the natural climate variability that occurs in any simulation of the chaotic climate system.

In initial screening of the RCM data for historic conditions we found that the regional spatial pattern in annual precipitation is rather well preserved (i.e. wet coastal areas and drier inland areas), but the absolute values can deviate considerably from observed data (e.g. GPCC). For temperature, the RCMs are more capable of reproducing historic conditions.

To quantify the performance of RCMs in simulating historic climate we used a composite measure, which is based on long-term spatio-temporal patterns of precipitation and temperature (for details see Kling et al., 2012). Figure 76 shows that some RCMs perform better than other RCMs for reproducing historic conditions. In general there is a tendency that SMHI simulations perform better than CLMcom simulations. However, climate model research showed that the climate model bias for historic conditions does not affect the projected climate change signals (Giorgi and Coppola, 2010). Therefore, we decided to base our results on all RCMs (instead of only the better performing RCMs).

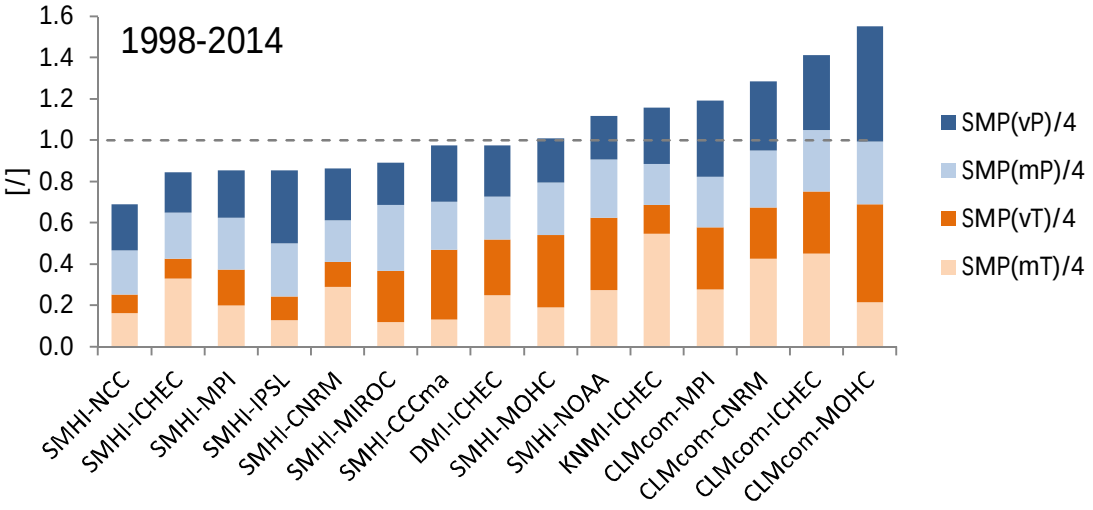


**Figure 76: Evaluation of performance of RCMs to simulate historic climate conditions in the period 1998-2014. Left to right: decreasing performance. Smaller bars indicate higher performance. Blue: performance for rainfall. Orange: performance for air temperature. Dark colors: performance for inter-annual variability. Light colors: performance for spatial variability. For details see Kling et al. (2012).**

In climate change studies the focus is usually on comparing historic and future long-term variables of e.g. 30-year periods. The reason is that the effect of natural climate variability should be minimized. For our study the selected periods are rather short, e.g. the reference period covers only 17 years from 1998-2014. This period was selected in order to reflect current, moderately wet hydrologic conditions in West Africa, as

opposed to the drought conditions in the 1980s. For the RCM runs first a smoothing of data was applied in order to average out the random variations from year to year. This allowed to compute more robust climate change signals between rather short periods of 1998-2014 vs. the two future periods 2026-2045 and 2046-2065.

Climate models in general have problems in simulating natural climate variability (instead they project gradual trends, and not cycles). Therefore, also the projections have to be interpreted as general trend projections. The climate model projections do not include possible natural cyclic behavior (which is not caused by climate change but is inherent to the climate system). As a consequence, the spread given in the simulation results for future discharge (median, upper and lower quartile) only reflects the uncertainty due to climate change projections, but not due to natural climate variability. Thus, the actual uncertainty in future discharge (including natural climate variability) is larger than given in our results.

On top of this, future discharge also depends on future decisions about water management, including:

- New irrigation withdrawals
- New large-scale reservoirs (evaporation losses)
- Agricultural practices and land-use change

Consideration of these local anthropogenic influences were beyond the scope of the presented regional assessment. Our study focusses on the impact of general climatic trends on the terrestrial water balance. The results show the expected change in future discharge given the most detailed climate model projections currently available for West Africa.

## 6.6 Conclusions

The climate change impact assessment is based on the most-detailed climate model projections currently available for Africa (CORDEX-Africa). The results of this study are therefore of interest not only for hydropower resources assessment, but relevant for all fields that may be affected by climate change (including e.g. agriculture).

The results of the climate change impact assessment lead to the following conclusions:

- Considerable warming is projected for West Africa in the next decades. The warming will be higher in inland regions than in coastal regions.
- In large parts of West Africa no pronounced change is projected for future mean annual rainfall. Mean annual rainfall is projected to increase in Guinea, Sierra Leone, Liberia and Côte d'Ivoire, whereas rainfall is projected to decrease in Senegal and The Gambia.
- The simulated future changes in mean annual runoff show the combined impacts of warming (increase in potential evapotranspiration) and changes in rainfall. In

large parts of West Africa a slight decrease or no considerable change is projected for future mean annual runoff. In Guinea, Sierra Leone, Liberia and Côte d'Ivoire runoff is projected to increase, whereas in Senegal and The Gambia runoff is projected to considerably decrease.

- For rivers having their source in the Fouta Djallon highlands (Senegal River, Niger River, etc.) the projected change in future mean annual discharge differs from the projected local changes in runoff (due to the flow routing from different regions):
    - The Niger River shows an increase in projected future discharge also in countries like Mali, Niger, and Nigeria (even though local runoff is projected to slightly decrease in these countries). These results are confirmed by a recent study for the Niger River by Oyerinde et al. (2016).
    - The Senegal River only shows a small decrease in projected future discharge, even though the local runoff in the lower stretches of the Senegal River is projected to significantly decrease. This is because the Senegal River has its source in a region where runoff is projected to increase.
- Overall the climate change impact assessment shows that in most parts of West Africa climate change is not a worst-case scenario for hydropower development.

# 7 COUNTRY REPORTS

## 7.1 Objective

The objective of the country reports is to provide a summary of the results of this study for each individual country.

## 7.2 Data sources

The main data source for the country reports are the GIS results of this study:

- Layer showing existing hydropower plants
- Layer D1 Climatic zones
- Layer D2 River network
- Layer D3 Sub-areas
- Climate change scenarios: Results incorporated into layers D1-D3

In addition also country statistics (population, GDP, etc.) of the tables included in ECOWAS Country Profiles in ECOWREX were used.

## 7.3 Methodology

The hydropower potential was summarized for each country by computing the sum of all river reaches located within the county. For river sections forming international borders (for example Senegal River) only half of the river section's hydropower potential is accounted for in the total potential of the country (and the other half is accounted for in the potential of the neighboring country).

For each country maps and tables were prepared showing the theoretical hydropower potential in attractive sub-catchments. In the selection of sub-catchments the focus was to present regions with attractive theoretical potential for pico/micro/mini and small HPP, whereas the focus was not on potential for medium/large HPP. The selected sub-catchments are only illustrative examples and there is no ranking between sub-catchments.

## 7.4 Results: Layer D4 country reports

The results of this study were summarized in 14 country reports. Overall the 14 country reports cover 242 pages and have about 100 tables, 150 maps and 150 figures.

Country reports are available for:

- Benin, 18 pages
- Burkina Faso, 16 pages
- Côte d'Ivoire, 18 pages

- The Gambia, 14 pages
- Ghana, 18 pages
- Guinea-Bissau, 16 pages
- Guinea, 19 pages
- Liberia, 18 pages
- Mali, 17 pages
- Niger, 17 pages
- Nigeria, 20 pages
- Senegal, 16 pages
- Sierra Leone, 18 pages
- Togo, 17 pages

Each country report includes text, maps, and figures in several sections:

- General information
  - Overview map
  - Table listing general country statistics (population, GDP, etc.)
- Climate
  - Map showing country's location on the regional climate map
  - Figures showing seasonality in rainfall and air temperature in the country's climate zones
- Hydrology
  - Map showing country's main river basins
  - Table listing percentage of country's area located in the largest river basins
  - Figures showing historic variation in (simulated) annual discharge from 1950 until 2014 for selected rivers
  - Figures showing seasonality in (simulated) mean monthly discharge in the period 1998-2014 for selected rivers
- Annual water balance

- Maps showing country's location and regional distribution of precipitation, actual evapotranspiration and runoff in West Africa

· Hydropower potential

- Figure showing how the total theoretical potential of the country is subdivided into theoretical potential for hydropower plants of different plant size.
- Table listing theoretical hydropower potential in country:
  - § Pico/micro/mini HPP
  - § Small HPP
  - § Medium/large HPP
  - § No attractive potential
  - § Total of all rivers in country
- Figures showing longitudinal profiles of selected rivers
- Detailed maps, table data and text description for the theoretical hydropower potential in selected sub-catchments

· Climate change

- Maps showing projections for the near future (2026-2045)
- Maps showing projections for the far future (2046-2065)
- Figures showing box-plots for projected change in discharge for selected gauges

Table 18 summarizes the theoretical hydropower potential for all countries, listing the classification results for pico/micro/mini, small and medium/large HPP (see also a graphical presentation of the results in Figure 77). The table data also lists the theoretical hydropower potential of rivers where no preferred plant size can be determined (due to too low specific hydropower potential). Nigeria has by far the highest theoretical hydropower potential of all countries in West Africa. Almost half of the theoretical hydropower potential of 14 ECOWAS countries is located in Nigeria. Interestingly, the theoretical hydropower potential for pico/micro/mini HPP is in Guinea almost as high as in Nigeria. Other notable countries for pico/micro/mini HPP are Sierra Leone, Liberia and Togo.

The data listed in Table 18 show that in all countries the theoretical hydropower potential for medium/large HPP is greater than for pico/micro/mini HPP. This is an expected result, as a very high number of small streams would be required to yield the same total potential as for one large river. However, the share of potential for different plant size differs considerably between countries. For example, Mali and Niger are countries where development of medium/large HPP shows considerable potential,

whereas the theoretical potential for small HPP or pico/micro/mini HPP is almost negligible in these two countries.

Guinea and Sierra Leone are two neighbouring countries with similar total theoretical hydropower potential, but the subdivision of the total potential for the country into potential for different plant size shows quite different results (Figure 78). Most of the total potential in Sierra Leone is classified as potential for medium/large HPP, whereas in Guinea medium/large, small and pico/micro/mini HPP have similar shares of the total potential.

**Table 18: Theoretical hydropower potential (MW) in individual countries, classified for different plant sizes.**

| Country | Pico/micro/ mini HPP | Small HPP | Medium/large HPP | No attractive potential | Total of all rivers in country |
|---|---|---|---|---|---|
| Benin | 5 | 90 | 239 | 415 | 749 |
| Burkina Faso | 1 | 16 | 10 | 244 | 271 |
| Côte d'Ivoire | 14 | 197 | 1580 | 1087 | 2878 |
| Ghana | 15 | 97 | 1041 | 890 | 2043 |
| Guinea | 524 | 1670 | 1980 | 1703 | 5877 |
| Gambia | 0 | 0 | 0 | 10 | 10 |
| Guinea Bissau | 0 | 1 | 97 | 82 | 180 |
| Liberia | 47 | 592 | 3164 | 675 | 4478 |
| Mali | 6 | 50 | 1086 | 1045 | 2187 |
| Niger | 0 | 3 | 312 | 214 | 529 |
| Nigeria | 678 | 3856 | 10691 | 4591 | 19816 |
| Senegal | 1 | 4 | 60 | 188 | 253 |
| Sierra Leone | 140 | 499 | 3148 | 594 | 4381 |
| Togo | 27 | 186 | 73 | 310 | 596 |
| 14 ECOWAS countries | 1458 | 7261 | 23481 | 12048 | 44248 |

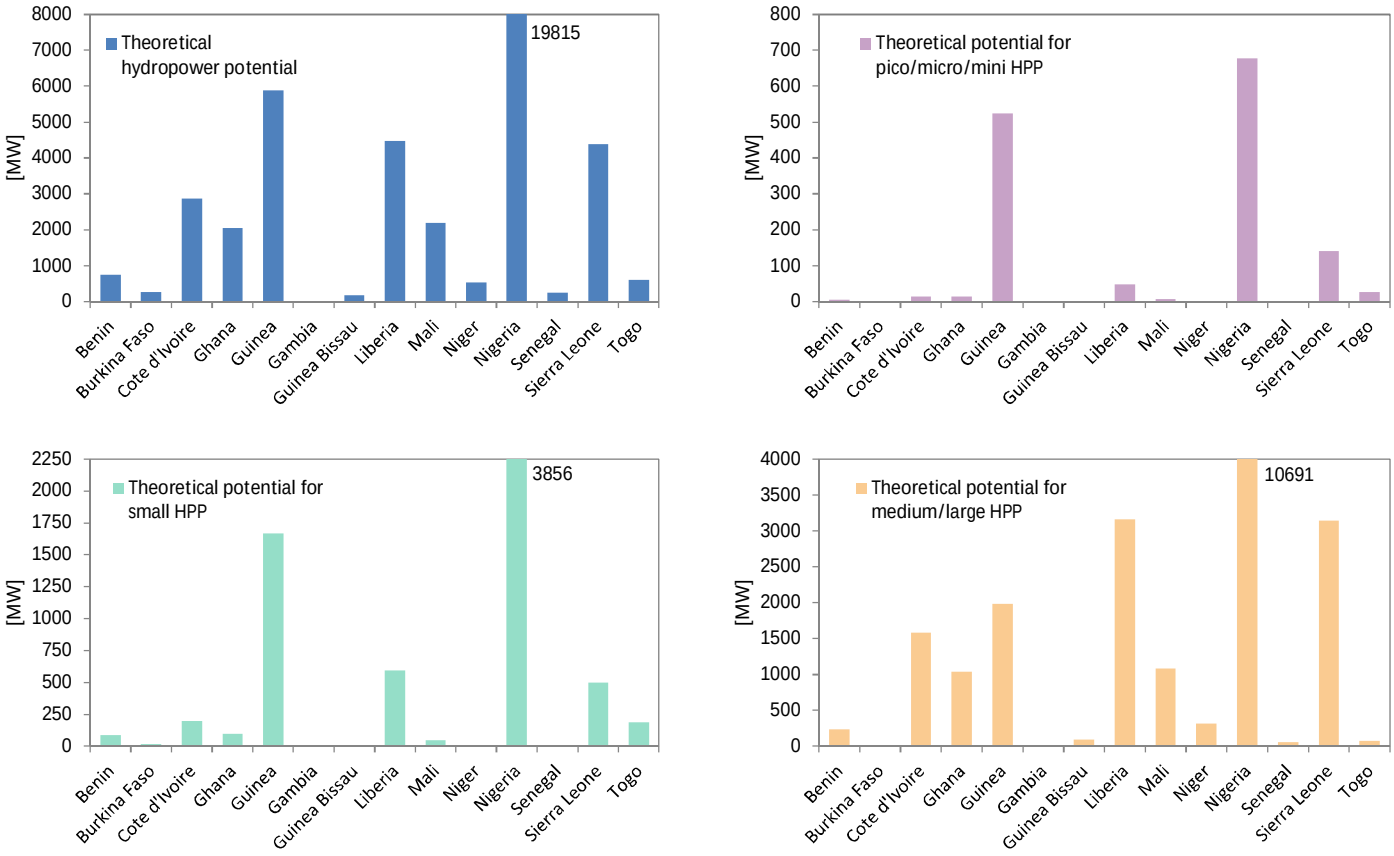


**Figure 77: Theoretical hydropower potential of countries.**

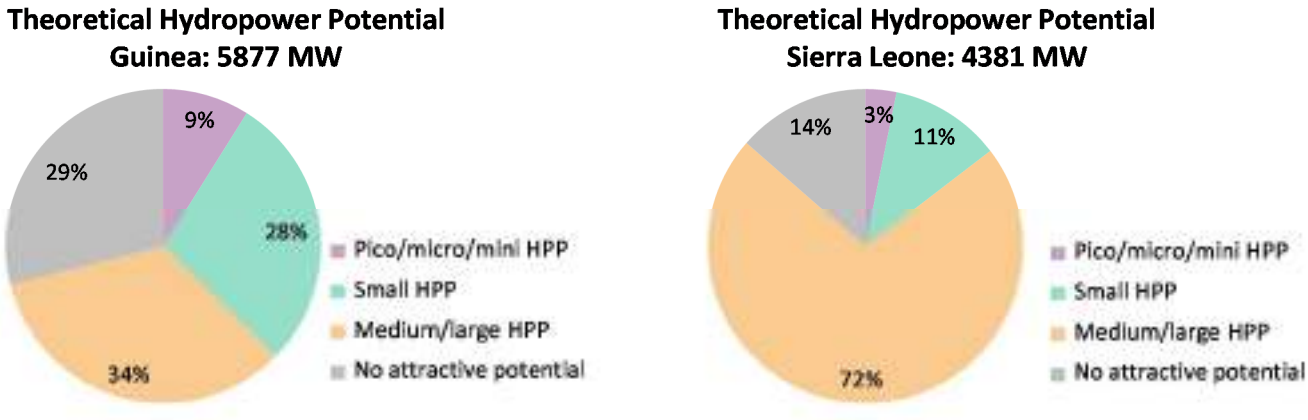


**Figure 78: Comparison of theoretical hydropower potential in Guinea (left) and Sierra Leone (right).**

## 7.5 Conclusions

In contrast to the detailed results provided by the GIS layers, the country reports provide a general overview about the theoretical hydropower potential and the expected impacts of climate change in individual countries in West Africa.

The results presented in the country reports allow the following general conclusions:

- Nigeria has by far the highest theoretical hydropower potential of all 14 ECOWAS countries studied.
- Other countries with high potential include Guinea, Liberia and Sierra Leone, followed by Côte d'Ivoire, Ghana and Mali.
- The subdivision of the total theoretical hydropower potential into potential for different plant sizes varies greatly between countries. For example, Guinea shows a high potential for pico/micro/mini and small HPP, whereas Liberia's potential is mainly for medium/large HPP. Countries like Mali and Niger solely have potential for medium/large HPP and are definitely not countries of interest for development of small and pico/micro/mini HPP.
- The climate change projections show that in most parts of West Africa no significant change is projected in future mean annual discharge, but there are regional variations in the projections:
    - In Guinea, Sierra Leone and Liberia future mean annual discharge is projected to slightly increase.
    - The Niger River, which has its headwater region in Guinea, is also projected to slightly increase.
    - Mean annual discharge of the Senegal River is projected to decrease in the future.

Overall, the country reports are a good reference that can be disseminated to ministries, hydrological services, river basin organizations, and hydropower investors. The country reports can also be used as a means to promote the detailed GIS results available via the ECOWREX system.

# 8 DEVIATIONS FROM THE TECHNICAL PROPOSAL

The execution of the hydropower resources mapping closely tried to follow Pöyry's original technical proposal. However, some deviations were made during the course of the project, which are summarized below:

- **River network:** Originally it was proposed to use the existing Hydrosheds river network, which consists of about 100,000 river reaches in West Africa. However, during project execution it was realized that this resolution is too coarse, as in humid regions many small streams that are potentially attractive for pico/micro/mini HPP would have been left out. Therefore, a new river network was created that consists of about 500,000 river reaches.

- **Country reports:** The contents of the country reports were not closely defined in Pöyry's original proposal. However, from the information provided in the TORs and Pöyry's technical proposal the country reports would mainly have been a table with a few entries (theoretical hydropower potential for three different plant sizes, country share of main river basins, etc.). Instead, during project execution it was realized that extensive country reports (with maps, tables, figures and accompanying text) would be a key outcome for this study. Therefore, 14 reports with overall 240 pages were prepared to give a general overview about the study results. Instead of presenting a summary of the results in the final report (this document) the results were presented in the country reports.

- **Layer Existing Hydropower Plants:** Pöyry's original proposal was to only include existing hydropower plants with an installed capacity greater than 30 MW (i.e. medium/large HPPs). In consultation with ECREEE it was agreed to also include smaller hydropower plants in the GIS layer. However, it cannot be guaranteed that all existing small HPPs were identified, as for some of the hydropower plants it was quite difficult to obtain the relevant information.

- **Diversions for irrigation:** Pöyry's technical proposal included an optional GIS layer showing diversions for irrigation in West Africa. This optional layer was not ordered by ECREEE. However, during water balance model calibration Pöyry realized that some large-scale irrigation schemes could not be ignored, as they have a significant impact on downstream discharge. The same applies to evaporation losses in floodplains. Therefore, Pöyry's water balance modelling approach was refined to consider the major diversion and floodplain losses at about 30 locations.

- **Longitudinal river profiles:** Pöyry did not prepare pre-computed graphs of thousands of longitudinal river profiles (as written in the original proposal), but instead provided code to ECREEE to automatically create longitudinal river profiles from the GIS river network layer. This code can be implemented in the ECOWREX system to dynamically create the graphs in the web-interface.

- **Preparation of training material:** In a contract extension Pöyry was invited to hold a two-day training workshop on GIS hydropower resources mapping, held in July 2016 in Dakar, Senegal. The contract extension covered some of the costs (flight, hotel, etc.), but excluded the costs for several days of preparation of

training materials (presentations) and practice examples for eight training sessions. The training materials were handed over to ECREEE for future use in similar training workshops.

The above deviations from Pöyry's original technical proposal were done in close consultation with ECREEE and were necessary adjustments to ensure optimal results for the project.

# 9 REFERENCES

Andersen I, Dione O, Jarosewich-Holder M, Olivry JC. 2005. *The Niger River Basin: A vision for sustainable management*. The World Bank, Washington D.C.

Budyko M I. 1974. *Climate and Life*. Academic, San Diego, Calif.

Choudhury BJ. 1999. *Evaluation of an empirical equation for annual evaporation using field observations and results from a biophysical model*. Journal of Hydrology, Issue 216, pages 99-110

Hay LE, Wilby RL, Leavesley GH. 2000. *A comparison of delta change and downscaled GCM scenarios for three mountainous basins in the United States*. Journal of the American Water Resources Association 36(2): 387-397

Fekete BM, Robarts RD, Kumagai M, Nachtnebel HP, Odada E, Zhulidov AV. 2015. *Time for in situ renaissance*. Science 349(6249): 685-686

Giorgi F, Jones C, Asrar GR. 2009. *Addressing climate information needs at the regional level: The CORDEX framework*. WMO Bulletin, Issue 58, pages 175-183

Giorgi F, Coppola E. 2010. *Does the model regional bias affect the projected regional climate change? An analysis of global model projections*. Climatic Change 100(3-4): 769-815

Gerrits AMJ, Savenije HHG, Veling EJM, Pfister L. 2009. *Analytical derivation of the Budyko curve based on rainfall characteristics and a simple evaporation model*. Water Resources Research 45, 15 pages

Kling H, Fuchs M, Paulin M. 2012. *Runoff conditions in the upper Danube basin under an ensemble of climate change scenarios*. Journal of Hydrology 424-425: 264-277

Kling H, Stanzel P, Fuchs M. 2016. *Regional assessment of the hydropower potential of rivers in West Africa*. Energy Procedia 97: 286-293

Kling H, Stanzel P, Fuchs M, Bauer H. 2017. *Theoretical hydropower potential for different plant sizes for all rivers in West Africa*. Conference Proceedings, Water Storage and Hydropower Development for Africa, Marrakech, Morocco, 14-16 March 2017

L`Hôte Y, Dubreuil P, Lerique J. 1996. *Carte des types de climats en Afrique Noire à l'ouest du Congo. Rappels, et extension aux régimes hydrologiques*. In: L'hydrologie tropicale: géoscience et outil pour le développement (Actes de la conférence de Paris, mai 1995). IAHS Publ. no. 238, p. 55-65

Lehner B, Verdin K, Jarvis A. 2008. *New global hydrography derived from spaceborne elevation data*. Eos Transactions, AGU, Issue 89(10), pages 93-94

Milly PCD, Dunne KA. 2002. *Macroscale water fluxes – 2. Water and energy supply control of the interannual variability*. Water Resources Research 38 (10), 9 pages

Oyerinde GT, Wisser D, Hountondji FCC, Odofin AJ, Lawin AE, Afouda A, Diekkrüger B. 2016. *Quantifying uncertainties in modeling climate change impacts on hydropower production.* Climate, Issue 4/34, 15 pages

Scheff J, Frierson D. 2014. *Scaling Potential Evapotranspiration with Greenhouse Warming*. J. Climate 27: 1539–1558

Zhang L, Dawes WR, Walker GR. 2001. *Response of mean annual evapotranspiration to vegetation changes at the catchment scale*. Water Resources Research 37(3): 701-708

# 10 LIST OF FIGURES

# 11 LIST OF TABLES